Rafaela Faria Malta

Development of lipid nanoparticles containing LEM2 for topical treatment of skin cancer

Dissertação do 2º ciclo de estudos conducente ao grau de mestre em Tecnologia Farmacêutica

Trabalho realizado sob a orientação de:
Prof. Doutora Helena Amaral (orientadora)
Prof. Doutora Lucília Saraiva (coorientadora)

Setembro, 2019

Agradecimentos

A elaboração e responsabilidade de uma tese de mestrado é, predominantemente, um ato individual. No entanto, este caminho não é percorrido na solidão. Dele fizeram parte várias pessoas que contribuíram com o seu conhecimento e o seu incentivo, deixando impressa a sua marca. Por isso, expresso a minha gratidão. Na impossibilidade de falar de todas, realço aquelas que merecem maior destaque:

À minha orientadora, Prof. Doutora Helena Amaral, e à minha coorientadora, Prof. Doutora Lucília Saraiva, um sincero obrigada pelo conhecimento científico partilhado, pela amabilidade, pela disponibilidade, pela compreensão, pelas críticas, pela ajuda, e, sobretudo, pelo voto de confiança.

Ao Prof. Doutor Paulo Costa, o qual faz parte deste projeto e foi um elemento bastante importante na realização deste trabalho, quero agradecer pela paciência, pela disponibilidade, pela atenção, pelos ensinamentos e pela preocupação.

Aos restantes Professores do Mestrado em Tecnologia Farmacêutica da Faculdade de Farmácia da Universidade do Porto, agradeço pelas competências e conhecimento científico que me transmitiram.

À Joana Loureiro, um elemento muito importante na realização deste trabalho, principalmente na parte final, quero agradecer toda a paciência e todos os ensinamentos.

Aos colegas de Mestrado que partilharam este percurso comigo, agradeço todo o apoio que me deram.

À Dona Conceição, obrigada pelo apoio prestado ao longo da execução laboratorial.

Aos meus pais, em especial, obrigada por acreditarem sempre em mim e obrigada por todas as oportunidades que me proporcionam.

Ao meu namorado e amigos, obrigada pela compreensão, pela paciência, e, sobretudo, pelo apoio.

The work was supported by UID/QUI/50006/2019 with funding from FCT/MCTES through national funds.

Abstract

Skin cancer affects millions of people around the world, being a major public health concern. Melanoma is the most worrying skin cancer type, because it is the most aggressive form of cancer and can even cause death. Thus, it is important to improve skin cancer treatment efficacy. Topical treatment of skin diseases is a good strategy since avoids systemic side effects that usually are associated with oral and parenteral drugs administration. LEM2 is a synthetic xanthone with proved antitumor effect in melanoma. However, it presents poor aqueous solubility, which is often related with poor bioavailability, limiting its therapeutic use. The use of lipid nanoparticles to encapsulate drugs can improve their bioavailability and seems to be very interesting for topical delivery of drugs due to their adhesion and occlusive properties.

In this work, unloaded lipid nanoparticles (SLNs and NLCs) were prepared by hot high-pressure homogenization (HPH) and ultrasonication. These nanoparticles were characterized (particle size, polydispersity index (PDI), zeta potential (ZP), and pH) and stability tests were performed for 60 days. NLCs were stable and ultrasonication showed to be an easier and faster method to prepare these nanoparticles when compared with hot HPH. So LEM2 was encapsulated in NLCs using the ultrasonication method and the final loaded NLCs had a mean particle size suitable for topical application, approximately 220 nm, and an encapsulation efficiency (EE) around 70%. This formulation seemed to be more cytotoxic against melanoma A375 cell line than unloaded NLC, possibly due to LEM2 antitumor activity, which means that NLCs could be used as a carrier to this drug, improving its bioavailability problems.

Keywords: skin cancer, melanoma, lipid nanoparticles, topical treatment, LEM2

Resumo

O cancro da pele afeta milhões de pessoas em todo o mundo, constituindo uma grande preocupação em termos de saúde pública. O melanoma é o tipo de cancro da pele mais preocupante por ser o mais agressivo, podendo até causar a morte. Deste modo, torna-se importante melhorar a eficácia do tratamento desta doença. O tratamento tópico de doenças da pele é uma boa estratégia, uma vez que evita os efeitos sistémicos colaterais, normalmente associados à administração de medicamentos por via oral ou parentérica. O LEM2 é uma xantona sintética com efeito anti-tumoral testada em células de melanoma. No entanto, este composto tem fraca solubilidade em meio aquoso, o que normalmente está relacionado com uma baixa biodisponibilidade, limitando o seu uso terapêutico. A utilização de nanopartículas lipídicas para encapsular fármacos pode melhorar a sua biodisponibilidade e este tipo de veículo parece ser bastante interessante para a administração cutânea de fármacos devido às suas propriedades de adesão e oclusão.

Neste trabalho, foram preparadas nanopartículas lipídicas (SLN e NLC) pelos métodos de homogeneização a alta pressão (HPH) e ultrasonicação. Estas nanopartículas foram caracterizadas (tamanho, índice de polidispersão (PDI), potencial zeta (ZP), e pH) e foram feitos estudos de estabilidade durante 60 dias. Os NLC pareceram ser mais estáveis e o método de ultrasonicação mostrou ser mais fácil e rápido em comparação com a HPH. Por estas razões, o LEM2 foi encapsulado em NLC usando o método de ultrasonicação e as nanopartículas finais resultantes apresentaram um tamanho adequado para a aplicação tópica do fármaco (aproximadamente 220 nm) e uma eficácia de encapsulação (EE) de cerca de 70%. Esta formulação mostrou ser mais tóxica para a linha celular A375 de melanoma do que as nanopartículas vazias, devido, possivelmente, à atividade anti-tumoral do LEM2, sugerindo que as NLC produzidas podem ser usadas como veículo para este fármaco, o que poderá melhorar o seu problema de biodisponibilidade.

Palavras-chave: cancro da pele, melanoma, nanopartículas lipídicas, tratamento tópico, LEM2

Index of contents

Index of figures

Index of tables

Abbreviations

ANOVA – One-way analysis of variance
ATCC – American Type Culture Collection
BCA – Bicinchoninic acid
BCC – Basal cell carcinoma
BSA – Bovine serum albumin
CV – Coefficient of variation
DBD – DNA-binding domain
DLS – Dynamic light scattering
ECL – Enhanced chemiluminescence
EDTA – Ethylene diamine tetra acetic acid
EE – Encapsulation efficiency
ELS – Electrophoretic light scattering
FBS – Fetal bovine serum
GAPDH – Glyceraldehyde 3-phosphate dehydrogenase
GI_{50} – 50% inhibition of the cell growth
GRAS – Generally recognized as safe
HPH – High-pressure homogenization
HPLC – High-performance liquid chromatography
HRP – Horseradish peroxidase
ICH – International Conference on Harmonization
k' – Capacity factor
LEM2 – 1-carbaldehyde-3,4-dimethoxyxanthone
N – Theorical plate number
NLC – Nanostructured lipid carrier
OD – Oligomerization domain
PBS – Phosphate buffered saline
PDI – Polydispersity index
PI – Propidium iodide
PVDF – Polyvinylidene difluoride
R^2 – Determination coefficient
RETRA – Reactivation of transcriptional reporter activity
RIPA – Radioimmunoprecipitation assay

RPMI – Roswell park memorial

RSS – Residual sum of squares

SCC – Squamous cell carcinoma

SD –Standard deviation

SDS-PAGE – Sodium dodecyl sulphate-polyacrylamide gel

SIMP – Small interfering mutant p53 peptide

SRB – Sulforhodamine B

SLN – Solid lipid nanoparticle

T – Tailing factor

TAD – Transactivation domain

TBS-T – Tris-buffered saline solution with 0.1% Tween® 20

t_0 – Unretained peak time

t_R – Retention time

UK – United Kingdom

USA – United States of America

US-FDA – US Food and Drug Administration

USP – United States Pharmacopeia

UV – Ultraviolet

ZP – Zeta potential

Chapter I – Introduction

1.1. Skin cancer

Skin cancer is a pre-eminent global public health concern, representing the most ordinary type of malignancy in Caucasian population and its incidence shows no signs of plateauing (1,2).

Skin cancer is mainly divided into two types: melanoma and non-melanoma skin cancer (3). Non-melanoma skin cancer includes basal cell carcinoma (BCC) and squamous cell carcinoma (SCC) (4). The different types of skin cancers are named according to the type of skin cell from which they arise (3,5). Most skin cancers develop in the uppermost layer of the skin, the epidermis (6).

Melanoma arises from epidermal melanocytes and can occur in any tissue that comprises these cells, including non-cutaneous sites, such as eye, oral mucosa, urinary tract, among others (7). It is the least common but most aggressive form of skin cancer (melanomas are fast to invade and metastasize) (6,8). According to Geller et al. (9), 132.000 new cases of melanoma and 50.000 melanoma-related deaths are diagnosed each year worldwide. In 2018, there were almost 300.000 new cases of melanoma, being Australia the country with the highest rate (Table 1) (9). The top 10 countries with the highest rates of melanoma of the skin in 2018 are given in Table 1.

Table 1 – Melanoma rates, both genders, all ages, in 2018 (9,10).

Rank	Country	Age-standardized rate per 100 000
1	Australia	33.6
2	New Zealand	33.3
3	Norway	29.6
4	Denmark	27.6
5	Netherlands	25.7
6	Sweden	24.7
7	Germany	21.6
8	Switzerland	21.3
9	Belgium	19.9
10	Slovenia	18.6

Fortunately, most melanomas arise on the skin surface, being therefore detectable by visual examination (1). Typical melanomas usually follow the “ABCDE” rule: asymmetry, border irregularity, color variation (especially red, black, blue or white hues), diameter more than 6 mm and evolving nature of the lesions (11,12) (Figure 1). Some lesions suggestive of melanoma will have some but not all of these characteristics (1). For example, some of the skin lesions caused by melanomas may be less than 6 mm, and thus it is important that even minor skin lesions with unusual appearance be considered for examination (13). Also, any alteration in a preexisting nevus, such as bleeding, ulceration, growth, pain or pigmentary changes, is a reason for concern (14).

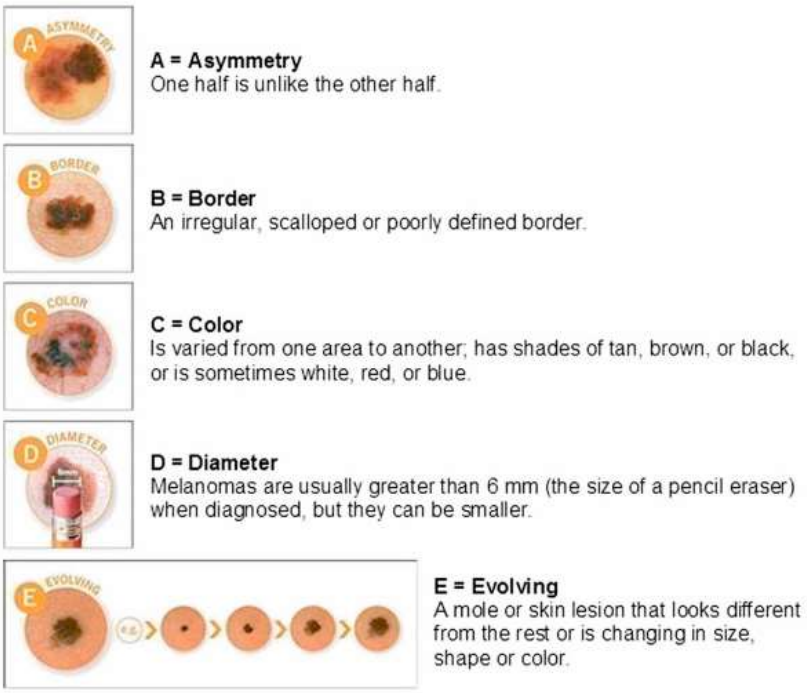

Figure 1 – The "ABCDE" signs of melanoma (13).

Numerous risk factors are associated with melanomas development, including endogenous factors (phototype, eye and skin color, individual or family history of skin cancer, number of melanocytic nevi, presence of dysplastic nevi) and exogenous factors (history of sunburn, type and degree of cumulative sun exposure) (1,15). Almost 90% of all skin cancer cases are caused by an overexposure to ultraviolet (UV) radiation, via sunlight or indoor tanning salons (16).

BCC and SCC make up 99% of all non-melanoma skin cancers. Other much fewer common forms of non-melanoma skin cancer includes Kaposi sarcoma, dermatofibrosarcoma, Merkel cell carcinoma, carcinosarcoma, and primary cutaneous B-cell lymphoma (17). The incidence of non-melanoma skin cancer is 18-20 times higher than that of melanoma (17,18). Yet, compared to melanoma, the epidemiology of this category of skin cancer is understudied (17).

BCC is the most common form of skin cancer and represents 75% of non-melanoma skin cancer cases (19). It is a slow growing, locally invasive epidermal tumor derived from the basal cells. Its metastatic rate is low (19,20). The most typical site of BCC lesions is uncovered skin directly exposed to the sun, such as head and neck areas (especially the eyelid and nose) (21,22). It develops characteristically into shiny papules, with pearly borders, prominent

engorged vessels on the surface (Figure 2, left), and a central ulcer. Sometimes, it could appear as yellowish-white flat, scar-like patches. Also, recurrent crusting or bleeding is common (1,22). Besides ultraviolet radiation, the most significant risk factors associated with the development of BCC includes genetic diseases (Gorlin-Goltz syndrome, for example), age, gender, immunosuppression, and fair skin (2,23,24).

Figure 2 – Examples of non-melanoma skin cancers lesions. Right – BCC, left – SCC (1,25).

SCC accounts for the majority of the remainder of non-melanoma skin cancers (19). This form of skin cancer arises from the epidermal keratinocytes, which could metastasize (1,23). The lesions induced by SCC may occur in areas usually exposed to the sun, such as face, lower lip, ears, neck, hands, arms, and legs (25). They can look like scaly red patches, crusted thick nodules (Figure 2, right), open sores, or warts, and they must crust over or bleed easily when bumped (1,25). Numerous risk factors have been associated with SCC, including cutaneous genetically inherited skin diseases (xeroderma pigmentosum, albinism, among others), some human papillomavirus types (16, 18, and 31), fair skin, and outdoor occupation (2,23).

1.2. Lipid nanoparticles

Lipid nanoparticles were introduced in the end of the 20th century by the research groups of Müller (Germany), Gasco (Italy), and Westesen (Germany) (26,27). At this moment, there are many research groups worldwide working on lipid nanoparticles for pharmaceutical applications, estimated by the published articles, which proves the increasing interest in the

field of these nanoparticles (28). They can be defined as particles composed of a lipid matrix that is solid at body and room temperature, with sizes mainly between 150-300 nm, although sizes less than 100 nm and near to 1000 nm may be present (29,30). Lipid nanoparticles are interesting lipid-based drug-delivery systems for many reasons, including biocompatibility, biodegradability, ease of large-scale production, low toxicity potential, and possibility of both hydrophilic and lipophilic drug incorporation (29,31).

There are two generations of lipid nanoparticles. The first generation of nanoparticles is named solid lipid nanoparticles (SLNs) and the second is called nanostructured lipid carriers (NLCs) (32). The main difference between them is the inner lipidic structure (32). The matrix of SLN is constituted by a solid lipid only, whereas the matrix of NLC is a combination of a solid lipid and a liquid lipid (Figure 3) (30,33,34). For a better understanding of the structural differences between these two generations of lipid nanoparticles, we can associate the SLN lipid organization with a perfect brick wall, while the NLC lipid organization can be compared with a disordered wall of stones with different dimensions and shapes (Figure 3). With this lipid organization, NLCs are able to overcome some of the shortcomings of SLNs. Thus, NLCs may increase drug loading, encapsulation efficiency, and physical stability (31,35) (Figure 3).

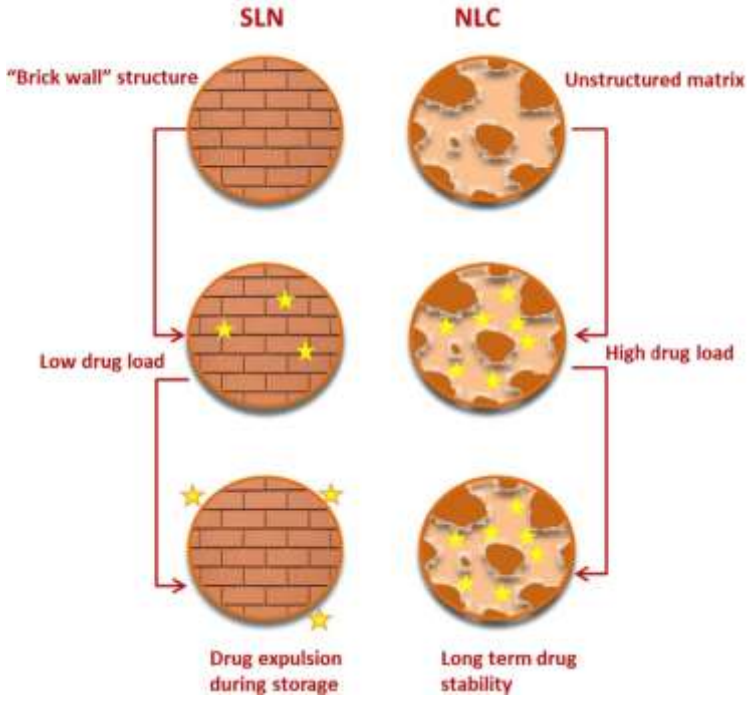

Figure 3 – Differences between SLNs and NLCs structure (28).

Typical lipid nanoparticles formulations are composed of a solid lipid (in case of SLN) or a mixture of solid and liquid lipids (in case of NLC), emulsifier(s), and water (29). Usually, the lipids used to prepare lipid nanoparticles are fatty acids, mono-, di-, and triglycerides, waxes, and fatty alcohols (29). The components of the lipid matrix must be carefully chosen, taking also into account the nature of the compound to be incorporated since it must be solubilized in the lipid matrix in order to have good encapsulation efficiency (36). Emulsifier or blend of emulsifiers are essential to stabilize lipid nanoparticle dispersions and prevent particles agglomeration (36). Tables 2 and 3 show some lipids and emulsifiers used for the preparation of lipid nanoparticles, respectively. All the excipients used in lipid nanoparticles formulations are generally recognized as safe (GRAS) substances, which mean that they are approved by the regulatory authorities for human use in medicine and food (26,34).

Table 2 – Commonly used lipids in lipid nanoparticles formulations.

Lipids	Examples	Physical form	References
Fatty acids	Oleic acid	Liquid	(37–46)
	Stearic acid	Solid	(41,47–50)
Triglycerides	Tripalmitin	Solid	(51–53)
	Tristearin	Solid	(52,54,55)
Long-chain (14-18C)	Corn oil	Liquid	(56,57)
	Soybean oil	Liquid	(42,58)
Medium chain (6-12C)	Glycerylcaprate (Miglyol® 810)	Liquid	(59,60)
	Glyceryltricaprylate (Miglyol® 812)	Liquid	(61–63)
Mono/di glycerides	Glyceryl palmitostearate (Precirol® ATO 5)	Solid	(43,44,64–68)
	Glyceryl monostearate	Solid	(43,69,70)
	Glyceryl dibehenate (Compritol® 888 ATO)	Solid	(43,64,66,70,71)
Waxes	Cetyl palmitate	Solid	(62,72–74)
	Carnauba wax	Solid	(75–77)
Phospholipids	Phosphatidylcholine	Solid	(52,78,79)
Other	α-tocopherol/vitamin E	Solid	(80–82)

Table 3 – List of some emulsifiers used in lipid nanoparticles formulations.

Type of emulsifier	Example	References
Hydrophilic emulsifier	Polysorbates (Tween® 80, Tween® 20)	(38,46,52,73,83–86)
	Poloxamer 88	(52,83,84)
	Sodium deoxycholate	(86–88)
Lipophilic emulsifier	Myverol® 18-04K	(67,89–91)
	Span® 20	(92,93)
Amphiphilic emulsifier	Lecithin	(38,84,94–96)

1.3. Examples of lipid nanoparticles used in skin cancer

Lipid nanoparticles have been widely studied due to their therapeutic efficacy via cutaneous administration route. Topical drug delivery systems that allow dermal penetration are administered for local treatment of pathological conditions, such as skin cancer. These formulations should let the drug reach the epidermis and the dermis without systemic effects (97). Compared to traditional drug delivery systems (oral and parenteral systems), topical delivery offers many advantages (6):

- Convenient and safe
- Increased patient acceptability, since it is noninvasive
- Avoid gastrointestinal tract and first pass effect of drugs
- Minimize side effects, and
- Avoid fluctuations in drug levels.

Some features of lipid nanoparticles, namely their small sizes and high surface area, allow them to achieve close contact with superficial junction of corneocyte clusters and channels of stratum corneum (Figure 4) (98). This is particularly important to improve drug accumulation and local drug depot formation, which can be used for controlled delivery of the compound over a long period of time (99,100). Besides, these nanoparticles possess an essential occlusive property (Figure 4), which may improve the penetration of compounds through the stratum corneum by reducing transepidermal water loss (100). However, it is important to note that the physicochemical properties of the molecules also play an important role on their skin penetration performance (27,101).

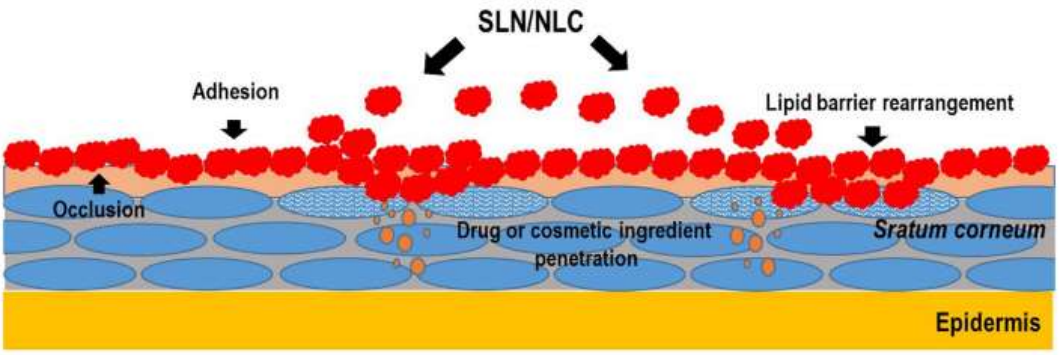

Figure 4 – Adhesion and occlusion effects of lipid nanoparticles in skin barrier (105).

Due to these high attractive features, various scientific groups worldwide have been studied the suitability of lipid nanoparticles to improve the topical delivery of drugs, including drugs to treat skin cancer. Numerous interesting intensive reviews of scientific publications can be found (3,102–104). Hence, only a few examples regarding the most recent publications in this area will be referred (Table 4). Considering the examples shown in Table 4, it can be concluded that the actual status of the studies related with topical lipid nanoparticles systems seems to be promising.

From the pharmaceutical technology point of view, lipid nanoparticles constitute aqueous dispersions with low viscosity for cutaneous application (100,105). Thereby, lipid nanoparticles dispersions need to be incorporated into commonly used dermal carriers, such as creams, gels, and ointments, to obtain semisolid formulations (100).

Table 4 – Examples of drugs encapsulated in lipid nanoparticles to treat skin cancer.

Compound	Type of lipid nanoparticle	Relevant conclusions	Reference
Topotecan	NLC	• Nanoparticle dispersions stable for up to 30 days • *In vitro* experiments showed that nanoencapsulation of the compound increased its cytotoxicity • NLCs with topotecan were incorporated in cellulose hydrogels, increasing the compound permeation	(106)
Doxorubicin	SLN	• The drug was successfully encapsulated in SLNs • *In vitro* and *in vivo* results indicated the superiority of cytotoxic performance of drug loaded SLN compared to free drug solution	(107)
Temozolomide	SLN	• Compared with free drug, drug loaded SLN exerted larger effects in cell proliferation and neoangiogenesis of melanoma cells • *In vivo* experiments showed that drug loaded SLN inhibit growth and vascularization of melanoma, without toxic effects	(108)
5-Fluorouracil	NLC	• Compared with free drug, drug loaded NLC showed significantly higher anticancer effect • NLC was incorporated in a hydrogel formulation for ease of application which has suitable occlusive and mechanical properties, viscosity and pH to improve patient compliance • There was a larger cumulative amount of the drug in dermal tissues after application of NLC enriched hydrogel when compared with 5-Fluorouracil hydrogel	(97)

Paclitaxel	SLN	• The drug was successfully encapsulated in SLN • SLN can be homogenously dispersed in a topical gel, showing a sustained release profile • *In vivo* experiments showed that the loaded topical gel is efficient in the treatment of skin cancer as compared to the free drug loaded gel	(109)
Chloroaluminum phthalocyanine (used as photosensitizer in photodynamic therapy)	NLC	• Lipid nanoparticles increased the retained amount of compound into the skin • NLC presented potent antitumoral effect • The presence of oleic acid in the NLC seems to potentialize the antitumoral effect	(110)

1.4. Skin cancer and TAp73

p53 is an important tumor suppressor that is vital in preserving cellular genomic integrity and controlled cell growth (111,112). Loss of p53 function results in the anomalous growth of cells, thus both the cellular expression and activity of p53 are tightly regulated (111). Under normal conditions, p53 is expressed at low levels in cells; however, in response to cellular stress like DNA damage, p53 is stimulated leading to cell cycle arrest and promotes DNA repair or induces apoptosis through transactivation of its target genes (113–116) (Figure 5).

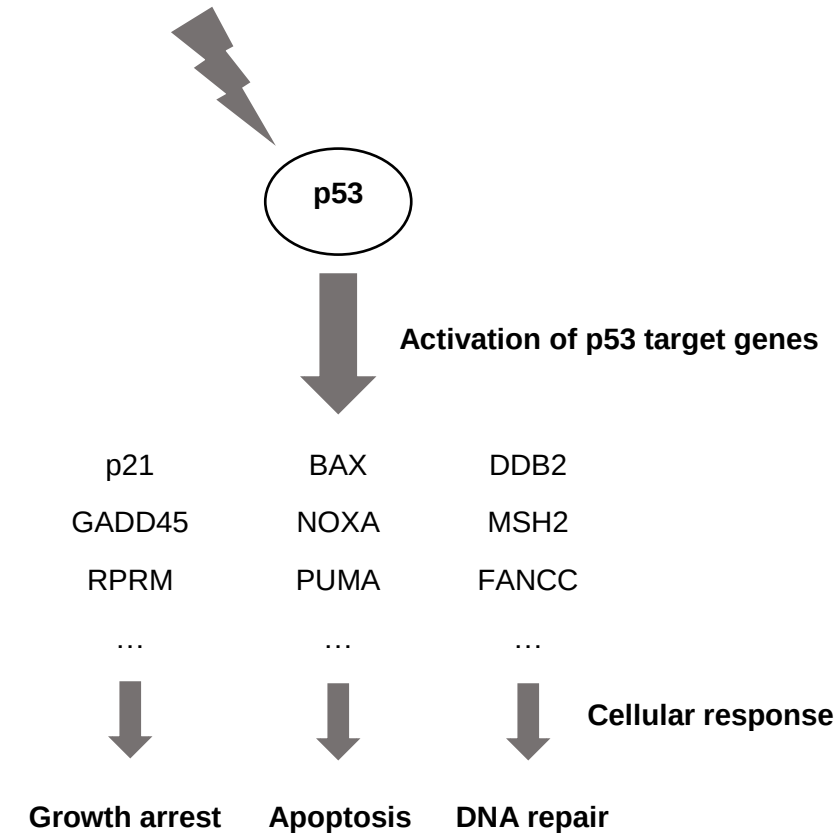

Figure 5 – Schematic representation of some responses mediated by p53 in stress conditions.

There are two p53-related genes, p63 and p73, that are structurally similar and functionally related to p53 (117). p53 family genes have three important structural elements: the N-terminal transactivation domain (TAD), which is the binding-site for positive/negative regulators of gene transcription; the C-terminal oligomerization domain (OD) which is subject to splicing and post-translational modifications; and the central DNA-binding domain (DBD) that binds to response elements of target genes (117–120) (Figure 6). p63 and p73 have an additional conserved domain (SAM), in the C-terminal, which is involved in protein-protein interactions (120) (Figure 6). The high level of sequence similarity in the DBD between p53 protein family members allows p63 and p73 to transactivate p53-responsive genes triggering cell cycle arrest and apoptosis (121,122).

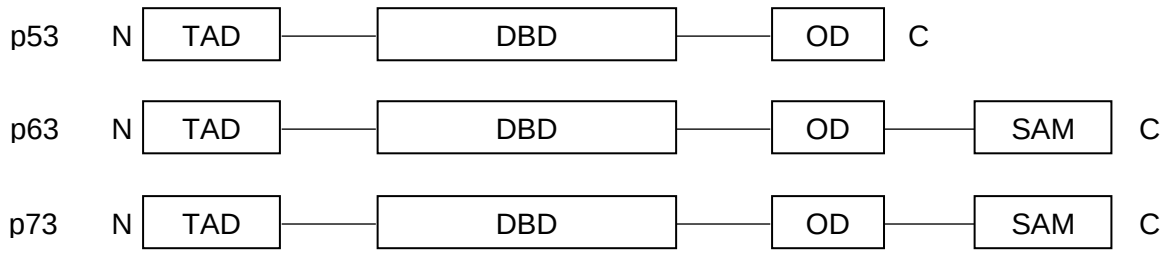

Figure 6 – Some important functional domains of p53 family member genes. TAD - transactivation domain; DBD - DNA-binding domain; OD - oligomerization domain; and SAM - sterile α-motif.

p73 is expressed mainly in two isoforms, ΔN and TA, that differs in their N-terminal region (123–125). ΔNp73 lacks an intact TAD, while retaining the DBD and OD (124,126). Consequently, ΔNp73 can act as dominant negative inhibitor for the functionally active p53 family proteins by competing with them for binding to target genes or by forming hetero oligomers with them (124). Thus, ΔNp73 acts as an oncogene (127,128). On the other hand, TAp73 contains an N-terminal TAD, like p53, and can activate p53 responsible genes (124). Hence, TAp73 acts as a tumor suppressor protein (125,129).

Unlike *TP53*, the *TP73* gene is rarely mutated in cancers, and the functional isoforms are expressed in most human tumors, including melanoma (125,130–133). However, TAp73 is often inactivated in cancer through interaction with mutant p53 and MDM2, the major negative regulator of p53 (134,135). Chemotherapeutic compounds able to trigger the tumor suppressor activity of TAp73, by disrupting the TAp73 interaction with mutant p53 and MDM2, may compensate the lack of a functional p53, increasing chemotherapeutic efficiency and overall survival of patients (134,136).

Nutlin-3, reactivation of transcriptional reporter activity (RETRA), small interfering mutant p53 peptides (SIMPs), prodigiosin, and benzyl isothiocyanate are some compounds capable of inhibiting MDM2-TAp73/mutant p53-TAp73 interactions with antitumor activity (135,137–142). More recently, it was discovered a new TAp73-activating agent named 1-carbaldehyde-3,4-dimethoxyxanthone (LEM2) with a potent antitumor activity (135). This synthetic xanthone was able to activate TAp73, releasing it from its interaction with both MDM2 and mutant p53, and enhancing TAp73 transcriptional activity, cell cycle arrest, and apoptosis (135).

1.5. Aim of the work

Skin cancer affects millions of people with an increasing incidence worldwide, making it a pre-eminent public health concern (1,2). The key for improving the treatment efficacy is to have a better understanding of the pathogenesis of the disease, early diagnosis, identification of individual molecular typing, and development of innovative and effective drugs, as well as their delivery systems.

Topical treatment of skin diseases, such as skin cancer, is very appealing since systemic load of drug and thus also systemic side effects are reduced, when compared to oral or parenteral drug administration (6). Furthermore, the direct drug application in the skin surface avoids major fluctuations of plasma levels caused by repeated administration of quickly eliminated drugs while it also allows to avoid the first passage of drugs through liver after intestinal absorption (6).

LEM2 (Figure 7) is a synthetic xanthone with tested antitumor effect in different cell lines, including melanoma (unpublished work). The antitumor activity of LEM2 has been related with an activation of TAp73, which is a major target in melanoma (135). However, this compound presents poor aqueous solubility, which is often related with poor bioavailability.

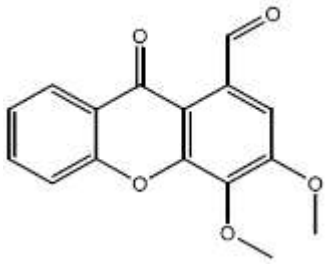

Figure 7 – LEM2 structure.

Encapsulated drugs using nanoparticles are advantageous due to properties, such as improved bioavailability, high stability, controlled drug release, longer blood circulation time, selective organ/tissue distribution, lower required dose, and minimal toxic side effects (143,144). Also, the use of lipid nanoparticles seems to be very interesting for topical delivery of drugs due to their adhesion and occlusive properties in stratum corneum (99,100).

Based on these considerations, the main objectives of this dissertation were:

- Development and optimization of blank (SLN and NLC) and drug loaded (NLC) lipid nanoparticles by different methodologies (hot high-pressure homogenization and

ultrasonication), using Precirol® ATO 5, oleic acid, Tween® 80, Cetrimide®, and LEM2, for topical application;

- Development of an HPLC method for the quantification of LEM2 in formulations;
- Characterization and evaluation of the stability of lipid nanoparticles;
- *In vitro* determination of growth inhibitory effect of drug-loaded lipid nanoparticles;
- Analysis of cell cycle arrest and apoptosis;
- Analysis of protein levels of TAp73 target genes.

Chapter II - Experimental methods

2.1. Materials and equipment

All the materials and equipment used in this work are listed in Tables 5 and 6, respectively.

Table 5 – List of substances and corresponding lot number and manufacturer used in this work.

Substance	Lot number	Manufacturer
Precirol® ATO 5	3092PPD	Gattefossé
Oleic acid	170285-P-1	Acofarma
Tween® 80	090725-C-8	Acofarma
Cetrimide®	DG/001/078/2001	Schutz
Roswell park memorial (RPMI) 1640 medium	00837042	Corning
Phosphate buffered saline (PBS)	8118127	Gibco
Fetal bovine serum (FBS)	830372	Gibco
Trypsin	985425	Gibco
Trypan blue	RNBC7180	Sigma-Aldrich
Sulforhodamine B (SRB)	SLKN5319	Sigma-Aldrich
Trichloroacetic acid	-	Sigma-Aldrich
Tris Base	-	Sigma-Aldrich
RNase A	RNBG5302	Sigma-Aldrich
Propidium iodide (PI)	MKBV9929	Sigma-Aldrich
Radioimmunoprecipitation assay (RIPA) buffer	RNTB2150	Sigma-Aldrich
Ethylene diamine tetra acetic acid (EDTA) -free protease inhibitor cocktail	NKML6130	Sigma-Aldrich

Enhanced chemiluminescence (ECL) Amersham kit t	14774055	GE Healthcare
Kodak GBX developer and fixer	-	Sigma-Aldrich

Table 6 – List of equipment and corresponding model and brand name used in this work.

Equipment	Model	Brand name	Country
Magnetic stirrer	C-MAG HS 7	IKA Labortechnik	Germany
Analytical balance	ABS-N/ABJ-NM	KERN & SOHN GmbH	Germany
High shear homogeneizer	Ultra-Turrax T25	IKA Labortechnik	Germany
High pressure homogenizer	SPCH-10	Stansted Fluid Power	United Kingdom (UK)
Ultrasonicator	VibraCell VCX130	Sonics & Materials, Inc	United States of America (USA)
Particle size/Zeta potential analyzer	ZetaPALS	Brookhaven Instruments Corporation	USA
Chromatograph	UltiMate 3000 Standard HPLC Systems	Dionex Corporation	USA
Spectrophotometer	V-650 UV-VIS Spectrophotometer	Jasco	Japan
Centrifuge	Centrifuge 5810	Eppendorf	Germany
Incubator	Heracell 150i	Thermo Fisher Scientific	USA
Inverted microscope	AE2000	Motic	China
Centrifuge	Heraeus Multifuge X1R Centrifuge	Thermo Fisher Scientific	USA
Microscope	BA210 Binocular	Motic	China
Microplate reader	Synergy MX	Biotek Instruments Inc.,	USA
Cytometer	BD Accuri C6 Flow cytometry	BD Biosciences	USA

2.2. Preparation of lipid nanoparticles

Blank lipid nanoparticles (SLN and NLC) were first developed to assess the suitability of these particles for the encapsulation of the drug. The excipients used and their quantities were chosen mainly based on previous experimental works performed at the Pharmaceutical Technology Laboratory, Department of Pharmaceutical Sciences, Faculty of Pharmacy, University of Porto (145,146). All of them are commonly used to prepare lipid nanoparticles, as shown in Tables 2 and 3.

Table 7 – Lipid nanoparticle formulations produced in this work.

Excipient (w/w %)	Unloaded SLN	Unloaded NLC	LEM2-loaded NLC (1)	LEM2-loaded NLC (2)
Precirol® ATO 5	10.00	7.00	7.00	7.00
Oleic acid	-	3.00	2.99	2.99
Tween® 80	2.50	2.50	2.50	2.50
Cetrimide®	0.10	0.10	0.10	-
LEM2	-	-	0.10	0.10
Water	87.40	87.40	87.31	87.41

The unload lipid nanoparticles were produced by two different methods, hot high-pressure homogenization (HPH) and ultrasonication. They were characterized and stability tests were performed during 60 days. Based on these results, it was decided to encapsulate LEM2 – 0.1% w/w – in NLC by the ultrasonication method. In this case, the amount of oleic acid was reduced to 2.99% (w/w) (Table 7). To perform the *in vitro* studies, were also prepared LEM2-loaded NLCs containing all the components mentioned before but without Cetrimide® by the ultrasonication method (Table 7).

2.2.1. Selection of a binary mixture of solid and liquid lipid for NLC

The selection of an appropriate lipid blend is crucial for successful production of NLC with appropriate physical and chemical characteristics (147). Thus, the solid and liquid lipids were mixed in different ratios – 50:50, 60:40, 70:30, 80:20, and 90:10 – in order to establish the miscibility of both lipids. Lipids were heated at 75ºC and stirred at 200 rpm for 15 minutes using

a magnetic stirrer (C-MAG HS 7, IKA Labortechnik, Germany). The mixtures were kept at room temperature until solidification. A portion of each lipid mixture was placed on a filter paper followed by visual observation. The presence of oil droplets on the filter paper indicates the lack of miscibility between the lipids.

2.2.2. Preparation of lipid nanoparticles

There are several production techniques described in literature to obtain both SLN and NLC (148). Most of them use two basic steps, emulsification and reduction to nanometric size (149). Hot HPH and ultrasonication have already proven its effectiveness in encapsulation of poorly water-soluble drugs and these were the two methods used in this work to prepare lipid nanoparticles (150) (Figure 8). Both methods have been preceded by high shear homogenization (Figure 8). Throughout this phase, the temperature used was about 10°C above the melting point of the Precirol® ATO 5 (50-60°C). All the lipid nanoparticles were produced in triplicate.

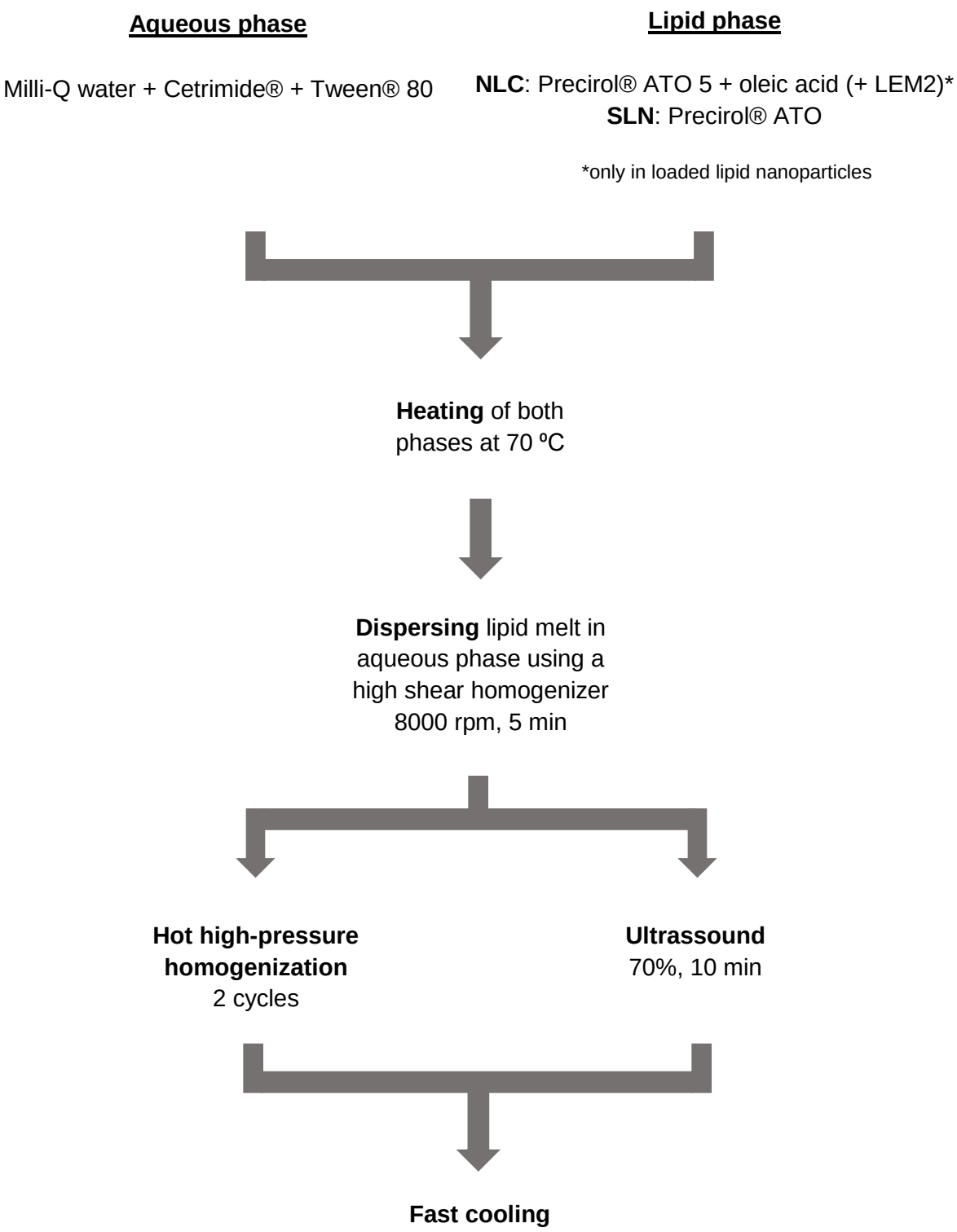

Figure 8 - Schematic overview of the production of lipid nanoparticles, SLN and NLC, by hot HPH and ultrasonication.

High shear homogenization

High shear homogenization is a technique widely used in the production of micro-dispersions. In practice, the lipid melt was dispersed in a hot aqueous phase (both at the same temperature) using a high shear homogenizer (Ultra-Turrax T25, IKA Labortechnik, Germany) at 8000 rpm for 5 minutes (Figure 8). This technique was combined with hot HPH or ultrasonication to reduce the size of the obtained microparticles (Figure 8).

Hot high-pressure homogenization (HPH)

High-pressure homogenization (HPH) is a simple, reliable, and easy to scale up technique for the preparation of lipid nanoparticles (149,151). In hot HPH, the hot pre-emulsion obtained by high shear homogenization is pushed under high pressure, approximately 1500 bar, through a micron size gap (Figure 8). The resulting shear stress and cavitation forces breaks down the accelerated particles to submicron size (151). In this study, the process was repeated 2 times (2 cycles) (Figure 8). The obtained hot nanoemulsion was cooled in an ice bath to form the lipid nanoparticles (Figure 8). The equipment used is shown in Figure 9.

Figure 9 - High pressure homogenizer used to prepare the lipid nanoparticles. SPCH-10, Stansted Fluid Power, UK.

Ultrasonication

Ultrasonication is a fast and highly reproducible method to prepare lipid nanoparticles (149). In this technique, the hot pre-emulsion obtained by high shear homogenization was converted into a nanoemulsion using a sonication probe (6 mm) with power-output amplitude of 70% for 10 minutes. It causes acoustic cavitation leading to disintegration of the lipid phase into smaller particles (152). The obtained hot nanoemulsion was cooled in an ice bath to form the lipid nanoparticles. The equipment is shown in Figure 10.

F**igure 10** – Ultrasonicator used to prepare the lipid nanoparticles. VibraCell VCX130, Sonics & Materials Inc, USA.

2.3. Characterization and stability studies of lipid nanoparticles

An adequate characterization of the lipid nanoparticles is essential for their quality control, but it can be very challenging due to their colloidal size, and their complexity and dynamic nature (151,153,154). Some important parameters that should be evaluated include particle size and polydispersity index (PDI), zeta potential (ZP), organoleptic features, pH, drug encapsulation, among others (151,153,154). There is a wide range of techniques for

characterizing lipid particles. Each one has its benefits and limitations and there is no universally applicable technique for all samples and situations (155). It is relevant to note that particle characterization techniques use a subsampling so it should be as representative as possible of the whole sample (155).

To characterize and study the stability of the lipid nanoparticles produced in this work, the parameters evaluated were particle size and PDI, ZP, organoleptic features, and pH, after their production, and after 30 and 60 days. The techniques used will be briefly described below. During this period, the lipid nanoparticles dispersions were stored in closed glass vials at 4°C. LEM2-loaded NLC formulations were also stored and evaluated likewise unloaded lipid nanoparticles.

2.3.1. Organoleptic characteristics

Organoleptic analysis of lipid nanoparticles dispersions allows a rapid assessment of formulation quality, since variations in their appearance/homogeneity are indicative of poor raw materials quality or problems during production and storage. The organoleptic examination of the lipid nanoparticles dispersions was performed by visual examination.

2.3.2. Particle size measurements

The mean particle size is considered the most important physical property of particle samples that has a direct influence on the physical stability of lipid nanoparticles (153). For particle size and size distribution measurements the dynamic light scattering (DLS) technique was used.

Dynamic light scattering (DLS)

Dynamic light scattering (DLS) is one of the most popular methods, well-established for the measurement of sizes and size distribution of nanoparticles, with the sensitivity of 1 nm to 10 µm (155,156). Some advantages of using DLS include fast analyses, small amount of sample required, and, because it is non-invasive, allows complete sample recovering (155).

DLS measures the variation of the intensity of scattered light caused by the movement of the particles. When the sample containing lipid nanoparticles is illuminated with a laser, the

intensity of the scattered light changes in very short time scales at a rate that depends on the particle size (Figure 11) (155,157,158).

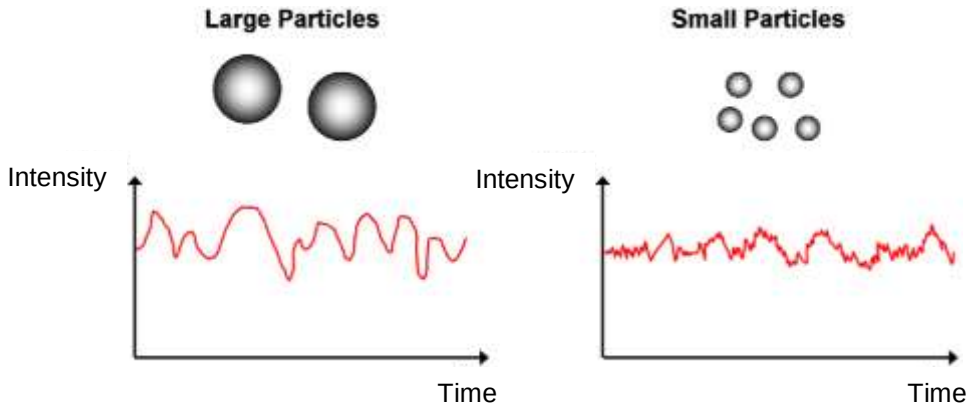

Figure 11 – Illustration of the effect of particle size on the variation of the intensity of scattered light (157).

Small, rapidly diffusing particles have a greater variation of intensity of the scattered light, whereas larger particles have a minor one (Figure 11). Thereby, the analyses of these intensity fluctuations depend on the speed of the Brownian motion and the particle size is then obtained using the Stokes-Einstein relationship (155,158). It should be noted that the particle diameter obtained by this technique is named hydrodynamic diameter and refers to how a particle diffuses within a fluid (155).

As mentioned before, DLS also measures the particle size distribution defined by PDI value. It ranges from 0.0 for a perfectly uniform sample, to 1.0 for a highly polydisperse sample with multiple particle size populations (159). In drug delivery applications using lipid-based carriers, a PDI of 0.3 and below is acceptable, indicating a homogenous population of lipid vesicles (159–161).

Particle size measurements and PDI values were obtained using a ZetaPALS (Brookhaven Instruments, USA) (Figure 12). Before the measurements, all samples were diluted by adding 20 µl of each sample and 1 ml of milli-Q water to a cuvette. Dilution of the original nanoparticle dispersions in water is necessary to obtain suitable scattering intensity from DLS measurements.

Figure 12 – ZetaPALS (Brookhaven Instruments, USA) used for particle sizes measurements and zeta potential (ZP) values.

2.3.3 Zeta potential (ZP) determination

When a colloidal particle develops a net surface charge, oppositely charged ions accumulate around the charged particle surface (162). This new arrangement leads to the formation of an electrical double layer around the particle (Figure 13) (162,163). It consists of two parts: an inner layer named the Stern layer (where ions are tightly bound with the particle) and the outer layer called the diffuse layer (where ions are less strongly associated) (Figure 13) (163–165). A theorical boundary lies inside the diffuse layer in which ions and the charged particle create a stable entity whereas ions further the boundary remain associated with the bulk fluid (162). The potential at this boundary is known as ZP, a potential difference between the bulk fluid and the layer of fluid containing oppositely charged ions that is associated with the particle (Figure 13) (162).

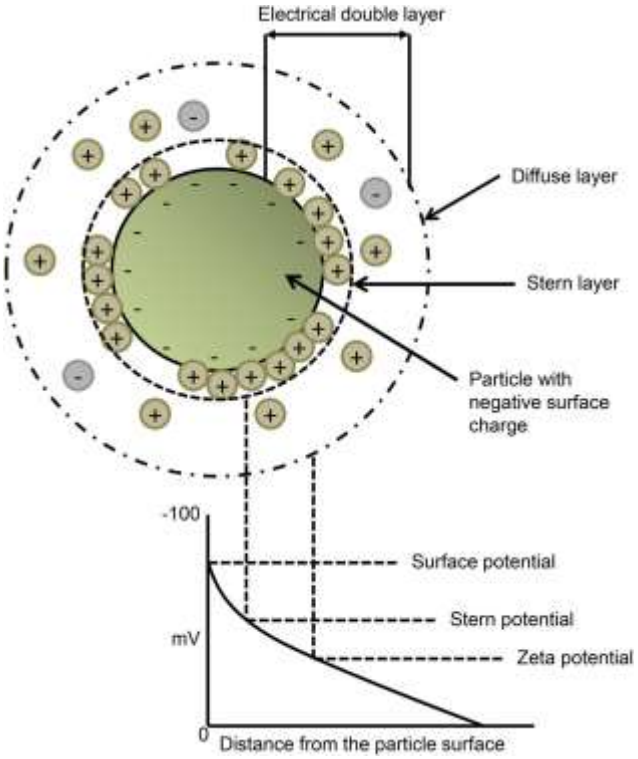

Figure 13 – Schematic representation of zeta potential (ZP) (161).

ZP is considered an important parameter in the predictions for long term stability of the formulations (166). Usually, dispersions with ZP values of ±0–10 mV are considered highly unstable, ±10–20 mV are relatively stable, ±20–30 mV are moderately stable, and > ± 30 mV are highly stable (167). The most significant factor that affects ZP is the pH of the medium (168,169).

The electrophoretic light scattering (ELS) was the technique used to evaluate this parameter.

Electrophoretic light scattering (ELS)

The electrophoretic light scattering (ELS) technique is used to measure the electrophoretic mobility of the dispersed particles or molecules in solution. In ELS, the velocity of particles is determined in a similar mode as in DLS, but under an applied electric field. In practice, the dispersion is inserted into a cell containing two electrodes causing the charged particles to migrate towards the oppositely charged electrode (Figure 14) (155,170). The magnitude of particle velocity is deduced from Doppler shift of laser light scattered from particles as they

move (168). Since the velocity of the particle is proportional to its charge in an electrical field, it is possible obtain its ZP value (168).

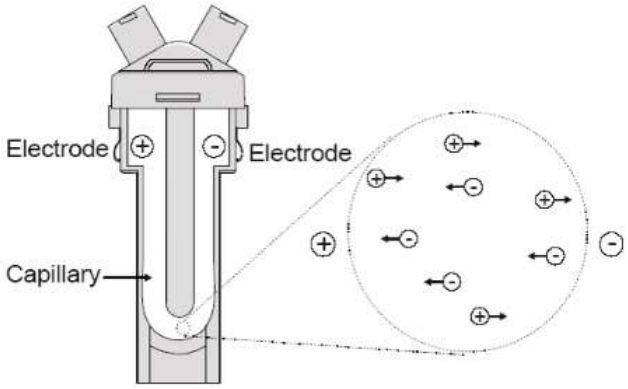

Figure 14 – Illustration of the movement of particles in electrophoretic light scattering (ELS) technique (169).

This technique is frequently used in combination with DLS in a single equipment, being able to measure both particle size and ZP with the same instrument (168).

The ZP values were determined by the same equipment used to obtain the size of the lipid nanoparticles, a ZetaPALS (Brookhaven Instruments, USA) (Figure 12). Before the measurements, all samples were diluted by adding 20 µl of each sample and 1 ml of milli-Q water to a cuvette.

2.3.4. pH

The pH of the colloidal dispersions of lipid nanoparticles may not correspond to the pH of the corresponding final preparation (e.g. cream, gel). However, this evaluation is relevant for assessing the stability of the preparations. The pH values were measured with Universal indicator paper.

2.4. Encapsulation efficiency (EE)

The encapsulation efficiency (EE) of LEM2-loaded NLC was determined by high-performance liquid chromatography (HPLC).

High-performance liquid chromatography (HPLC)

High performance liquid chromatography (HPLC) is an analytical technique used for the separation, identification, and quantification of the components in a mixture (171). HPLC is the most versatile, fastest, and safest chromatographic method for the quality control of drug components (172). Basically, HPLC pumps at high pressure a sample (analyte) dissolved in a solvent (mobile phase) through a column with an immobilized chromatographic packing material (stationary phase) (173). Each individual component of the sample has different affinity with mobile and stationary phases and, consequently, they will migrate down the column at different speeds and times (173). Analytes with strongest interactions with the mobile phase will migrate faster through the column, while analytes with greater affinity for the stationary phase will migrate slowly through the column (172). The time at which a specific component elutes (comes out of the end of the stationary phase) is named retention time and is unique for each component at specific conditions (171,172). The separation of compounds in a sample can be accomplished via an isocratic elution or via a gradient elution; in the first one, the composition of the mobile phase remains constant while in the second one the composition of the mobile phase is changed over the course of the separation (173). At the exit of the column, the mobile phase passes through a detector (e.g. UV-absorbance detector), which creates a signal correlating to the amount of analyte emerging from the column (172–174). The representation of these signals over the time constitutes the chromatogram. The peaks in the chromatograms provide qualitative and quantitative information about the analyzed sample (175). The qualitative information is obtained from the retention times and the quantitative information from the areas, or height, of the peaks (175).

2.4.1. HPLC method development and optimization

The sensitivity of the HPLC method which uses UV detection depends upon the proper selection of the wavelength. A solution of LEM2 in ethanol (50 µg/ml, see 2.4.2. section) was prepared and using a spectrophotometer (Jasco V-650 UV-VIS Spectrophotometer, Japan) the UV spectrum of the drug was performed with the wavelength ranging from 200 to 400 nm. The wavelength used to detect the drug by HPLC method was 242 nm, which is a wavelength of maximum absorbance. The HPLC method was developed using an UltiMate 3000 Standard HPLC Systems (Dionex Corporation, USA).

The selection of suitable stationary and mobile phases can offer a simple and quick analytical HPLC procedure (176). Take into consideration methodology already developed and described in (178), were conducted tests under the analytical conditions described with slight changes. The stationary phase used was a C18 column (Thermo Fisher Scientific Acclaim™ 120 C18) with a particle size of 5 µm, with a length of 25 cm and internal diameter of 4.6 mm. The choice of the mobile phase is also important since it runs the solute through the stationary phase, thus the solvent in the mobile phase should be pure, avoiding any material that can degrade the column or HPLC device. Common mobiles phases used include any miscible combination of water or organic liquids and the most common are methanol and acetonitrile (172). Many combinations of water and acetonitrile – 0:100; 5:95; 10:90; 15:85; 20:80; 25:75; 30:70; 35:65; 40:60; and 45:55 – were tested being chosen the ratio 40:60. It was used an isocratic elution with a flow rate of 1.0 ml/min. Comparing with a gradient elution, an isocratic elution is less expensive so its preferred for simple samples with few components (177).

The chromatographic conditions used to determine the encapsulation efficiency of LEM2-loaded NLC are summarized in Table 8.

Table 8 – Chromatographic conditions used to determine the encapsulation efficiency of LEM2-loaded NLC.

Chromatographic conditions	
Injection volume	20 µl
UV detection	242 nm
Flow rate	1.0 ml/min (isocratic elution)
Mobile phase composition	Water: acetonitrile 40:60 v/v
Stationary phase	C18 column (5 µm, 25 cm x 4.6 mm)
Temperature	25ºC
Run time	6-7 min

2.4.2. Preparation of standard solutions

A stock solution containing 50 µg/ml of LEM2 in ethanol was prepared. Six standard solutions – 5, 10, 20, 30, 40, and 48 µg/ml – were prepared by diluting the adequate amount of stock solution with ethanol in a 10 ml volumetric flask.

2.4.3. Validation of the HPLC method

The validation of an analytical method is important to demonstrate that the method developed is suitable for its intended purpose and it works in a reproducible manner when used by different operators, employing the same equipment in the same/different laboratories (178). For pharmaceutical HPLC methods validation, guidelines from the US Food and Drug Administration (FDA), US Pharmacopeia (USP), and International Conference on Harmonization (ICH) provides a framework for performing such validation (179). The HPLC method developed in this work was validated in accordance with ICH guideline Q2 (R1): "Validation of analytical procedures: text and methodology" (180). For identification tests and assay procedures, typical parameters recommended by this entity are accuracy, precision, specificity, linearity, and range (Figure 15) (181,182). System suitability test parameters are also essential during method validation (179,180).

Type of analytical procedure characteristics	IDENTIFICATION	TESTING FOR IMPURITIES quantitat.	 limit	ASSAY - dissolution (measurement only) - content/potency
Accuracy	-	+	-	+
Precision				
Repeatability	-	+	-	+
Interm.Precision	-	+ (1)	-	+ (1)
Specificity (2)	+	+	+	+
Detection Limit	-	- (3)	+	-
Quantitation Limit	-	+	-	-
Linearity	-	+	-	+
Range	-	+	-	+

- signifies that this characteristic is not normally evaluated

+ signifies that this characteristic is normally evaluated

(1) in cases where reproducibility (see glossary) has been performed, intermediate precision is not needed

(2) lack of specificity of one analytical procedure could be compensated by other supporting analytical procedure(s)

(3) may be needed in some cases

Figure 15 – Parameters of interest during HPLC method validation, considering the goal of the analytical procedure (180).

System suitability

Before performing any validation experiments, it is important to ensure that the HPLC system can provide data of acceptable quality (179). System suitability tests are based on the concept that the equipment, analytical operations, electronics, and samples form an integral system that can be evaluated as a whole. Therefore, system suitability is the checking of a system to ensure system performance before or during the analysis of the analytes (179). Parameters such as theorical plate number (is a measure of column efficiency, N), tailing factor (is a measure of peak tailing, T), capacity factor (is an indication of how long the analyte is retained on the chromatographic column, k'), and injection repeatability (coefficient of variation (CV) of retention time and peak area for a minimum of five repetitions) need to be determined and compared with the specifications set (183). The CV was calculated by the ratio to the standard deviation with mean values and the k' was calculated as follows:

$$k' = \frac{t_R - t_0}{t_0}$$

where t_R is the retention time of LEM2 and t_0 represents the unretained peak time. The other parameters were calculated and provided directly by the software.

The system suitability of the method was studied by injecting six replicates of the LEM2 standard solution 30 µg/ml and calculating the parameters mentioned before.

Specificity

In HPLC method, developing a separation involves demonstrating specificity, which is the ability of an analytical method to differentiate and quantify the analyte in the presence of all potential sample components. The response of the analyte in test mixtures containing the analyte and all potential components (excipients, placebo formulation, impurities, among others) should be compared with the response of a solution containing only the analyte (179,180).

This parameter was determined by comparing the chromatograms of LEM2 standard solution 30 µg/ml and the supernatant of a blank NLC formulation (obtained as described in section 2.3.5.4.).

Linearity and range

The linearity of the method is its ability to obtain test results that are directly proportional to the concentration of analyte in a sample over the working range (178,179). Range is the interval between the higher and lower levels of analyte that have been demonstrated to be determined with precision, accuracy, and linearity using the method as written (179). The ICH guidelines recommend a minimum of five concentration levels, along with certain minimum specified ranges (180). For assay procedures, the minimum specified range is from 80-120% of the target concentration (180). Acceptability of linearity data is usually judge by examining the correlation coefficient (R^2) and residual sum of squares (RSS) of the linear regression line for the response versus concentration plot (180).

This parameter was determined by the calculation of a regression line from the peak areas plot *versus* LEM2 concentration of the standard solutions (5 - 48 µg/ml, 12.5 - 120% of target concentration) using the minimum squares method. The resulting plot slope, intercept, R^2 and RSS were used to estimate the quality of the curve. It was also done an analysis of the deviation of the real data points from the regression line (residual plot), since it is also useful for the evaluation of linearity. The standard solutions were injected in triplicate in increasing order of concentration.

Precision

Precision expresses the nearness of agreement between a group of measurements got from multiple sampling of the same homogenous sample under the similar analytical conditions (179). According to ICH guidelines, precision may be performed at three levels, namely repeatability, intermediate precision, and reproducibility (180). In this work, only repeatability was studied. Repeatability is the result of the method operating over a short period of time in the same circumstances (intra-assay precision) (179). It should be determined from a minimum of nine determinations covering the specified range of the procedure (three concentration levels in triplicate), or from a minimum of six determinations at 100% of the target concentration (180). The precision is expressed and evaluated through CV (180).

The precision of the method was studied by assaying three concentration levels in triplicate – 30, 40, and 48 µg/ml – during the same day and under the same experimental conditions and the CV values of peak areas were calculated.

Accuracy

The accuracy of a measurement is defined as the closeness of the measured value by the analytical method to the value accepted as true (179). Accuracy can be determined by spiking analyte in blank matrices (179). The added amount corresponds to the true value. For assay methods, the ICH guidelines recommend preparing spiked samples in triplicate at three concentration levels over the specified range (180). Accuracy is represented as percent recovery by the assay of know added amount of analyte in the sample (180).

To study the accuracy of the method, the procedure recommended by ICH guidelines was not followed due to the low amount of drug available. Instead, it was added standard solution 40 µg/ml to a blank NLC dispersion as described in 2.3.5.4., swapping ethanol for standard solution. The process was repeated for three formulations and the recovery percentage was calculated as follows considering the dilution factor associated to the procedure:

$$Recovery\ (\%) = \frac{amount\ of\ LEM2\ recovered\ (\mu g/ml)}{amount\ of\ LEM2\ added\ (\mu g/ml)} \times 100$$

2.4.4. Encapsulation efficiency (EE)

Separation of the free drug from that incorporated in lipid nanoparticles is a key step in determining the encapsulation efficiency (EE). The amount of incorporated drug can be determined directly or indirectly by many techniques. In a direct method, the lipid nanoparticle dispersion is diluted and filtered so that the unincorporated drug is removed and only lipid nanoparticles remain. Thereafter, the drug is released from the lipid nanoparticles by the addition of an organic solvent like ethanol, methanol, and others.

To determine the amount of LEM2 encapsulated in NLC, a procedure described in (186) was performed with slightly changes. The freshly prepared LEM2-loaded NLC dispersion (1 ml) was diluted with milli-Q water (4 ml). Then, 1 ml of the diluted formulation was added to a 4 ml of ethanol and thoroughly mixed to extract the drug from the lipid matrix. The mixture was centrifuged (Eppendorf Centrifuge 5810) at 5000 rpm for 10 minutes. The supernatant was filtered through a 5 µm cellulose nitrate syringe filter (Biotech GmbH, Germany) to remove unencapsulated drug crystals and the amount of the drug in the filtered supernatant was

measured by HPLC. EE was calculated as follows considering the dilution factor associated to the procedure:

$$EE(\%) = \frac{amount\ of\ LEM2\ in\ the\ filtered\ formulation\ (\mu g/ml)}{total\ amount\ of\ LEM2\ (\mu g/ml)} \times 100$$

2.5. Cell culture

2.5.1. Tumor cell line and growth conditions

The human melanoma A375 cell line was obtained from American Type Culture Collection (ATCC, Rockville, MD, USA). The cells were maintained in Roswell Park Memorial (RPMI) 1640 medium supplemented with 10% fetal bovine serum (FBS), at 37^0C with 5% CO_2. Cells were subcultured every 2-3 days.

2.5.2. Routine laboratory procedures

Cell subculture

In adherent cultures, when the cells occupy all the disposable substrate and have no room left for expansion (i.e., reach confluence), cell proliferation is extremely reduced. In order to keep them at an optimal density for continuous growth and to stimulate further proliferation, the culture must be divided, and fresh medium supplied. Subculturing (or passaging) consists of removing the medium and transferring the cells from a previous culture into fresh growth medium, a procedure that allows the further propagation of the cell line.

The cultures were observed using an inverted microscope (Motic AE2000 Inverted Microscope, China) to assess the degree of cell confluency and to confirm the absence of microbial contamination. When cells reached around 80% confluence, they were subcultured. Initially, the medium was aspirated, and the cells washed with phosphate buffered saline (PBS). Then, trypsin was added to detach the adherent cells from the flask and the flask was left in the incubator at 37^0C for 3 minutes. After cell detaching, it was added medium to neutralize the trypsin. The culture suspension was transferred to a sterile tube and was centrifuged at 1500

rpm for 5 minutes (Thermo Fisher Scientific Heraeus Multifuge X1R Centrifuge, USA). The supernatant was removed, and the pellet was resuspended in fresh medium. It was removed a sample to determine the total number of cells using a hemacytometer (Neubauer chamber) and the desired number of cells was used to start a new cell culture flask or used for cellular assays in culture plates. The flasks/plates were incubated at 37^0C, 5% CO_2 in air atmosphere. This protocol is schematically represented in Figure 16 (184).

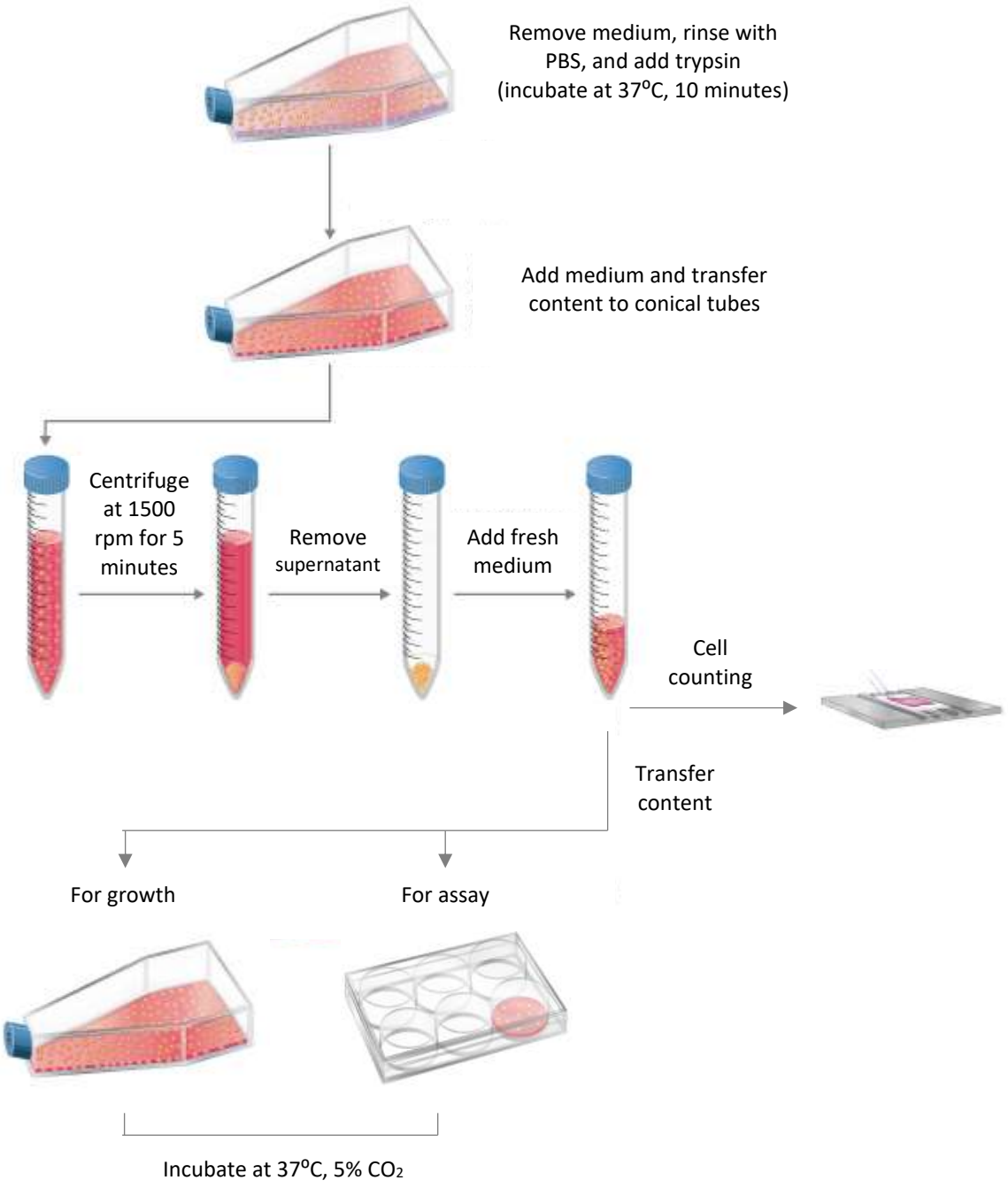

Figure 16 – Schematic representation of cell subculture protocol. Adapted from (182).

Cell counting

To count the cells a hemocytometer was used, namely a Neubauer chamber. It is composed of 2 chambers, each one divided into nine squares with the dimension of 1 x 1 mm. A cover glass was supported 0.1 mm over these squares so that the total volume over each one was 1.0 mm^2 x 0.1 mm or 0.1 mm^3 or 10^{-4} cm^3. Thus, the cell concentration per milliliter will be the average count per square x 10^4.

First, 10 µl of cell suspension was added to 90 µl of trypan blue and then placed in a Neubauer chamber. The Neubauer chamber was placed in the microscope under a 10X objective. Non-viable cells stain blue while viable cells remain opaque. The viable cells found in the four large corners squares were counted (Figure 17). To calculate the cell concentration, the average number of viable cells in the four squares was multiplied by 10^4 to get the number of cells per milliliter. Therefore, this number was multiplied by the dilution factor from the trypan blue addition. This final value corresponds to the number of viable cells per milliliter in the original cell suspension.

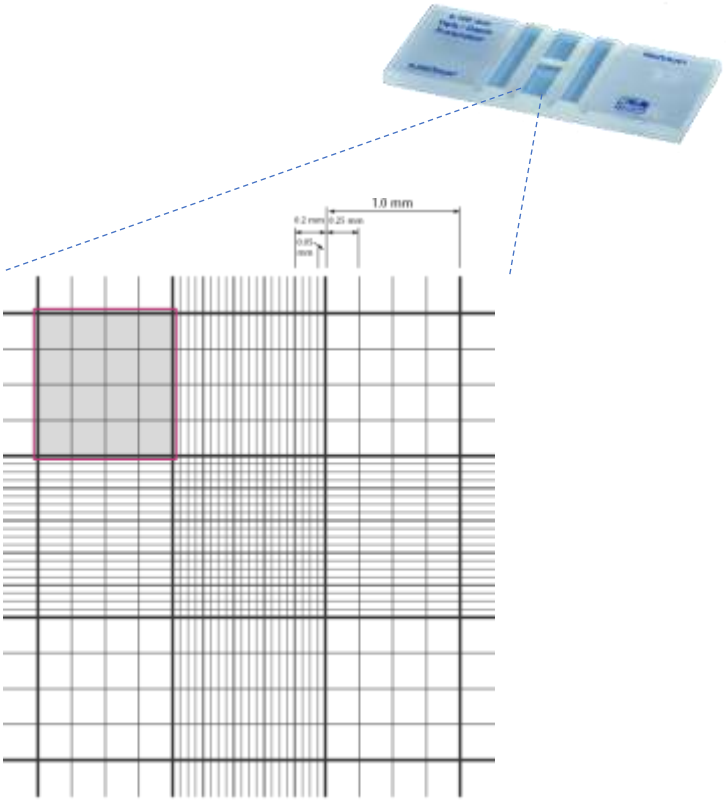

Figure 17 – Neubauer chamber.

2.5.3. *In vitro* assays

To study the effect of lipid nanoparticles on cell growth, both formulations of LEM2-loaded NLCs were used. For the subsequent studies only the formulation without Cetrimide® was used. All the procedures in this section were performed as described in (185).

2.5.3.1 Effect of lipid nanoparticles on cell growth

Cells were seeded in 96-well plates at a final density of 4.5 x 10^3 cells/well. Two types of plates were prepared, one to determine cell growth fixed at the time of the addition of the lipid nanoparticles to cells (T0) and the other to determine the cell growth at 48 hours after treating the cells with the lipid nanoparticles (T48). Cells were incubated for 24 hours to allow them to adhere. Then, cells were treated with serial dilutions of LEM2-loaded and blank lipid nanoparticles, ranging from 5 to 0.010 µM LEM2, for 48 hours. The solvent of lipid nanoparticles (water) was included as control. The effect of the lipid nanoparticles was analyzed using the sulforhodamine B (SRB) assay. The SRB dye is used as a quantitative indicator of the protein content of the cell culture and this content is proportional to the cell density. After the incubation, cells were fixed by adding 25% trichloroacetic acid (Sigma-Aldrich, Sintra, Portugal) for 1 hour at 4°C, stained with 0.4% SRB (Sigma-Aldrich, Sintra, Portugal) for 30 minutes, and washed with 1% acetic acid solution. Then, the bound dye was solubilized with 10 mM Tris Base and the absorbance was measured at 510 nm using a microplate reader (Biotek Instruments Inc., Synergy MX, USA). The concentration that caused 50% inhibition of the cell growth (GI_{50}) was determined for all tested lipid nanoparticles. The plate design is shown in Figure 18.

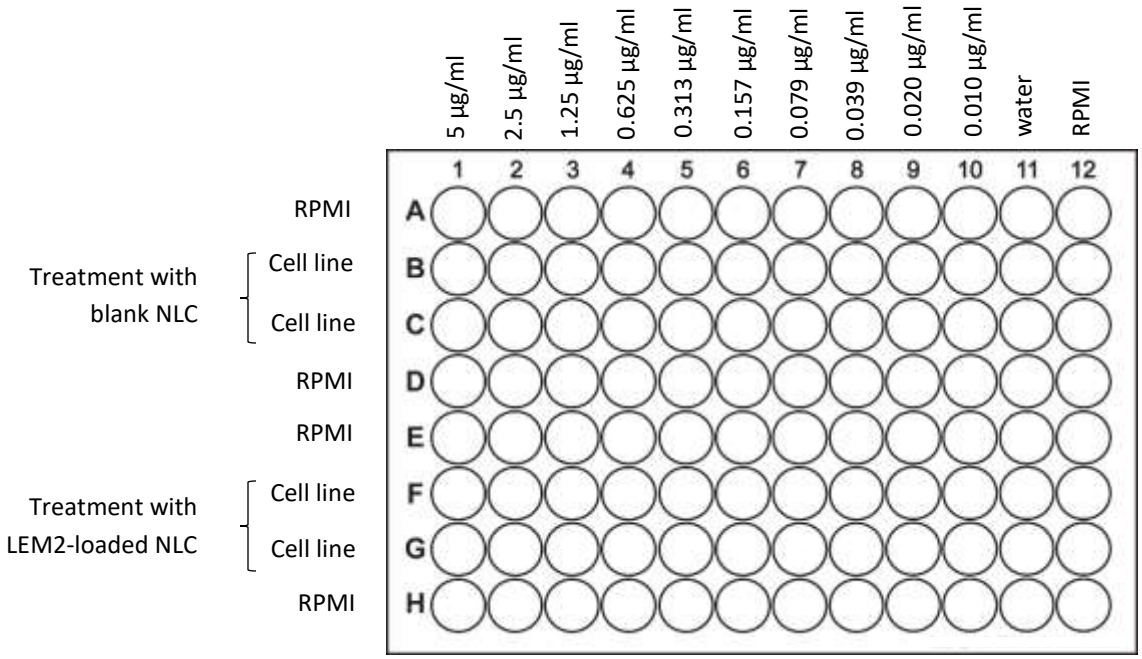

Figure 18 – Plate design used to study the effect of lipid nanoparticles on A375 melanoma cells growth.

2.5.3.2. Analysis of cell cycle and apoptosis in tumor cell lines

Cells were seeded in a 6-well plate at a final density of 1.5 x 10^5 cells/well and incubated at 37^{0}C and 5% CO_2 for 24 hours to adhere. Then, the cells were treated with LEM2-loaded NLC (formulation without Cetrimide®) at 1.0 µM (GI_{50} concentration) and 2.0 µM (two-fold GI_{50} concentration), or water only (control) for 24 or 48 hours for cell cycle or apoptosis analyses, respectively.

For cell cycle analyses, after trypsinization and centrifugation, cells were fixed with ice-cold 70% ethanol for 15 minutes. Later, cells were incubated with RNase A (200 µg/mL; Sigma–Aldrich, Sintra, Portugal) at 37^{0}C for 15 minutes, and further incubated with propidium iodide (PI) (0.5 mg/mL; Sigma-Aldrich, Sintra, Portugal) for 30 minutes. DNA content of the cells was analyzed using flow cytometry (BD Accuri™ C6 Flow cytometry, USA) by analyzing at least 30 000 events per sample. The percentage of cells in the different phases of cell cycle were determined using the FlowJoX 10.0.7 (Treestar, USA) software.

Apoptosis analyses were performed using the trypan blue assay. After trypsinization and centrifugation, 10 µl of cell suspension was added to 12 µl of trypan blue and then placed in a

Neubauer chamber. Non-viable cells (in blue) and viable cells (opaque) were counted in the four large squares of the chamber using a microscope (10X objective). To obtain the percentage of cell death induced by LEM2-loaded NLC, the average number of dead cells was divided by the average number of total cells and multiplied by 100.

The plate design used is shown in Figure 19.

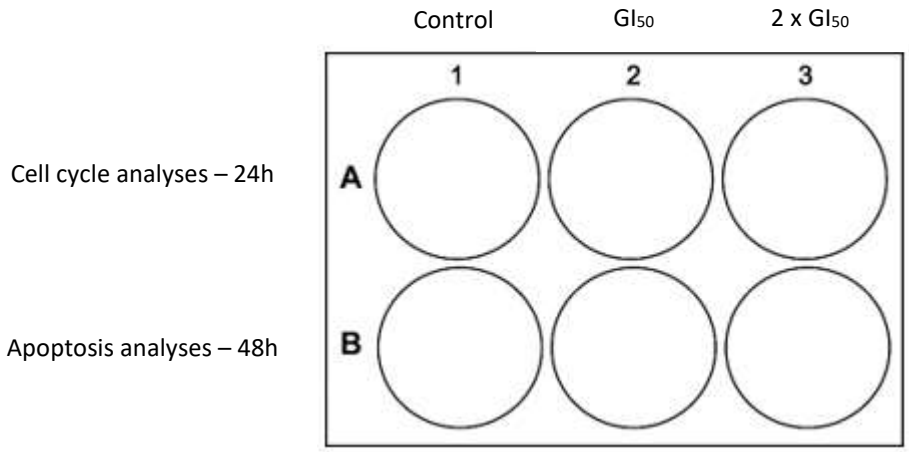

Figure 19 – Plate design used to study the effect of lipid nanoparticles on cell cycle and apoptosis in A375 melanoma cells.

2.5.3.3. Analyses of protein expression (western blot)

The western blot is used to detect specific proteins from a complex mixture of proteins extracted from cells (186,187). The first step is to separate the proteins in a sample using gel electrophoresis. Then, the separated proteins are transferred to a membrane, usually of nitrocellulose or polyvinylidene difluoride (PVDF). This membrane has to be blocked to prevent any nonspecific binding of antibodies to the surface of the membrane. Usually, the transferred protein is then probed with a combination of antibodies (188). One antibody specific to the protein of interest (primary antibody) and another one specific to the host species of the primary antibody (secondary antibody). The secondary antibody is conjugated with labelled chemiluminescent or fluorescent molecule, which will produce a detectable signal. Finally, the intensity of this signal reflects antigen/antibody binding (189,190). A schematic representation of the procedure is shown in Figure 20.

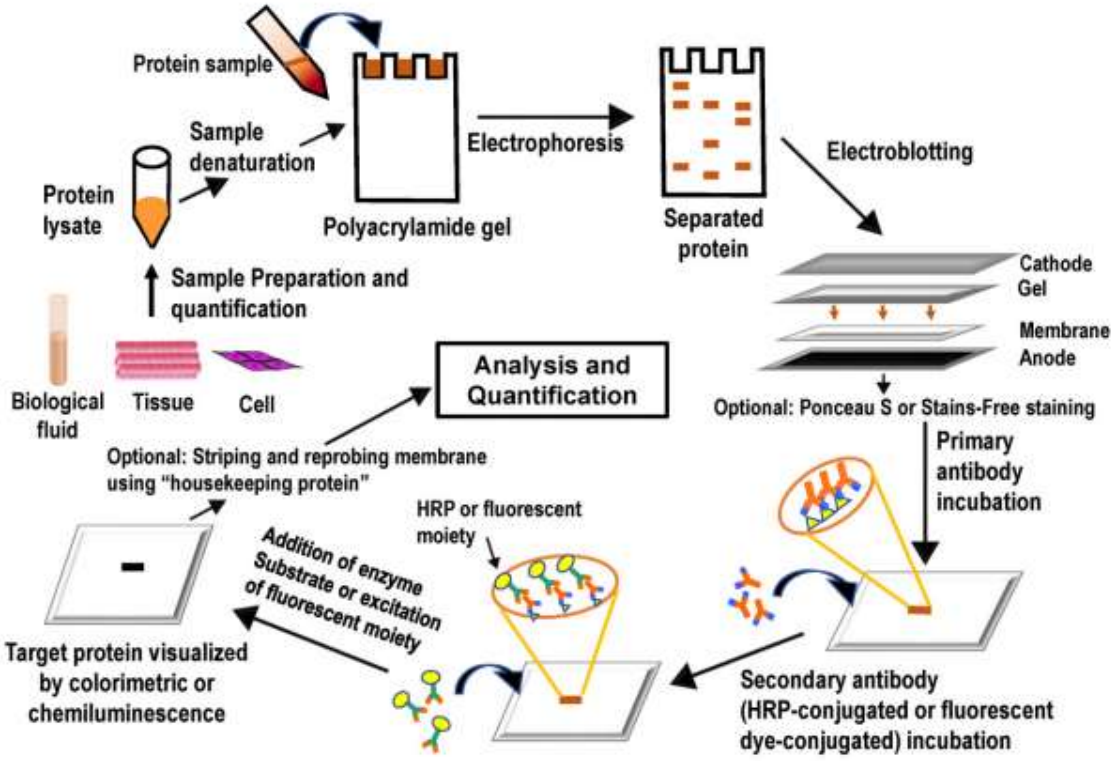

Figure 20 – Schematic representation of western blot technique (185).

To analyze the protein expression in cell lines, cells were seeded in 6-well plates at a final density of 1.5 x 10^5 cell/well and incubated for 24h, at 37^0C, 5% CO_2. Cells were then treated with LEM2-loaded NLC (formulation without Cetrimide®) at 1.0 and 2.0 µM, or water only for 24 hours. After treatment, the proteins were extracted by lysing the cells with radio-immunoprecipitation assay (RIPA) buffer (Sigma-Aldrich, Sintra, Portugal) in the presence of an ethylene diamine tetra acetic acid (EDTA) -free protease inhibitor cocktail (Sigma-Aldrich, Sintra, Portugal) for 1 hour at 4^0C (to prevent proteolysis, dephosphorylation, and denaturation of the proteins) with agitation. The supernatants, corresponding to cellular proteins, were obtained after centrifugation at 13000 rpm, at 4^0C, for 10 minutes. The total cellular protein was quantified using a bicinchoninic acid (BCA) assay and bovine serum albumin (BSA) as protein standard. After protein quantification, proteins (40 µg) were separated according to their molecular weight on 10% sodium dodecyl sulphate-polyacrylamide gel (SDS-PAGE) at 120 volts for 1 hour and 30 minutes and transferred to a nitrocellulose membrane (Protan, VWR, Carnaxide, Portugal) at 100 volts for 1 hour and 30 minutes. The membrane was blocked with tris-buffered saline solution with 0.1% Tween® 20 (TBS-T) containing 5% milk (w/v), for 1 hour

with agitation at room temperature. The membrane was then incubated overnight at 4^0C with the following primary antibodies: rabbit anti-p21 (1:100), mouse anti-MDM2 (1:150), mouse anti-PUMA (1:50), mouse anti-TAp73 (1:100), mouse anti-BAX (1:100), and mouse anti-BCL-2 (1:200), all from Santa Cruz Biotechnology (Frilabo, Porto, Portugal). The membrane was washed with TBS-T and was incubated for 2 hours at room temperature with the corresponding secondary antibodies: anti-rabbit horseradish peroxidase (HRP)-conjugated secondary antibody from Santa Cruz Biotechnology (Frilabo, Porto, Portugal) for p21 detection and anti-mouse horseradish-peroxidase (HRP)-conjugated secondary antibody from Abcam (Cambridge, United Kingdom). For loading control, a mouse anti- glyceraldehyde 3-phosphate dehydrogenase (GAPDH) antibody from Santa Cruz Biotechnology (Frilabo, Porto, Portugal) was used. The signal was detected with the enhanced chemiluminescence (ECL) Amersham kit t from GE Healthcare (VWR, Carnaxide, Portugal) and the Kodak GBX developer and fixer (Sigma-Aldrich, Sintra, Portugal). The intensity of the bands was quantified using the Bio-Profil Bio-1D++ software (Vilber-Lourmat, Marne La Vallée, France).

2.6. Statistical analyses

The results were statistically analyzed using independent Student's *t-test* and one-way analysis of variance (ANOVA) to compare two or multiple groups, respectively, after confirmation of normality and homogeneity of the variance through Shapiro-Wilk and Levene tests. Differences between more than two groups were compared using post hoc test (Tukey HSD). Samples were analyzed using a significance level of 95% ($\alpha = 0.05$). All statistical analyses were performed with the SPSS software (v 21.0; IBM, Armonk).

Chapter III – Results and Discussion

3.1. Unloaded lipid nanoparticles

3.1.1. Formulation optimization

Lipid nanoparticles are mainly composed of lipids (solid in the case of SLN, and a mixture of solid and liquid in the case of NLC), emulsifier(s), and water. SLN formulations are normally composed of 0.1% to 30% (w/w) of solid lipids dispersed in an aqueous medium, stabilized with 0.5% to 5% (w/w) of surfactant (28). To obtain the lipidic blend of NLC, the solid lipid must be mixed with the liquid lipid preferably in a ratio of 70:30 up to a ratio of 99.9:0.1 (28,147). It is important to ensure that both lipids are miscible at the desired concentration, meaning that macroscopic phase separation cannot occur at a temperature below the melting point of the lipid (147).

The composition of lipid nanoparticles has been adopted from the previously reported studies performed at Faculty of Pharmacy, University of Porto (146,147). Unloaded lipid nanoparticles (SLN and NLC) were first developed to assess the suitability of these particles for the encapsulation of the drug, using the following excipients: Precirol® ATO 5 (solid lipid), oleic acid (liquid lipid), Tween® 80 (surfactant), Cetrimide® (preservative), and water. Precirol® ATO 5 and oleic acid are lipids commonly used to prepare lipid nanoparticles, besides they are recognized as GRAS substances which means that they are approved in Europe and in the USA for clinical use, as well as Tween® 80 (191). The use of oleic acid in NLC formulations is also advantageous because this component can function as a skin penetration enhancer, increasing the flux of drugs through the skin (192–194). Cetrimide® was included in the formulations to prevent any contamination during the storage.

Before lipid nanoparticles preparation, namely NLC, the compatibility of Precirol® ATO 5 and oleic acid was assessed by visual examination of cooled samples of the lipidic mixture onto filter paper. The results showed that both lipids are miscible in all proportions tested, with no oil droplets in the filter paper (Appendix I). The consistency of the cooled samples was also analyzed. The cooled samples corresponding to the proportions 50:50 and 60:40 (solid lipid: liquid lipid) showed a semisolid consistency, whereas the others showed solid consistency. The

ratio 70:30 was the chosen one to prepare NLC, since it is the proportion with higher amount of liquid lipid in which the different mixtures remain with a solid consistency (note that the lipid matrix should remain solid at body temperature). The final formulations of unloaded lipid nanoparticles prepared are shown in Table 7 previously presented in 2.2.

The unloaded lipid nanoparticles were prepared by two different methods, ultrasonication and hot HPH, in order to select the most advantageous to continue the studies with LEM2-loaded lipid nanoparticles. The conditions used in each method has been also adopted from the previously studies reported in literature (41,146). It was verified that the ultrasonication method is easier and faster when compared with hot HPH.

After the preparation of unloaded lipid nanoparticles, these were characterized and stability tests were performed (days 0, 30, and 60) in order to choose the most suitable/stable type of lipid nanoparticles to encapsulate LEM2.

3.1.2. Characterization and stability studies

To characterize and study the stability of the unloaded lipid nanoparticles, some parameters, including organoleptic characteristics, particle size and PDI, ZP, and pH were evaluated after their production, and after 30 and 60 days of storage at 4 ºC.

Organoleptic characteristics

The analyses of the organoleptic characteristics after the production of the lipid nanoparticles dispersions give a first impression of the quality of the preparation. Despite the simplicity of this assessment, problems in the appearance and/or homogeneity of the preparations are indicative of poor raw materials quality or problems during production and storage. After their preparation, all the unloaded lipid nanoparticles dispersions were liquid, with milky white aspect, homogeneous, and without any phase separation (Appendix II). During 30 and 60 days of storage, there were no changes in the aspect of the dispersions developed, suggesting that all have good quality (Appendix II)

Particle size and polydispersity index (PDI)

The particle size of lipid vesicles has been shown to have a significant influence on drug delivery into the skin (195,196). Since the purpose of the lipid nanoparticles are for topical

administration of LEM2, their size must allow them to remain on the skin with a minimal or no amount of LEM2 reaching the systemic circulation. However, it is necessary that the drug cross the outermost layer of the skin (stratum corneum), in order to be effective. As indicators of stability, the particle size and its distribution should maintain a narrow range during storage. An increase in particle size indicates agglomeration and hence physical instability.

After the production of unloaded lipid nanoparticles, the particle size and their distribution were evaluated by DLS and the results are presented in Table 9. Unloaded NLC prepared by HPH had sizes varying from 133.2 ± 0.8 nm to 145.4 ± 0.8 nm and PDI values varying from 0.227 ± 0.004 to 0.276 ± 0.005; the other ones prepared by ultrasonication had sizes ranging from 133.2 ± 0.7 nm to 150.4 ± 0.8 nm and PDI values ranging from 0.269 ± 0.004 to 0.293 ± 0.006. Unloaded SLN prepared by HPH showed sizes varying from 129.1 ± 1.5 nm to 137.4 ± 1.2 nm and PDI values varying from 0.241 ± 0.005 to 0.323 ± 0.006; the SLN produced by ultrasonication had sizes ranging from 140.4 ± 0.6 nm to 155.8 ± 1.6 nm and PDI values between 0.229 ± 0.006 and 0.362 ± 0.007.

Table 9 – Results of particle size, polydispersity index (PDI), and zeta potential (ZP) for all unloaded lipid nanoparticles formulations after production either by hot pressure homogenization (HPH) or by ultrasonication.

Preparation method	Batch	Particle size (nm) [(a)]	PDI [(a)]	ZP (mV) [(b)]
HPH	NLC_1	133.2 ± 0.8	0.276 ± 0.005	32.76 ± 1.47
	NLC_2	145.4 ± 0.8	0.246 ± 0.006	34.62 ± 2.04
	NLC_3	142.5 ± 1.2	0.227 ± 0.004	25.65 ± 0.89
	SLN_1	129.1 ± 1.5	0.323 ± 0.006	32.81 ± 0.85
	SLN_2	134.3 ± 1.1	0.241 ± 0.005	27.13 ± 1.26
	SLN_3	137.4 ± 1.2	0.284 ± 0.006	26.47 ± 0.94
Ultrasonication	NLC_1	133.2 ± 0.7	0.289 ± 0.005	31.85 ± 1.97
	NLC_2	142.7 ± 0.5	0.269 ± 0.004	26.32 ± 0.43
	NLC_3	150.4 ± 0.8	0.293 ± 0.006	34.82 ± 2.04
	SLN_1	149.9 ± 0.6	0.229 ± 0.006	27.93 ± 3.06
	SLN_2	140.4 ± 0.6	0.296 ± 0.002	38.04 ± 0.25
	SLN_3	155.8 ± 1.6	0.362 ± 0.007	46.47 ± 1.18

[(a)] n=3, mean value ± SD

[(b)] n=6, mean value ± SD

There are evidences that vesicles and particles with sizes ≤300 nm are able to deliver their contents to some extent into the deeper skin layers, and only the ones with sizes ≤70 nm have shown maximum deposition of compounds in both viable dermal and epidermal layers (195,197). Thus, the mean particle size of the unloaded lipid nanoparticles prepared are adequate for topical administration of LEM2. Also, PDI values ≤0.3, in drug delivery applications using lipid-based carriers, are considered to be acceptable and indicates a homogenous distribution of particles (160,161,198).

The mean particle size and the PDI values were also measured 30 and 60 days after the production of the unloaded lipid nanoparticles. For NLC produced by HPH and ultrasonication, it was noted a small increase in particle size, however, no statistically significant differences were found (Figures 21 and 22). By contrast, the mean particle size of SLN produced by either HPH or ultrasonication significantly increased after their storage (Figures 23 and 24). This indicates physical instability of SLN produced by both methods. For all unloaded lipid nanoparticles, the PDI values also increased, however, they were similar to those measured after their production (Figures 25, 26, 27, 28).

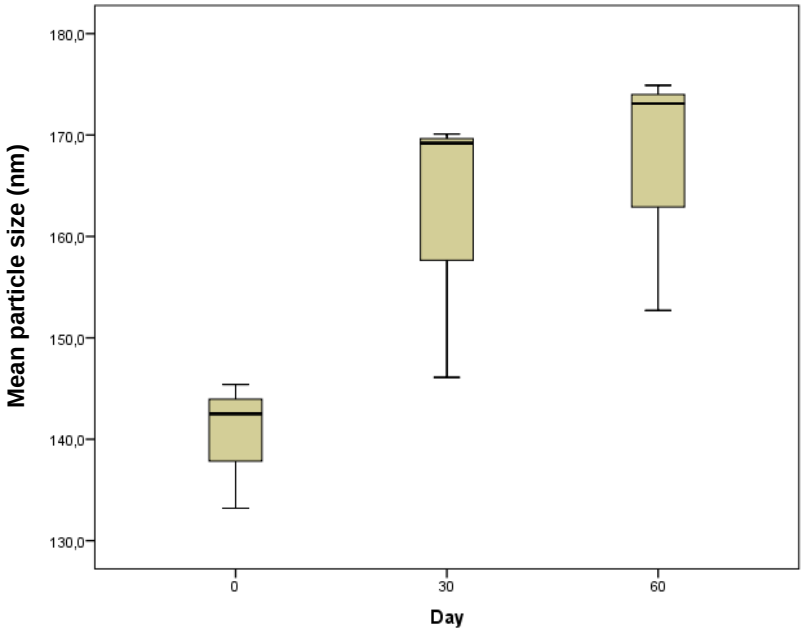

Figure 21 – Results of mean size, in nm, of the unloaded NLC prepared by HPH after preparation, and after 30 and 60 days of storage. Each box represents 3 different batches. Statistical significance: p=0.059

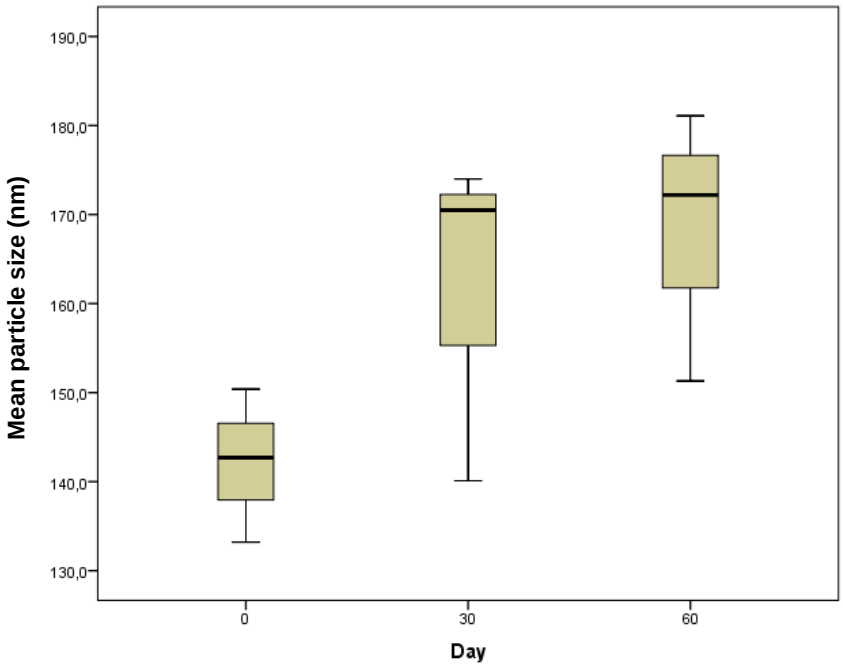

Figure 22 – Results of mean size, in nm, of the unloaded NLC prepared by ultrasonication after preparation, and after 30 and 60 days of storage. Each box represents 3 different batches. Statistical significance: p=0.160

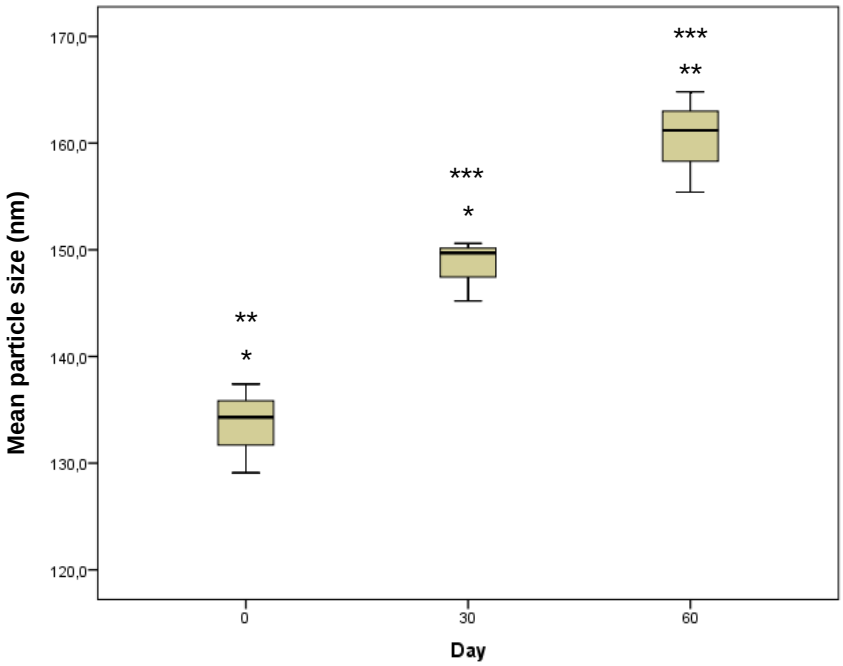

Figure 23 – Results of mean size, in nm, of the unloaded SLN prepared by HPH after preparation, and after 30 and 60 days of storage. Each box represents 3 different batches. Statistical significance: *p=0.009, **p<0.001, ***p=0.025

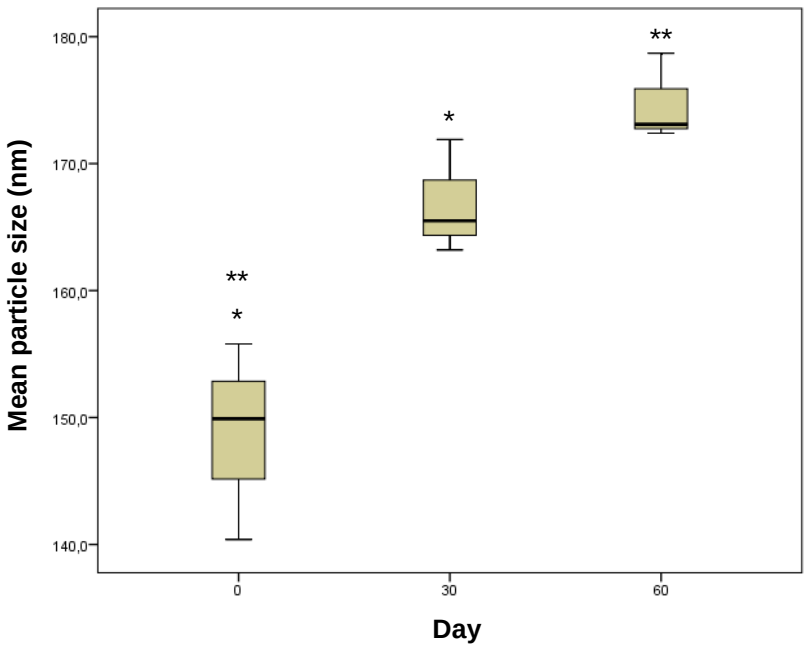

Figure 24 – Results of mean size, in nm, of the unloaded SLN prepared by ultrasonication after preparation, and after 30 and 60 days of storage. Each box represents 3 different batches. Statistical significance: *p=0.017, **p=0.003

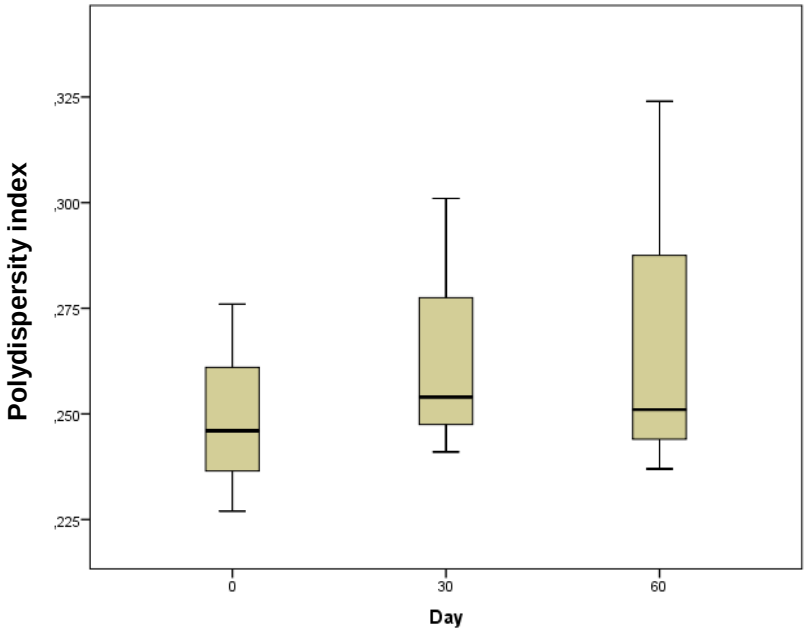

Figure 25 – PDI values of the unloaded NLC prepared by HPH after preparation, and after 30 and 60 days of storage. Each box represents 3 different batches. Statistical significance: p=0.763

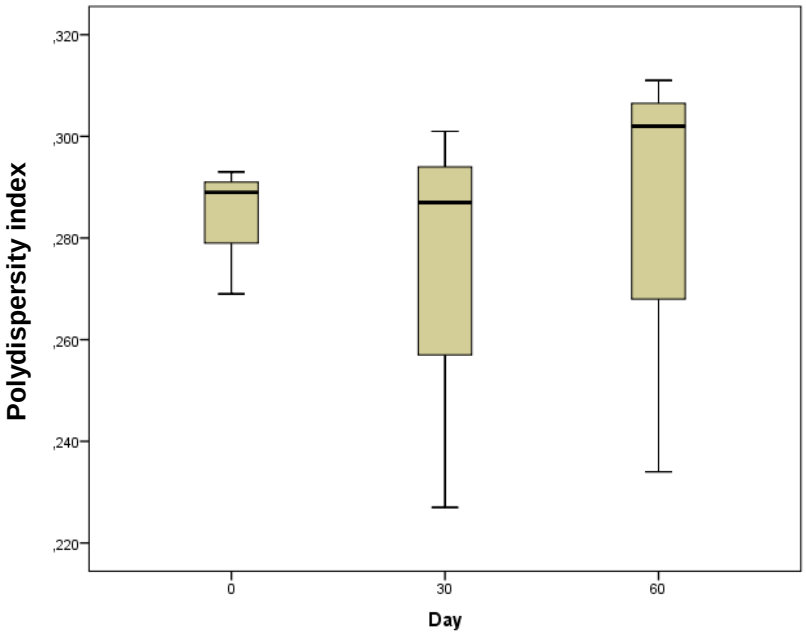

Figure 26 – PDI values of the unloaded NLC prepared by ultrasonication after preparation, and after 30 and 60 days of storage. Each box represents 3 different batches. Statistical significance: p=0.896

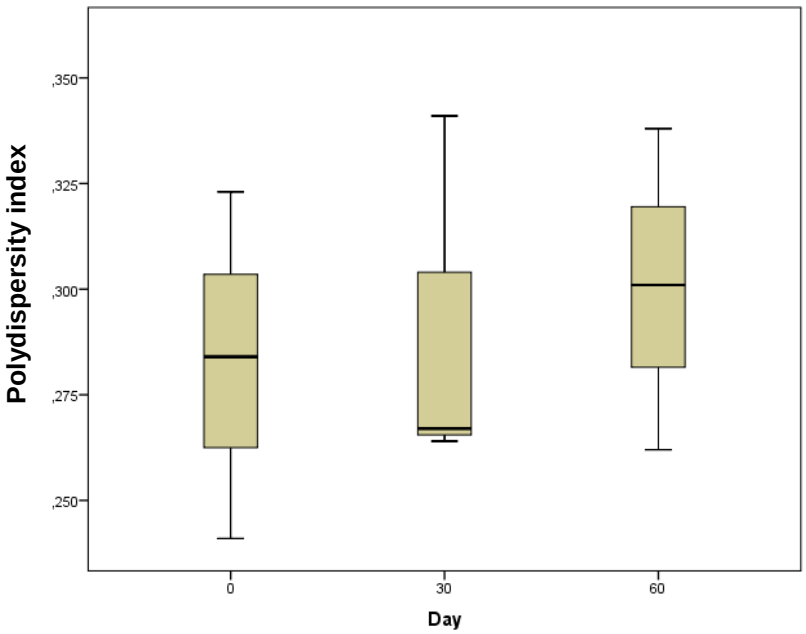

Figure 27 – PDI values of the unloaded SLN prepared by HPH after preparation, and after 30 and 60 days of storage. Each box represents 3 different batches. Statistical significance: p=0.872

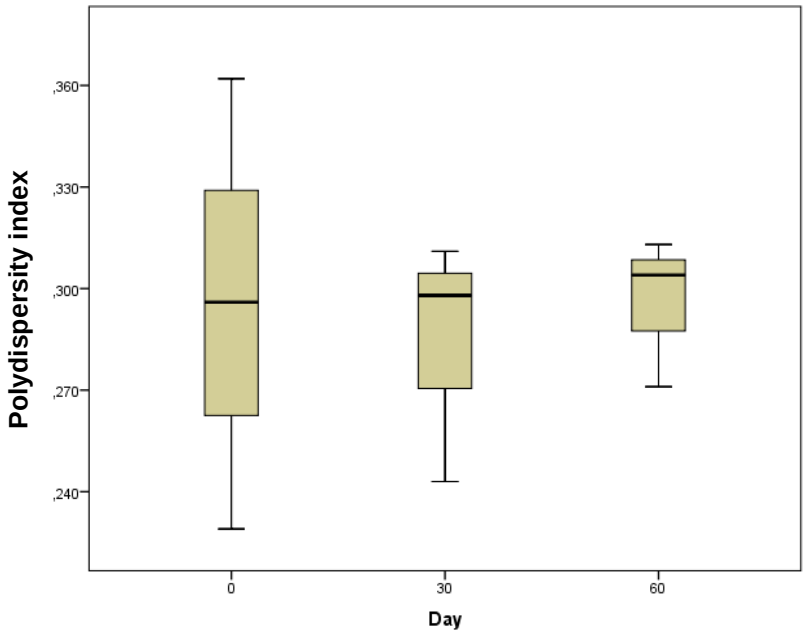

Figure 28 – PDI values of the unloaded SLN prepared by ultrasonication after preparation, and after 30 and 60 days of storage. Each box represents 3 different batches. Statistical significance: p=0.935

Zeta potential (ZP)

ZP is another important factor used to characterize and study the stability of lipid nanoparticles dispersions. After the production of lipid nanoparticles, the ZP values were measured by ELS and the results are presented in Table 9. Unloaded NLC prepared by HPH had ZP values varying from 25.65 ± 0.89 mV to 34.62 ± 2.04 mV; the other ones prepared by ultrasonication had ZP values ranging from 26.32 ± 0.43 mV to 34.82 ± 2.04 mV. Unloaded SLN prepared by HPH showed ZP values varying from 26.47 ± 0.94 mV to 32.81 ± 0.85 mV; SLN produced by ultrasonication had ZP values ranging from 27.93 ± 3.06 mV to 46.47 ± 1.18 mV. According to literature, dispersions with ZP values of ±20–30 mV are moderately stable, and > ± 30 mV are highly stable, so it is possible that the unloaded lipid nanoparticles dispersions prepared in this study remain stable during storage (168).

The ZP values were also measured 30 and 60 days after the production of the unloaded lipid nanoparticles. In all formulations was noted a slightly decrease in the ZP values, however, comparing the results on the production day and after 30 and 60 days, it was possible to verify

that there are not statistically significant differences in these values (Figures 29, 30, 31, and 32). Although the ZP has decreased slightly, the values remained between 20 and 30 mV, which could indicate that particle aggregation is unlikely to occur. Nevertheless, by the analysis that has been made to the particle size, it was found that in the case of unloaded SLN formulations, the particle size significantly increased during storage, suggesting a possible aggregation of particles over time.

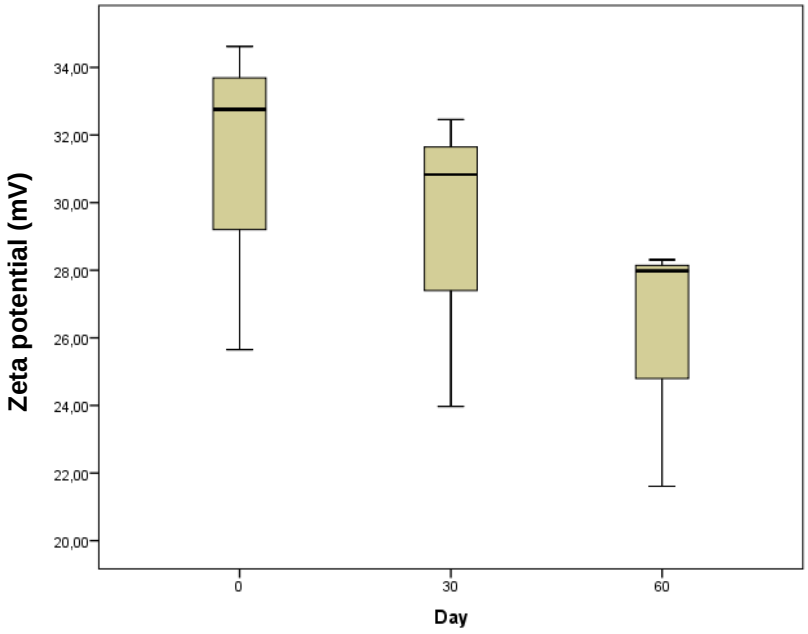

Figure 29 – Results of zeta potential (ZP), in mV, of the unloaded NLC prepared by HPH after preparation, and after 30 and 60 days of storage. Each box represents 3 different batches. Statistical significance: p=0.415

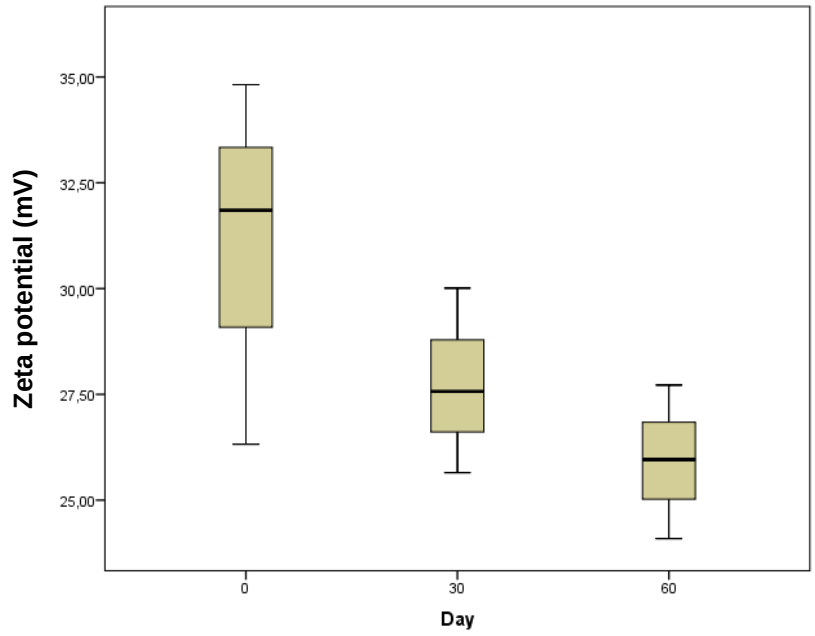

Figure 30 – Results of zeta potential (ZP), in mV, of the unloaded NLC prepared by ultrasonication after preparation, and after 30 and 60 days of storage. Each box represents 3 different batches. Statistical significance: p=0.189

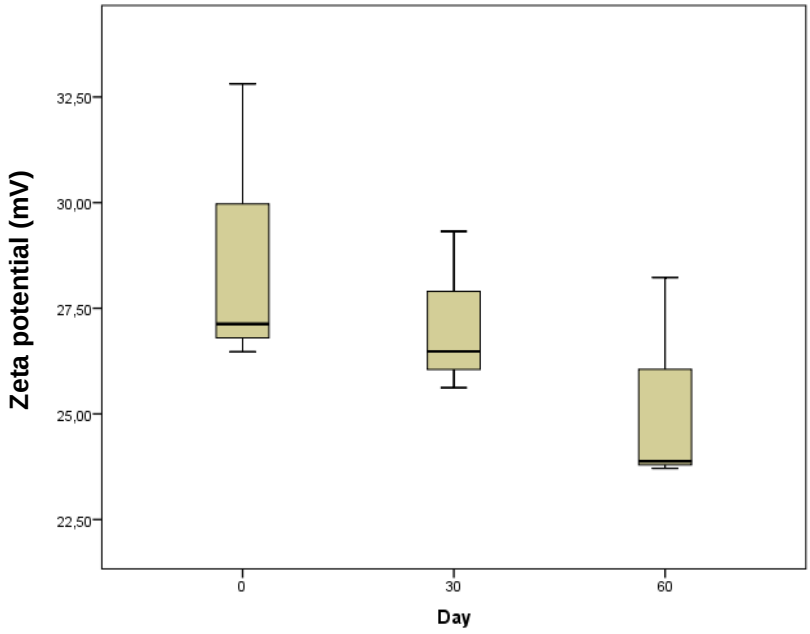

Figure 31 – Results of zeta potential (ZP), in mV, of the unloaded NLC prepared by ultrasonication after preparation, and after 30 and 60 days of storage. Each box represents 3 different batches. Statistical significance: p=0.352

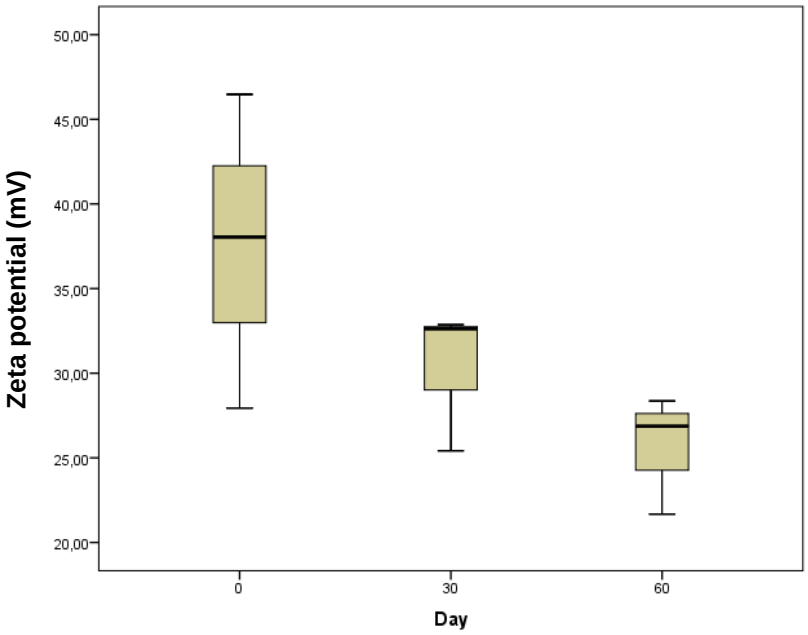

Figure 32 – Results of zeta potential (ZP), in mV, of the unloaded SLN prepared by ultrasonication after preparation, and after 30 and 60 days of storage. Each box represents 3 different batches. Statistical significance: p=0.142

pH

The pH was also used to characterize and predict the stability of the lipid nanoparticles dispersions. After the production of lipid nanoparticles, the pH values were measured with Universal indicator paper. It was not possible use a potentiometer since the sample volume was too small to dip the electrode. The results showed that all unloaded lipid nanoparticles produced by both methods had pH values varying from 5.50 to 5.83 (Table 10).

The values were also measured 30 and 60 days after the production of the unloaded lipid nanoparticles. The results presented in Table 10 showed that pH values had some variations during storage time, however, there are no statistically significant differences between them when compared with t measured after the production (Table 11).

Table 10 – pH values of unloaded lipid nanoparticles after their production and after 30 and 60 days. The values were obtained from 3 different batches of each formulation.

Day	NLC [(a)]		SLN [(a)]	
	HPH	Ultrasonication	HPH	Ultrasonication
0	5.83 ± 0.29	5.50 ± 0.50	5.67 ± 0.29	5.67 ± 0.29
30	5.50 ± 0.50	5.67 ± 0.29	5.67 ± 0.29	5.67 ± 0.29
60	5.50 ± 0.00	5.83 ± 0.29	5.67 ± 0.29	5.50 ± 0.00

[(a)] n=3, mean value ± SD

Table 11 – Significance levels obtained from the statistical analysis of the pH of lipid nanoparticles during the 60 days of storage.

Type of lipid nanoparticle	Method of preparation	Significance level
NLC	HPH	0.179
	Ultrasonication	0.670
SLN	HPH	0.846
	Ultrasonication	0.304

3.2. Loaded lipid nanoparticles

Since NLC proved to be stable during 60 days of storage at 4 ºC and ultrasonication showed to be an easier and faster method to prepare lipid nanoparticles when compared with hot HPH, it was decided to encapsulate LEM2 in NLC produced by ultrasonication.

During the development of the LEM2-loaded NLC, it was noted that the drug has relatively poor solubility in the lipid mixture, which will influence the EE and subsequent effectiveness of these particles. To overcome this problem, it is important to do some drug-in-lipid solubility tests before the development of lipid nanoparticles, however, in this work it was not possible to do this test due to the low amount of LEM2 available.

Two different LEM2-loaded NLC formulations were prepared, with and without the preservative Cetrimide® (Table 8). Initially, it was prepared the formulation containing this

preservative, however, this formulation showed high toxicity during *in vitro* tests (see results section 3.4.1.). So, to continue the work, it was necessary to remove this component from the formulation.

3.2.1. Characterization and stability studies

The parameters used to characterize the empty nanoparticles (organoleptic characteristics, particle size and PDI, ZP, and pH) were also used to characterize LEM2-loaded NLC dispersions. The stability studies were also carried out likewise unloaded lipid nanoparticles.

3.2.1.1. LEM2-loaded NLC – formulation containing Cetrimide®

Organoleptic characteristics

The organoleptic characteristics of LEM2-loaded NLC dispersions were assessed after their preparation and, as well as unloaded lipid nanoparticles dispersions, they were liquid, with milky white aspect, homogeneous, and without any phase separation. After 30 and 60 days, there were no changes in their appearance, suggesting that the dispersions have good quality.

Particle size and PDI

After the production of LEM2-loaded NLC, the mean particle size and the PDI values were obtained by DLS and the results are presented in Table 12. Their sizes ranged from 171.7 ± 1.3 nm to 176.3 ± 1.3 nm.

Comparing with the results obtained for unloaded NLC, the encapsulation of LEM2 significantly increased the mean particle size (Figure 33). This increase is not considered important because the developed particles continued to be adequate for topical application of LEM2. However, the mean particle size significantly increased after 30 and 60 days of storage, probably due to the formation of lipid aggregates, which suggests that the LEM2-loaded NLC formulation with Cetrimide® is physically unstable (Figure 34).

Table 12 – Results of particle size, polydispersity index (PDI), and zeta potential (ZP) for LEM2-loaded NLC (formulation containing Cetrimide®) after production by ultrasonication.

Batch	Mean particle size (nm) [(a)]	PDI [(a)]	ZP (mV) [(b)]
1	171.7 ± 1.3	0.254 ± 0.004	26.34 ± 1.41
2	176.3 ± 1.3	0.237 ± 0.006	27.71 ± 1.03
3	173.6 ± 0.9	0.301 ± 0.004	26.52 ± 0.98

[(a)] n=3, mean value ± SD
[(b)] n=6, mean value ± SD

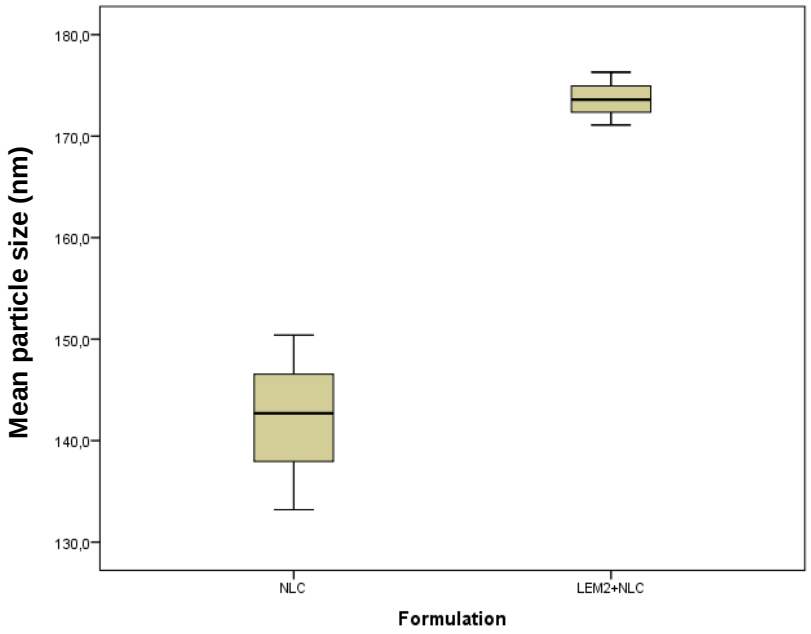

Figure 33 – Particle sizes of unloaded NLC and LEM2-loaded NLC (formulation with Cetrimide®) after their production by ultrasonication method. Each box represents 3 different batches. Statistical significance: p=0.004

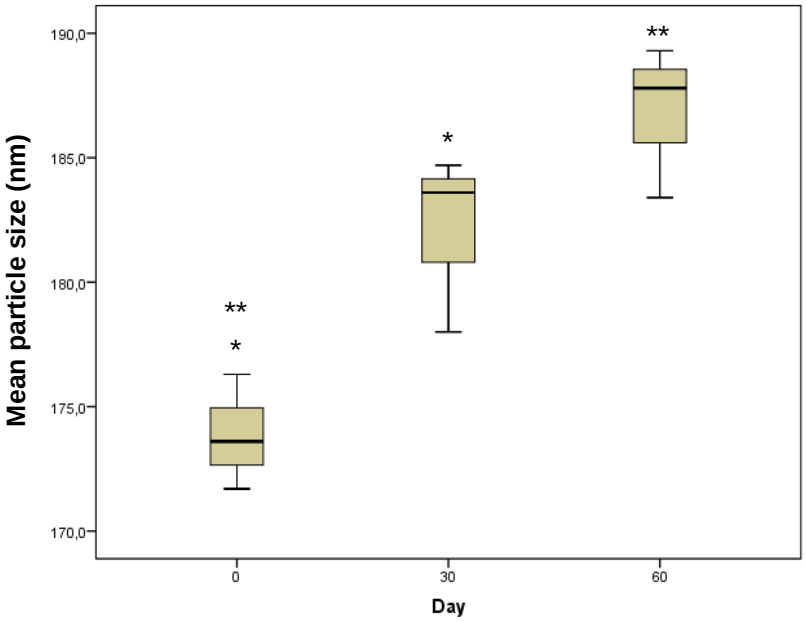

Figure 34 – Results of mean size, in nm, of LEM2-loaded NLC (formulation with Cetrimide®) prepared by ultrasonication after preparation, and after 30 and 60 days of storage. Each box represents 3 different batches. Statistical significance: *p=0.037, **p=0.005

The PDI values measured after the production of LEM2-loaded NLC vary between 0.237 ± 0.006 and 0.301 ± 0.004, indicating a homogenous distribution of lipid nanoparticles (Table 10). These values were similar to those obtained for unloaded NLC (Figure 35). On days 30 and 60, it was noted a small increase in the PDI values, however, comparing these results and those obtained on the production day, it was possible to verify that there are not statistically significant differences (Figure 36). These results showed that the distribution of lipid nanoparticles remained homogeneous, even though there was an increase in their size over time.

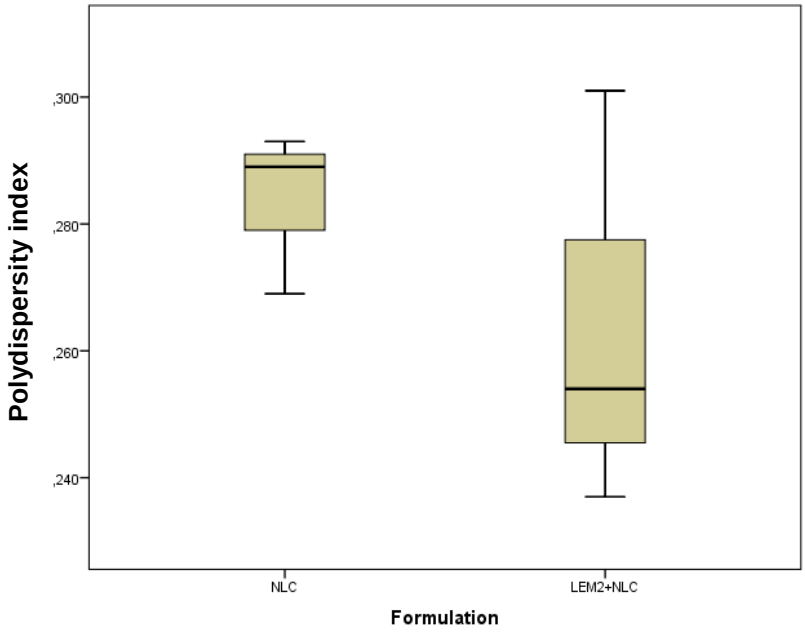

Figure 35 – PDI values of unloaded NLC and LEM2-loaded NLC (formulation with Cetrimide®) after their production by ultrasonication method. Each box represents 3 different batches. Statistical significance: p=0.392

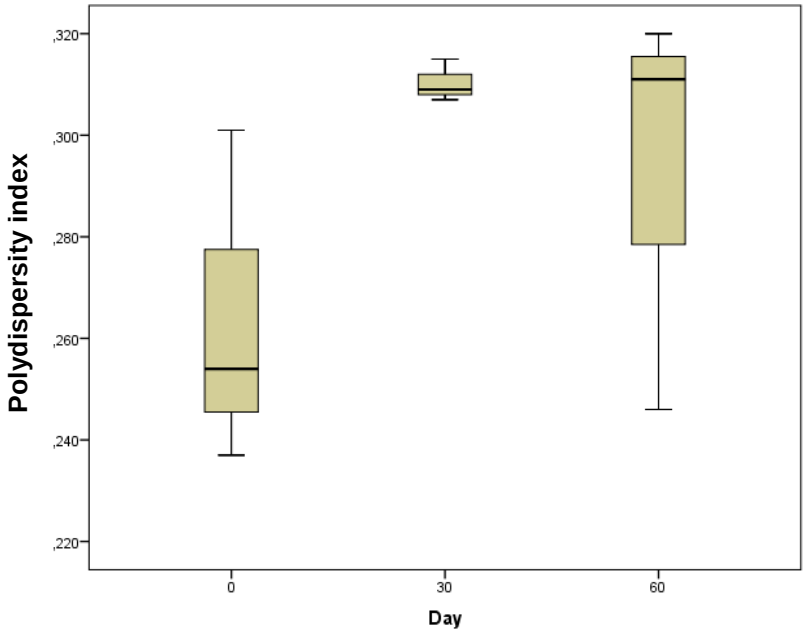

Figure 36 – PDI values of LEM2-loaded NLC (formulation with Cetrimide®) prepared by ultrasonication after preparation, and after 30 and 60 days of storage. Each box represents 3 different batches. Statistical significance: p=0.246

ZP

After the production of LEM2-loaded NLC, the values of ZP obtained by ELS range from 26.34 ± 1.41 mV to 27.71 ± 1.03 mV (Table 12). Comparing with the results obtained for unloaded NLC, the encapsulation of LEM2 slightly decrease the ZP values, however, it was possible to verify that there are not statistically significant differences (Figure 37).

On days 30 and 60, it was noted a small decrease in ZP, however, there are not statistically differences between these values and those measured after the production, which could mean that particle aggregation is unlikely to occur (Figure 38). However, by the analysis that has been made to the particle size, it was found that the particle size of LEM2-loaded NLC significantly increased during storage, suggesting a possible aggregation of particles over time.

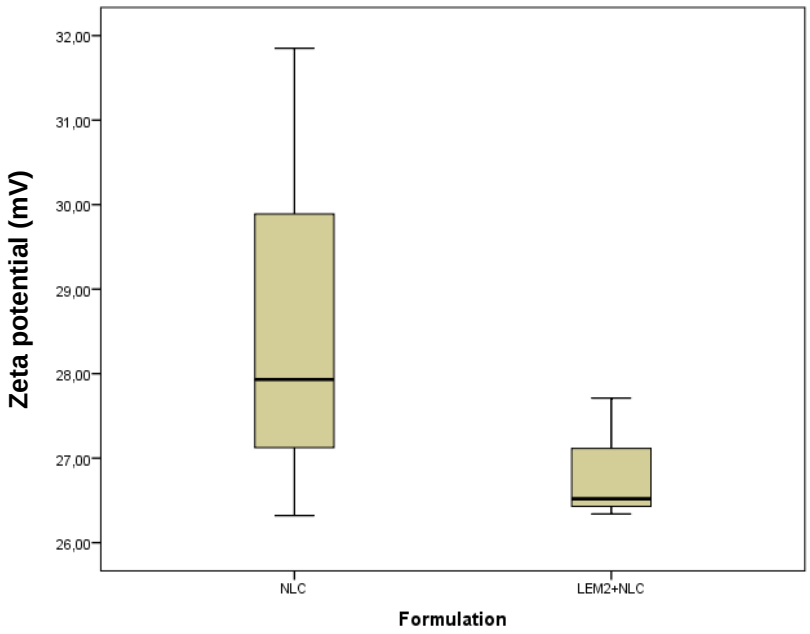

Figure 37 – ZP values of unloaded NLC and LEM2-loaded NLC (formulation with Cetrimide®) after their production by ultrasonication method. Each box represents 3 different batches. Statistical significance: p=0.339

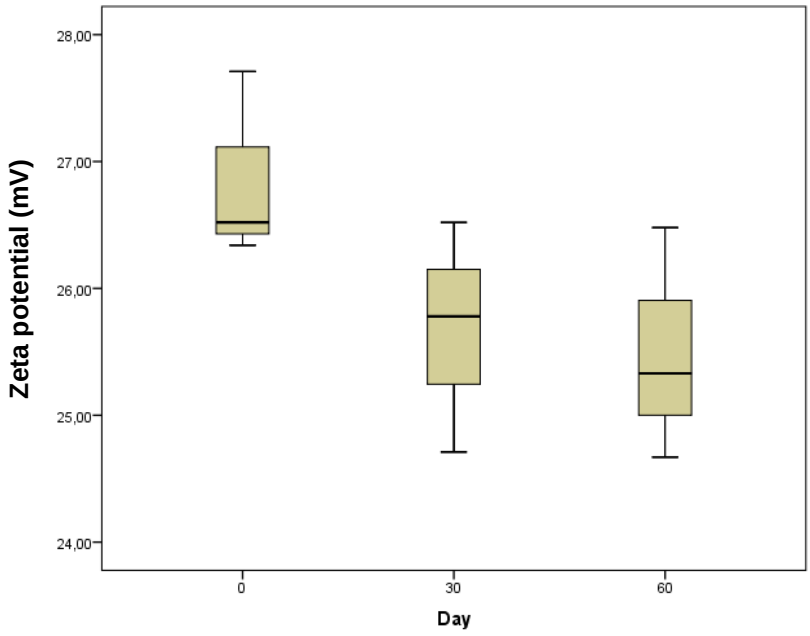

Figure 38 – ZP values of LEM2-loaded NLC (formulation with Cetrimide®) prepared by ultrasonication after preparation, and after 30 and 60 days of storage. Each box represents 3 different batches. Statistical significance: p=0.189

pH

After the production of LEM2-loaded NLC, the values of pH measured with Universal indicator paper ranged from 5.17 to 5.67 (Table 13), likewise unloaded NLC.

Table 13 – pH values of LEM2-loaded NLC (formulation with Cetrimide®) after their production and after 30 and 60 days.

Day	pH [(a)]
0	5.67 ± 0.29
30	5.17 ± 0.29
60	5.17 ± 0.29

[(a)] n = 3, mean value ± SD

On days 30 and 60, it was noted a small decrease in pH (Table 13), however, comparing these results with those obtained on the production day, it was possible to verify that there are no statistically significant differences (significance level equal to 0.141).

3.2.1.2. LEM2-loaded NLC – formulation without Cetrimide®

Organoleptic features

After preparation, the LEM2-loaded NLC dispersions without Cetrimide® were liquid, milky white, homogeneous, and without any phase separation, as well as unloaded NLC and LEM2-loaded NLC formulations with Cetrimide®. At days 30 and 60, there was no alterations in their appearance, suggesting that the dispersions have good quality.

Particle size and PDI

After the production of LEM2-loaded NLC, the mean particle size and the PDI values were obtained by DLS and the results are showed in Table 14. Their sizes range from 197.6 ± 1.4 nm to 207.2 ± 2.2 nm. Comparing with both unloaded NLC and LEM2-loaded NLC formulation containing Cetrimide®, the sizes of LEM2-loaded NLC without this preservative are significantly larger (Figure 39), but still suitable for topical administration of LEM2. The particle size increased during storage time; however, statistically significant differences were found only at day 60, suggesting a possible aggregation of particles (Figure 40).

Table 14 – Results of particle size, polydispersity index (PDI), and zeta potential (ZP) for LEM2-loaded NLC (formulation without Cetrimide®) after production by ultrasonication.

Batch	Mean particle size (nm) [(a)]	PDI [(a)]	ZP (mV) [(b)]
1	214.6 ± 1.6	0.261 ± 0.004	25.21 ± 1.39
2	225.1 ± 2.2	0.307 ± 0.004	22.96 ± 2.01
3	219.3 ± 1.4	0.278 ± 0.005	26.47 ± 1.28

[(a)] n = 3, mean value ± SD
[(b)] n = 6, mean value ± SD

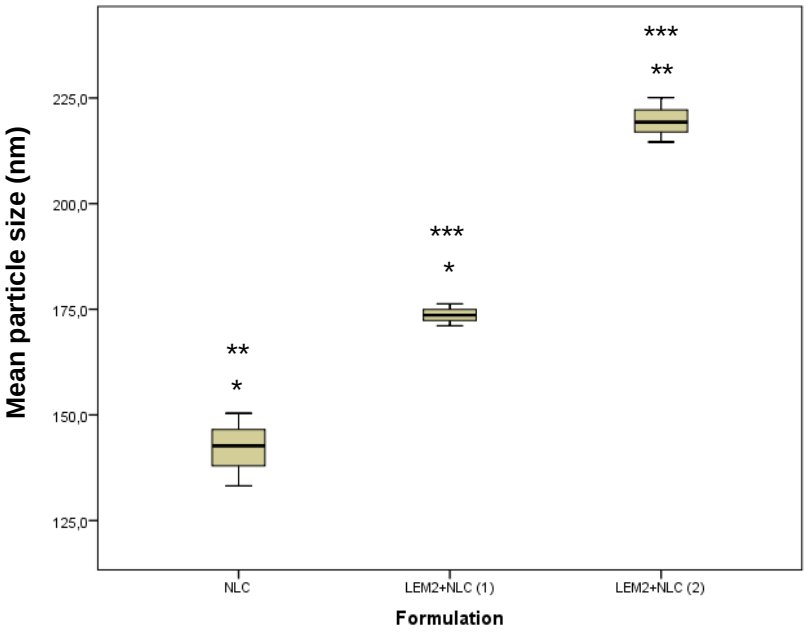

Figure 39 – Particle sizes of unloaded NLC and LEM2-loaded NLC with (LEM2+NLC (1)) and without (LEM2+NLC (2)) Cetrimide®, after their production by ultrasonication method. Each box represents 3 different batches. Statistical significance: *p=0.004, **p<0.001, ***p<0.001

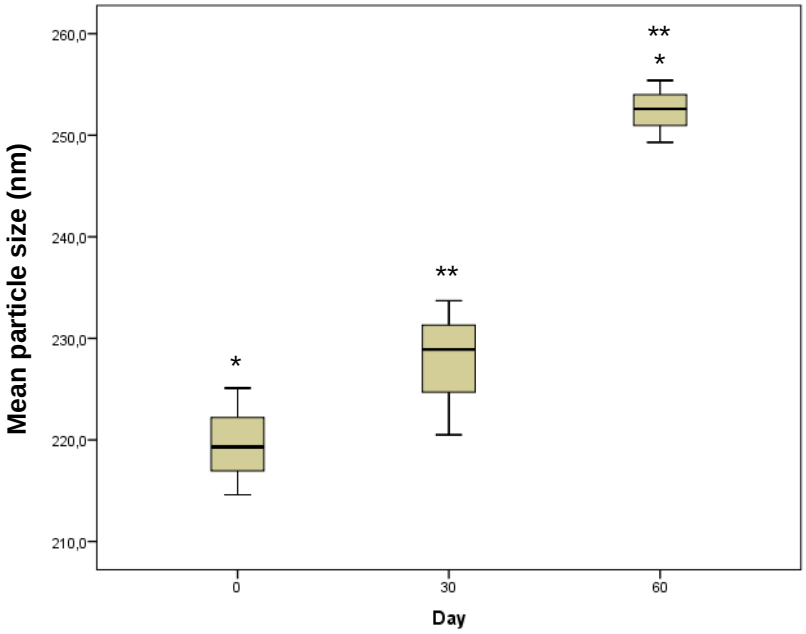

Figure 40 – Results of mean size, in nm, of LEM2-loaded NLC (formulation without Cetrimide®) prepared by ultrasonication after preparation, and after 30 and 60 days of storage. Each box represents 3 different batches. Statistical significance: *p=0.001, **p=0.003

The PDI values measured after the production of LEM2-loaded NLC vary between 0.261 ± 0.004 and 0.307 ± 0.004, indicating a homogenous distribution of lipid nanoparticles (Table 14). The obtained values were similar to those measured in unloaded NLC and LEM2-loaded NLC formulation containing Cetrimide® (Figure 41). On days 30 and 60, it was noted a small increase in the PDI values, however, comparing these results with those obtained on the production day, it was possible to verify that there are not statistically significant differences (Figure 42). The results showed that the populations of lipid nanoparticles remained homogeneous, even though there was an increase in their size over time.

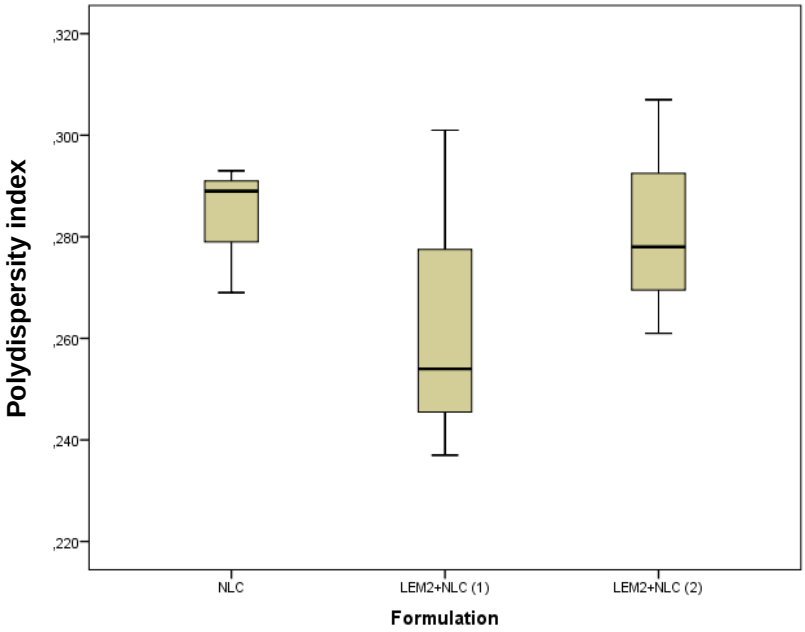

Figure 41 – PDI values of unloaded NLC and LEM2-loaded NLC with (LEM2+NLC (1)) and without (LEM2+NLC (2)) Cetrimide®, after their production by ultrasonication method. Each box represents 3 different batches. Statistical significance: p=0.582

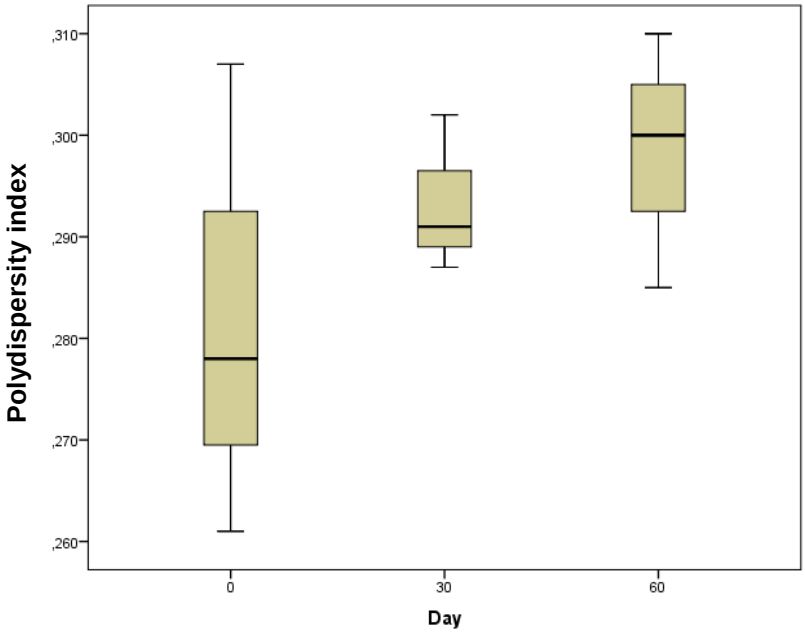

Figure 42 – PDI values of LEM2-loaded NLC (formulation without Cetrimide®) prepared by ultrasonication after preparation, and after 30 and 60 days of storage. Each box represents 3 different batches. Statistical significance: p=0.481

ZP

After the production of LEM2-loaded NLC, the values of ZP obtained by ELS range from 22.96 ± 2.01 mV to 26.47 ± 1.28 mV (Table 14). Comparing with both unloaded NLC and LEM2-loaded NLC formulation containing Cetrimide®, the ZP values of LEM2-loaded NLC without Cetrimide® are lower, however, there is not statistically significant differences between them (Figure 43). During the storage there was a decrease in the ZP, but only at day 60 were verified significant differences (Figure 44). These lower values of ZP at day 60 indicate that particle aggregation is more likely to occur, which are in accordance with the results obtained in particle size at the same day. This could mean that the formulation remained stable for at least 30 days. These results confirm that Cetrimide®, being a cationic compound, is important for adjusting ZP and for preventing particle agglomeration.

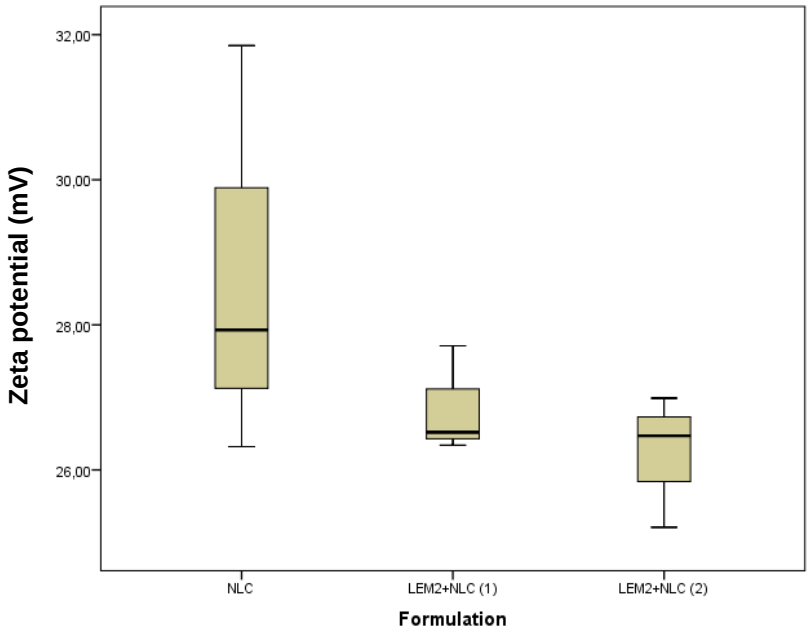

Figure 43 – ZP values of unloaded NLC and LEM2-loaded NLC with (LEM2+NLC (1)) and without (LEM2+NLC (2)) Cetrimide®, after their production by ultrasonication method. Each box represents 3 different batches. Statistical significance: p=0.283

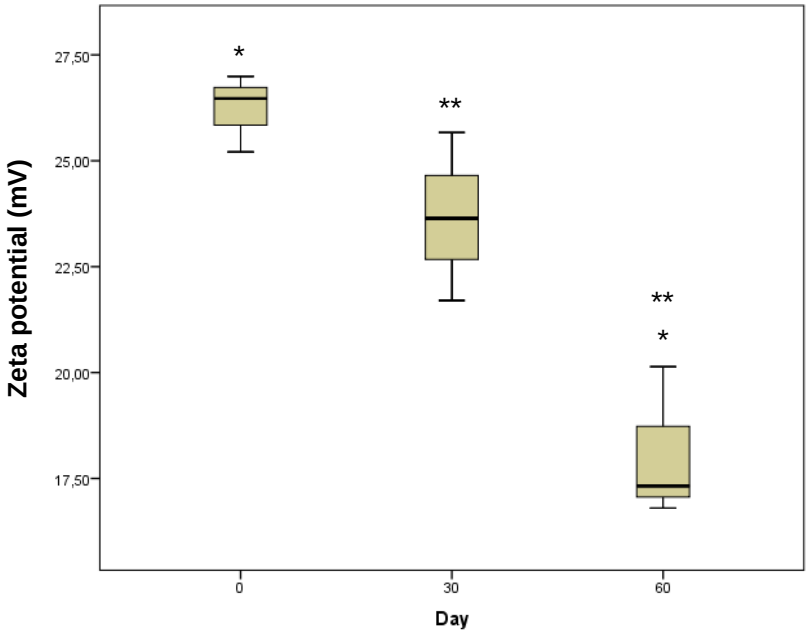

Figure 44 – ZP values of LEM2-loaded NLC (formulation without cetrimide) prepared by ultrasonication after its preparation, and after 30 and 60 days. Each box represents 3 different batches. Statistical significance: *p=0.002, **p=0.014

pH

After the production of LEM2-loaded NLC without Cetrimide®, the pH values obtained with Universal indicator paper ranged from 5.25 to 5.50 (Table 15), similarly, to unloaded NLC and LEM2-loaded NLC with Cetrimide®.

Table 15 – pH values of LEM2-loaded NLC (formulation without Cetrimide®) after their production and after 30 and 60 days.

Day	pH [(a)]
0	5.33 ± 0.58
30	5.50 ± 0.50
60	5.25 ± 0.29

[(a)] n = 3, mean value ± SD

Comparing the pH values measured on days 30 and 60 with those obtained on the production day, it was possible to verify that there are no statistically significant differences (significance level equal to 0.656).

3.3. Encapsulation efficiency (EE)

After the preparation of LEM2-loaded NLC (both formulations), the amount of LEM2 incorporated into nanoparticles was determined by HPLC, but first it was necessary to optimize and validate the method.

3.3.1. HPLC method development and optimization

To identify and measure an analyte in a given sample by HPLC, certain conditions (e.g. injection volume, detection wavelength, mobile phase composition and flow rate, column type, among others) need to be first defined. In a first approach, some of the analytical conditions adopted were chosen considering methodology already developed and described in (178). The type of column (C18), temperature (25ºC), and flow rate (1.0 ml/min) were selected based on the work mentioned before, whereas the detection wavelength and the composition of mobile phase were studied in order to achieve the best conditions for the identification and quantification of LEM2.

To detect LEM2 by the HPLC method is important to choose the right wavelength. So, the UV spectrum of a LEM2 solution in ethanol (50 µg/ml, stock solution) was performed (Figure 45). The maximum absorption of LEM2 occurs at the wavelengths 242 nm and 326 nm. The wavelength used was 242 nm.

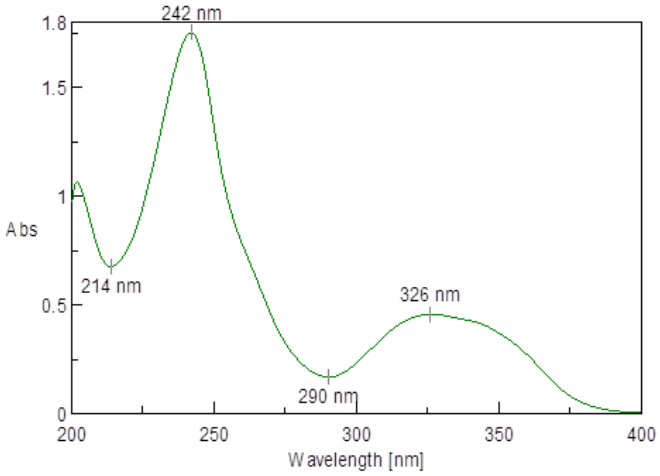

Figure 45 – UV spectrum of LEM2 in ethanol.

To choose the mobile phase composition, many combinations of water and acetonitrile were tested – 0:100; 5:95; 10:90; 15:85; 20:80; 25:75; 30:70; 35:65; 40:60; and 45:55 – and the selection of the most suitable one was based on the k' (capacity factor) values calculated. This parameter is very important since it is a mean of measuring the retention of an analyte on the chromatographic column, and the aim of any HPLC method is to provide a well-resolved peak in the shortest amount of time. High k' value indicates that the analyte is highly retained and has spent too much time interacting with the stationary phase and, consequently, the elution takes a very long time (199). Ideally, the k' value for an analyte should be more than 2, which indicates a certain level of interaction (202). The most effective and convenient way to change the k' value of a peak is to adjust the solvent strength of the mobile phase. This is usually achieved by altering the amount of organic solvent in the mobile phase mixture. The HPLC system used has a non-polar stationary phase, so enhancing the polarity of the mobile phase will progressively repel the hydrophobic parts of the analyte molecules into the stationary phase and the analyte will be retained for longer on the column (higher k' values). The converse is also true, which means that at high mobile phase organic solvent composition, the retention time and k' values are lower. The obtained results (Figure 46) are in agreement with the literature since at lower percentages of acetonitrile in the mobile phase the k' values and the retention time obtained are higher than those obtained at highest percentages of acetonitrile. Values of k' higher than 2 were obtained for the percentages of 60% and 55% of acetonitrile (Table 16). The percentage of acetonitrile selected was 60%, being possible to reduce the run times and consequently the eluent expense.

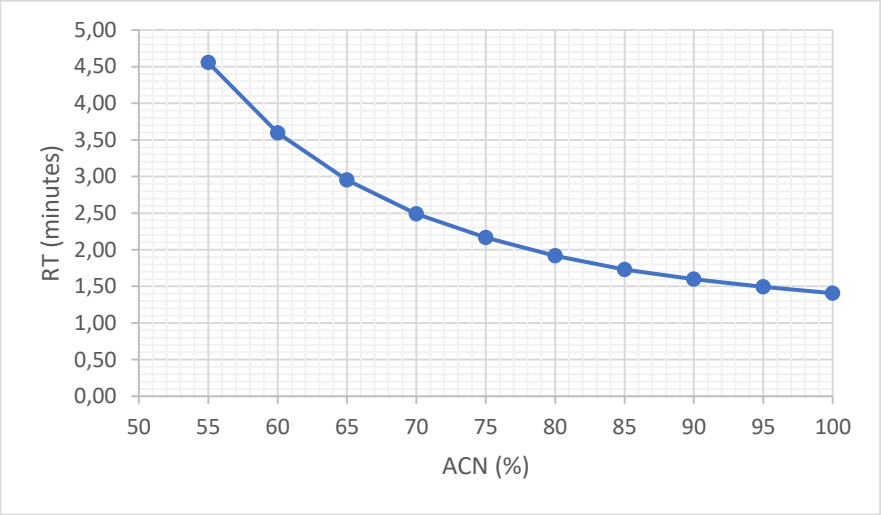

Figure 46 – Graphic representation of retention time (RT) of LEM2, in minutes, versus amount of acetonitrile (ACN) in the mobile phase, in percentage.

Table 16 – Results obtained for capacity factor (k'). ACN – acetonitrile; TR – retention time.

ACN (%)	RT 1 (minutes)	RT 2 (minutes)	Mean RT (minutes)	k'
100	1.41	1.41	1.41	0.41
95	1.49	1.49	1.49	0.49
90	1.60	1.60	1.60	0.60
85	1.73	1.73	1.73	0.73
80	1.91	1.92	1.92	0.92
75	2.16	2.17	2.17	1.17
70	2.47	2.50	2.49	1.49
65	2.94	2.96	2.95	1.95
60	3.59	3.60	3.60	2.60
55	4.55	4.56	4.56	3.56

After the chromatographic conditions were defined, it was obtained the chromatogram in Figure 47. The chromatogram shows some peaks: the first and the last peaks probably

correspond to impurities (the purity degree of LEM2 is unknown); and the second and major peak corresponds to LEM2. The retention time of LEM2 was about 3.6 minutes.

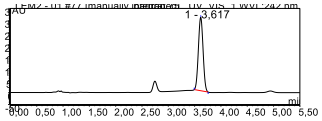

Figure 47 – Chromatogram of a standard LEM2 solution (30 µg/mL).

3.3.2. Method validation

System suitability

To assess the system suitability, the LEM2 standard solution (30 µg/mL) was injected 10 times and some parameters such as k', T, and N were calculated. The results (Table 17) showed that the values of all parameters are in accordance with the recommendation limits proposed by US-FDA guidance Validation of Chromatographic Methods, except the injection repeatability. In this parameter, the tighter the value, the more precise or sensitive to variation will be the results. The obtained value was higher than 1%, which means that the method does not meet this requirement.

Table 17 – System suitability parameters obtained for the HPLC system. k' – capacity factor; T – tailing factor; N – theorical plate number; CV – coefficient of variation. (183)

Parameters	Obtained values [(a)]	Recommendation
k'	2.595 ± 0.008	Generally, >2.0
T	1.020 ± 0.062	It should be ≤2
N	7586 ± 133.2	In general, should be >2000
Injection repeatability	32.718 ± 1.302, CV – 2.08%	CV≤1% for N≥5 is desirable

[(a)] n=10, mean value ± SD

Specificity

Method specificity was assessed regarding the possibility of occurring interferences of the components of the lipid nanoparticles on the LEM2 retention time. The existence/absence of any interference was confirmed by comparing the chromatograms of LEM2 standard solution (30 µg/mL) with the supernatant of an unloaded NLC formulation (Figures 47 and 48, respectively). As shown in Figure 48, the supernatant of the unloaded NLC formulation did not exhibit any peak at LEM2 retention time (3.6 minutes). Therefore, no interferences from NLC components were observed, meaning that the method is specific for the purposed application.

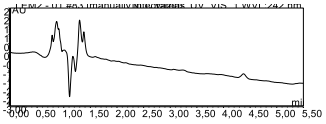

Figure 48 – Chromatogram of the supernatant of a blank NLC formulation.

Linearity

Quantitative analytical methods are highly influenced by the quality of the calibration curve, so it is important to ensure a linear relationship between the peak area and the LEM2 concentration in the standard solutions used – 5, 10, 20, 30, 40, and 48 µg/mL. The standard solutions were injected in triplicate. The calibration curve was obtained by simple linear regression using the minimum squares method. The results (Figure 49) showed a linear relationship between the peak area and LEM2 concentration from 5 to 48 µg/mL and the following general linear equation was obtained: y = 1.0586x + 0.0042, where y is the peak area and x is LEM2 concentration at µg/ml. The high R^2 value, 0.9991, indicates a good linear relationship between the 2 variables and the low RSS value, 0.0015, indicates that the regression model fits the data well (200). Figure 50 shows that the residuals of the concentration values of LEM2 standard solutions are randomly dispersed, reinforcing the linearity of the method.

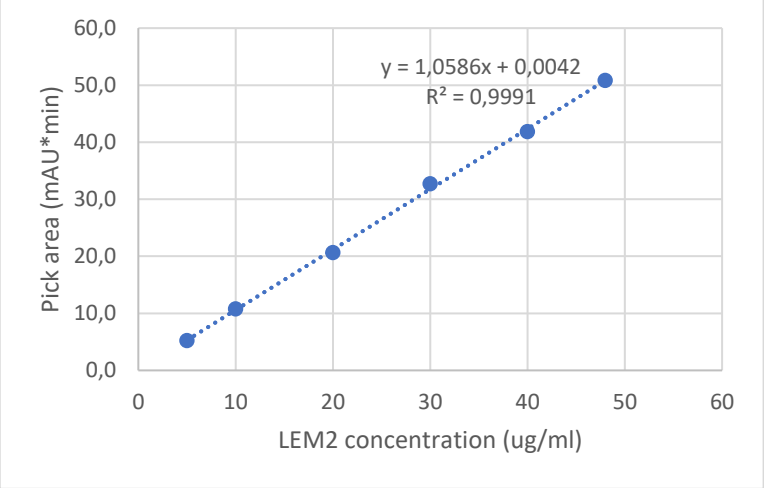

Figure 49 – Calibration curve of peak areas versus LEM2 concentration of standard solutions (5 - 48 µg/mL).

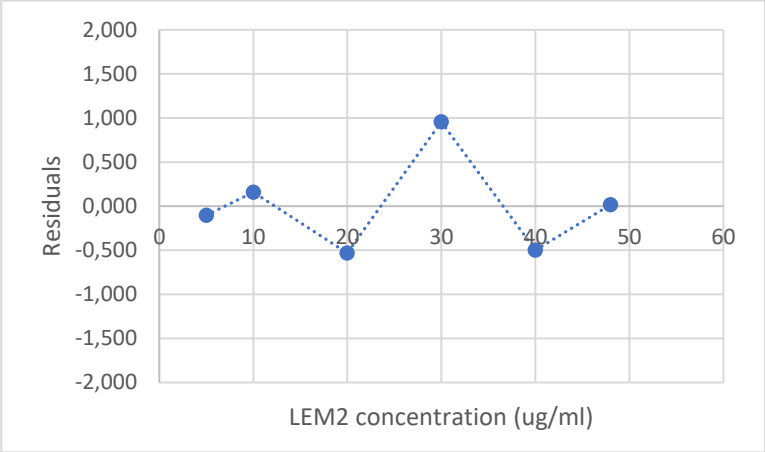

Figure 50 – Graphic representation of the residuals of concentration values of LEM2 standard solutions.

Precision

To study the precision of the method, only reproducibility was assessed. The standard solutions of LEM2 30, 40, and 48 µg/mL were injected in triplicate during the same day and under the same experimental conditions. The CV values obtained (Table 18) are acceptable since the limit is 2%, however, some values slightly exceed the limit which means that HPLC can provide less precise data.

Table 18 – Results obtained for intra-assay precision of the method. SD – standard deviation; CV – coefficient of variation.

Validation parameter	Concentration (ug/ml)	Peak area (mAU*min)	Mean (mAU*min)	SD	CV (%)
Repeatability	30	32.239	32.385	0.745	2.300
		33.192			
		31.724			
	40	41.329	41.516	0.850	2.046
		42.443			
		40.775			
	48	51.037	50.833	0.953	1.876
		49.794			
		51.668			

Accuracy

The accuracy of the method was studied by adding a certain amount of LEM2 standard solution (40 µg/mL) to an unloaded NLC dispersion as described in section 2.3.5.4. The peak area of the resulting supernatant was measured in HPLC and the amount of LEM2 recovered at the end of the procedure was calculated with the linear equation $y = 1.0586x + 0.0042$, where y is the peak area and x is LEM2 concentration (Table 19). The obtained values are close to 100%, ranging from 94-96% approximately, which means that the recovery is satisfactory and, consequently, the method can be expected to be accurate.

Table 19 – Obtained values for recovery studies.

Formulation	Peak area (mAU*min)			Mean (mAU*min)	LEM2 recovered (ug/mL)	Recovery (%)
1 [(a)]	33.925	31.743	31.809	32.492	30.690	96
2 [(a)]	32.964	31.352	30.948	31.755	29.993	94
3 [(a)]	30.625	32.571	32.164	31.787	30.024	94
4 [(b)]	32.976	31.395	33.182	32.518	30.714	96

[(a)] formulation with Cetrimide®

[(b)] formulation without Cetrimide®

3.3.3. Encapsulation Efficacy determination

The EE of LEM2 in NLC was determined by a direct measurement of the drug that was encapsulated in the formulation, as described in section 2.3.5.4. The quantification of LEM2 was performed by HPLC. The peak area of the resulting supernatant was measured by HPLC and the amount of LEM2 in the supernatant was calculated with the following linear equation y = 1.0586x + 0.0042, where y is the peak area and x represents LEM2 concentration. The dilution factor associated to the procedure was 25. The values obtained for EE in formulations containing Cetrimide® are around 43 - 51% (Table 20 – Formulations 1, 2, and 3), whereas the EE obtained for the formulation without Cetrimide® was about 72% (Table 20 – Formulation 4). These low values were already expected and can be justified not only by the non-complete dissolution of the drug in the lipid mixture during the preparation of NLC, but also by the losses caused by the method used to determine the EE of LEM2. This increase in EE in LEM2-loaded NLC without Cetrimide® could be the reason why particle size has also increased significantly comparing with the sizes of LEM2-loaded containing Cetrimide®.

Table 20 – Results achieved for encapsulation efficiency (EE) of LEM2 in NLC.

Formulation	Peak area (mAU*min)			Mean (mAU*min)	LEM2 concentration (ug/ml)	EE (%)
1 [(a)]	17.964	20.591	20.167	19.574	18.487	46
2 [(a)]	22.569	21.075	21.239	21.628	20.427	51
3 [(a)]	19.198	17.852	17.977	18.342	17.323	43
4 [(b)]	33.910	27.879	29.625	30.472	28.780	72

[(a)] formulation with Cetrimide®

[(b)] formulation without Cetrimide®

3.4. *In vitro* assays

3.4.1. Effect of lipid nanoparticles on cell growth

Before applying NLC as a drug delivery system its potential cytotoxicity was determined. The cytotoxicity of both unloaded NLC and LEM2-loaded NLC against A375 melanoma cells was investigated using the SRB assay, and the GI_{50} was calculated.

The results obtained with LEM2-loaded NLC and unloaded NLC, using a formulation with Cetrimide® (Figure 51), showed that these nanoparticles were toxic to the cells. The same corresponding amount of unloaded NLC had a similar growth inhibitory effect on cells to LEM2-loaded NLC. It was not expected such toxicity due to NLC components, however Cetrimide® used in the formulation to improve stability and adjust zeta potential is a component that can cause cell damage by emulsification of the cell wall lipids (201–203). In fact, it has been demonstrated that Cetrimide® and other quaternary ammonium surfactants can be toxic to some types of cells (201,204–207). Therefore, the same experiment was performed with a Cetrimide® solution with the same concentration used in the formulation (3 mM). The results showed that a concentration of Cetrimide® above 0.157 µM also causes cell death (Figure 52), which indicated that the toxicity of the nanoparticles prepared was probably due to this component. Because of that, the followed *in vitro* studies were performed using formulations without Cetrimide®.

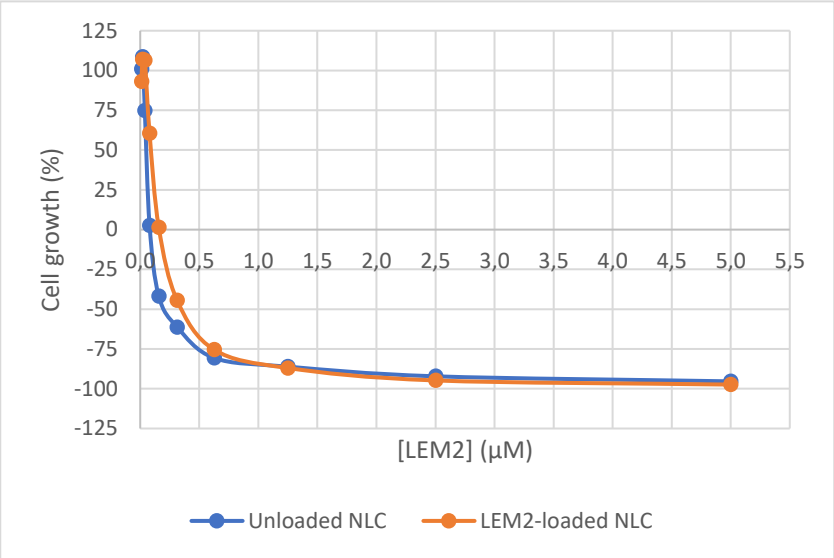

Figure 51 – Dose-response curves for the growth inhibitory activity of 0.010 - 5 µM of LEM2 in NLC (formulation with Cetrimide®) and unloaded NLC in A375 melanoma cells, determined by SRB assay, after 48 hours of treatment (n=4).

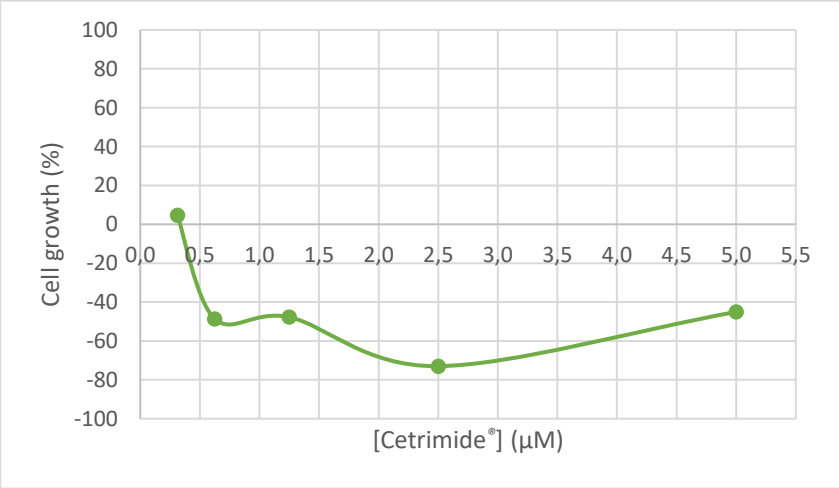

Figure 52 – Dose-response curve for the growth inhibitory effect activity of 0.313 - 5 µM of a Cetrimide® solution in A375 melanoma cells, determined by SRB assay, after 48 hours of treatment (n=4).

Without Cetrimide®, the developed nanoparticles were less toxic to the cells (Figure 53). For LEM2 concentrations between 0.313 and 1.250 µM, loaded NLC inhibited cell growth, causing cell death for concentrations above 1.250 µM, with a higher potency than unloaded NLC. The inhibited cell growth and induction of cell death by unloaded NLC were not expected since NLCs are composed of safe and well-tolerated FDA GRAS substances. Despite this, loaded nanoparticles showed to be more cytotoxic than unloaded NLC, possibly due to LEM2 antitumor activity, which means that NLCs could be used as a vehicle to this drug, improving its bioavailability problems. The GI_{50} value of LEM2-loaded NLC was equal to 1.0 µM.

Despite this, we wanted to know if the encapsulation would interfere with the molecular mechanism of action previously described for LEM2 (135). With this aim the following analysis were carried out.

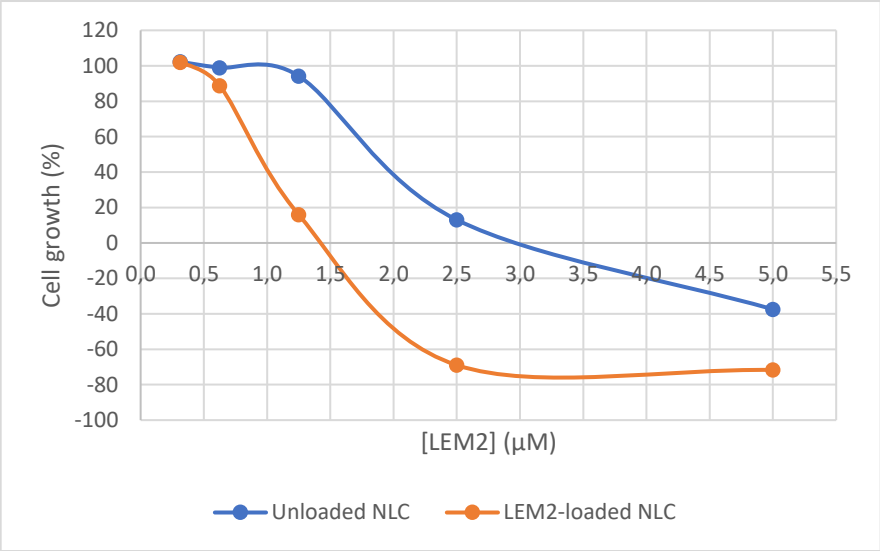

Figure 53 – Dose-response curves for the growth inhibitory activity of 0.313 - 5 µM of LEM2 in NLC (formulation without Cetrimide®) and unloaded NLC in A375 melanoma cells, determined by SRB assay, after 48 hours of treatment (n=4).

3.4.2. Effects of LEM2-loaded NLC on apoptosis and cell cycle arrest

The effects of LEM2-loaded NLC on apoptosis in A375 cells was determined for 48 hours treatment with trypan-blue assay. The results showed that LEM2-loaded NLC induced apoptosis on A375 cells in both tested concentrations after 48h treatment (Figure 54). Only

10.9 ± 0.5 % of dead cells were observed in control group whereas the percentage of dead cells increased up to 23.6 ± 0.9 % and 35.3 ±1.9 % in cells treated with GI_{50} (1 µM) and $2GI_{50}$ (2 µM) concentration, respectively. These results indicate that the LEM2-loaded NLC has a marked and dose-dependent effect on cellular apoptosis in A375 cells.

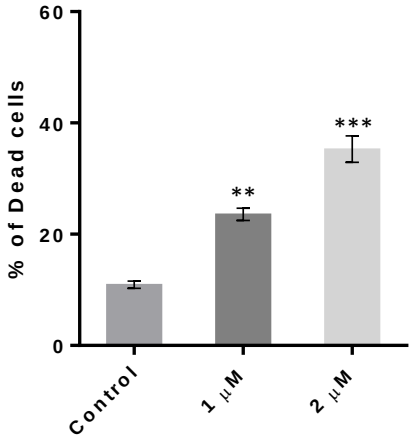

Figure 54 – Percentage of cell death induced by LEM2-loaded NLC was determined for 48 hours treatment by trypan-blue assay in A375 cells; data are mean ± SEM of three independent experiments. Values significantly different from control (**p < 0.01, ***p<0.001), unpaired Student's t-test.

The effect of LEM2-loaded NLC on the cell cycle of A375 melanoma cells was also evaluated. Thereby, the nuclear DNA content of the cells was analyzed by flow cytometry following 24 hours treatment with LEM2-loaded NLC. The results showed that in cells treated with the GI_{50} concentration of LEM2-loaded NLC (1 µM) there were no major alterations in the percentage of cells in different phases of the cell cycle (Figure 55). However, in cells treated with $2xGI_{50}$ concentration (2 µM) there was a statistically significant increase in the percentage of cells in the G2/M phase of the cell cycle (Figure 55). The results therefore suggested that LEM2-loaded NLC induced cell cycle arrest in G2/M phase.

Consistently, in our previous work, it was shown that LEM2 induced G2/M phase cell cycle arrest and apoptosis in colon adenocarcinoma HCT116 cells (2 µM) and in breast adenocarcinoma MDA-MB-468 cells (1.5 µM) (136).

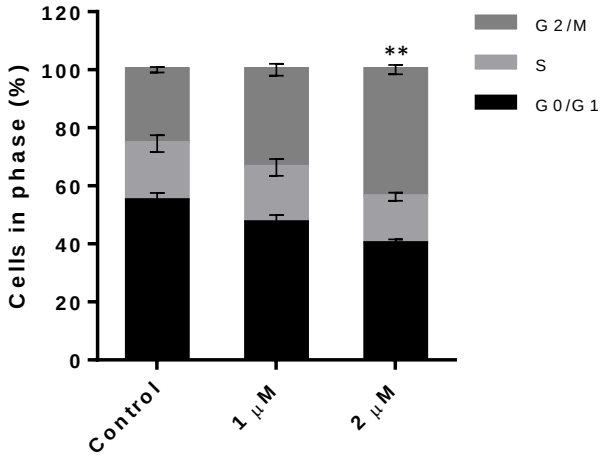

Figure 55 – Cell cycle arrest was determined for 24 hours treatment with LEM2-loaded NLC in A375 cells; data are mean ± SEM of three independent experiments. Values significantly different from control (**p < 0.01), unpaired Student's t-test.

3.4.3. Western blot analyses

In the study developed by Gomes et al., the LEM2-induced growth inhibition was also associated with regulation of many p53-family transcriptional targets, in different cell lines (135). In particular, in colon adenocarcinoma HCT116 cells (1 μM), the treatment with LEM2 increased the protein levels of TAp73α, MDM2, p21, and BAX, while reduced Bcl-2; in breast adenocarcinoma MDA-MB-468 cells (1.5 μM), LEM2 increased the protein levels of TAp73α, p21, and PUMA, and decreased Bcl-2; and in neuroblastoma SH-SY5Y cells, it increased TAp73α, p21, MDM2, and BAX (1.4 μM) (135).

In order to confirm that the mechanism of LEM2 anticancer effects was conserved in LEM2-loaded NLC, the protein expression levels of numerous key targets of TAp73α, involved in the cell cycle and apoptosis, were assessed by western blot analysis after 24 hours of treatment.

The results showed that the treatment with LEM2-loaded NLC increased the expression levels of p73, p21, PUMA, BAX, and MDM2, while reducing BCL-2 (Figure 56).

These results were already expected since LEM2 can activate TAp73 by disrupting its interaction with mutant p53 and/or MDM2. Activated TAp73 is able to regulate the transcription of p53 target genes, like *CDKN1A* (*p21*; cell cycle arrest), *PUMA*, *BAX,* and *BCL-2* (apoptosis) (208).

These results showed that the used nanoparticles did not interfere with LEM2 molecular mechanism of action.

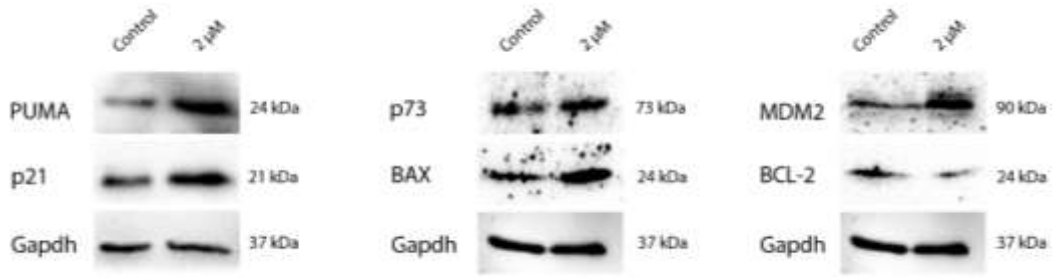

Figure 56 – Analysis of protein levels of p73 target genes. Western blot analysis was performed after 24 hours treatments with LEM2-loaded NLC in A375 cells. Immunoblots are representative of three independent experiments.

Chapter IV – Conclusions

Skin cancer affects many people worldwide, especially Caucasians, and its incidence continues to increase year after year. Of all types of skin cancer, the most worrying is melanoma because it is the most aggressive form of cancer and can even cause death. Therefore, it is important to improve skin cancer treatment efficacy. In this perspective, topical treatment of skin diseases is very appealing, comparing with oral or parenteral drug administration, mainly because systemic load of drug and thus also systemic side effects are reduced (these formulations should let the drug reach the epidermis and the dermis only). Besides, the topical administration of drugs may increase patient acceptability, since it is noninvasive.

LEM2 is a synthetic xanthone with tested antitumor effect in melanoma A375 cell line (unpublished work). However, this compound presents poor aqueous solubility, which is often related with poor bioavailability, limiting its therapeutic use. The use of nanoparticles to encapsulate drugs can improve their bioavailability and particularly the use of lipid nanoparticles seems to be very interesting for topical delivery of drugs due to their adhesion and occlusive properties.

In this work, both types of lipid nanoparticles produced by either ultrasonication or hot HPH showed good and similar physical characteristics after their production, mainly particle size. However, by the analyses of the stability studies (60 days), it was found that SLNs produced by the two methods can be physically instable, because there was an increase of the particle size, suggesting that particle aggregation occurred. On the other hand, the NLCs produced by both methods appear to be stable. During the production of lipid nanoparticles, it was noted that the ultrasonication method is easier and faster when compared with hot HPH. Given these results, LEM2 was encapsulated in NLCs using the ultrasonication method. It was noted that LEM2 has relatively poor solubility in the lipid mixture, which affected the encapsulation efficiency (EE), 50% approximately.

The new loaded lipid nanoparticles prepared without Cetrimide® had a higher EE, 72% approximately, and a larger mean particle size (also suitable for topical application). The stability tests revealed that particle size and ZP increased over the time. This highlights the importance of the cationic compound (Cetrimide®) for adjusting ZP and for preventing particle

agglomeration. Unloaded NLCs without Cetrimide® showed some unexpected cytotoxicity to melanoma A375 cell line. Loaded NLCs seemed to be more cytotoxic against melanoma A375 cell line than unloaded NLC, possibly due to LEM2 antitumor activity, which means that NLCs could be used as a vehicle to this drug, improving its bioavailability problems. Besides, the used nanoparticles did not interfere with LEM2 molecular mechanism of action.

Chapter V – Future work

In a future work, before doing further *in vitro* tests, it is important reconsider and improve the lipid nanoparticle formulations. First, as the drug has poor solubility in the lipids mixture, more drug-in-lipid solubility tests should be done before the development of new lipid nanoparticles, because this problem will influence the EE and subsequent effectiveness of these nanoparticles. More parameters should be used to characterize the lipid nanoparticles, for more reliable information, such as degree of crystallinity and lipid modification by differential scanning calorimetry, and surface morphology by scanning electron microscopy. In addition, the stability tests should be done for a long period of time. The cytotoxicity of the new lipid nanoparticles should also be evaluated. Then, since dispersions of lipid nanoparticles have low viscosity, they need to be incorporated into dermatological bases, such as creams or gels, in order to have a suitable semisolid consistency for topical application. The semisolid formulation should be characterized through rheological measurements, texture and color analyses, and stability tests should be performed for a significant period of time.

Appendix

Appendix I

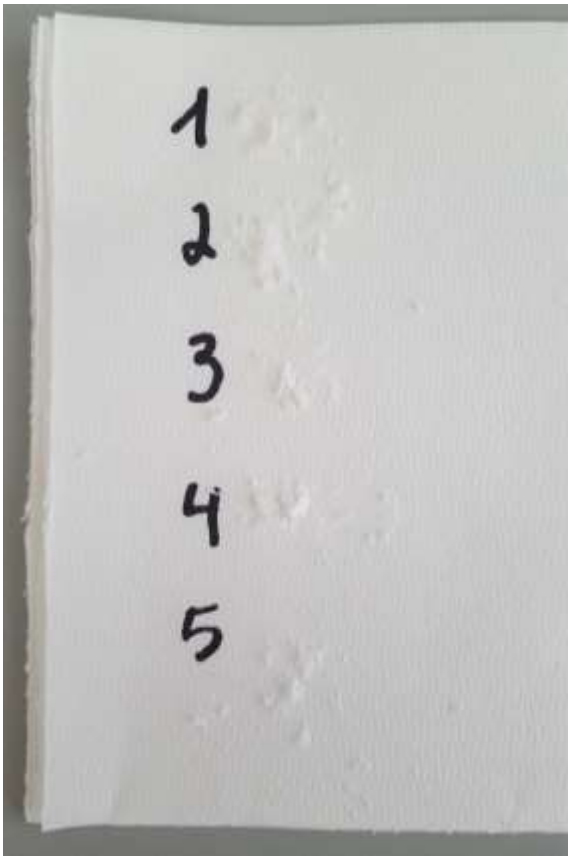

Figure 57 – Cooled samples of the lipid mixture between Precirol® ATO 5 and oleic acid. The numbers on the filter paper represents the proportions used, beginning in 50:50 until 60:40 (solid lipid: liquid lipid).

Appendix II

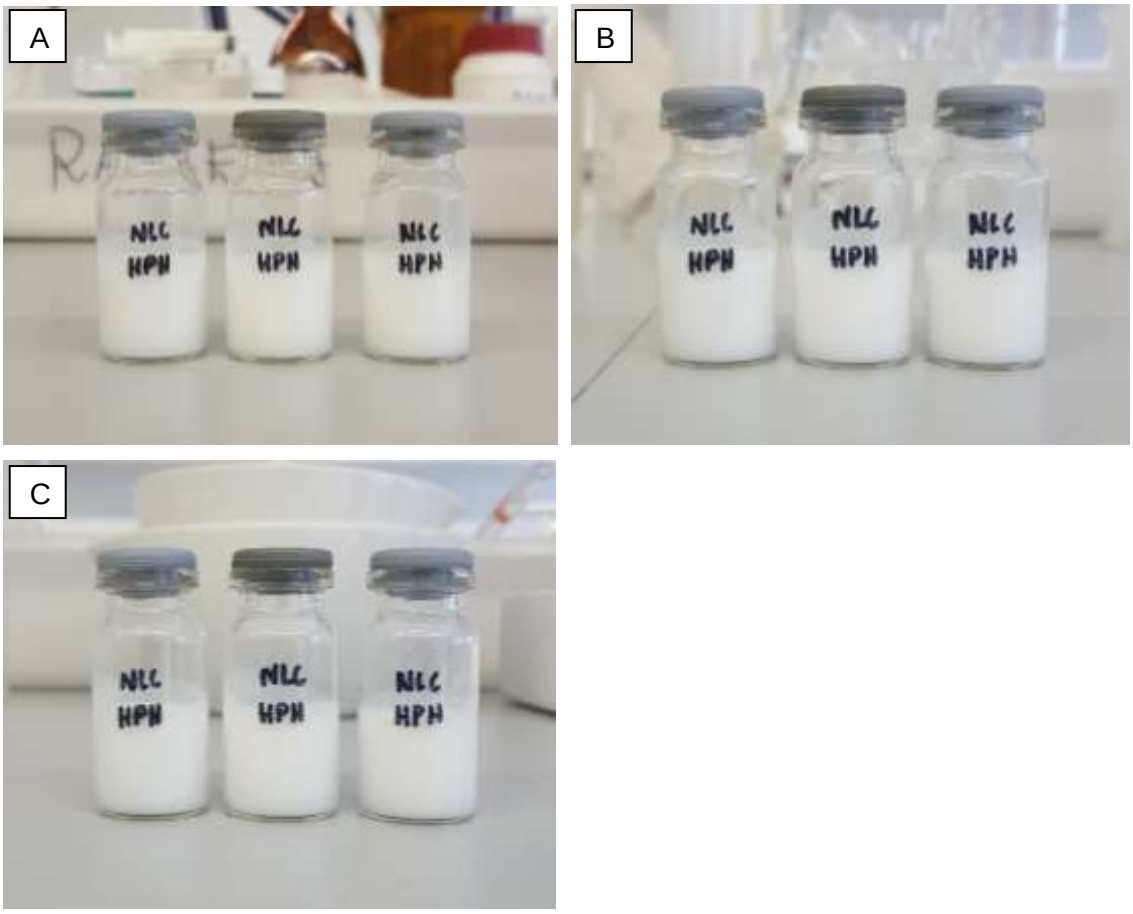

Figure 58 – Aspect of unloaded NLC dispersions prepared by hot HPH (A) after their preparation and after (B) 30 and (C) 60 days of storage at 4 ºC.

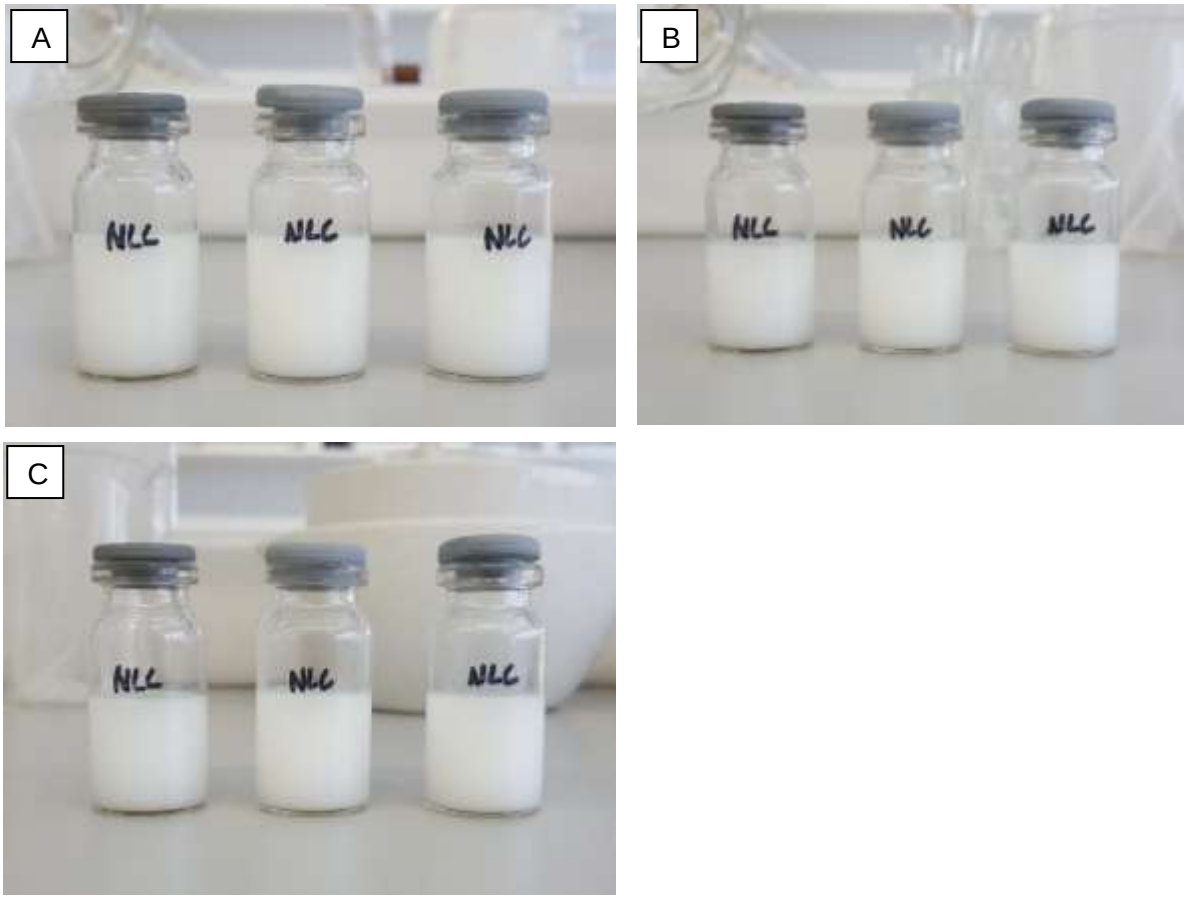

Figure 59 – Aspect of unloaded NLC dispersions prepared by ultrasonication (A) after their preparation and after (B) 30 and (C) 60 days of storage at 4 ºC.

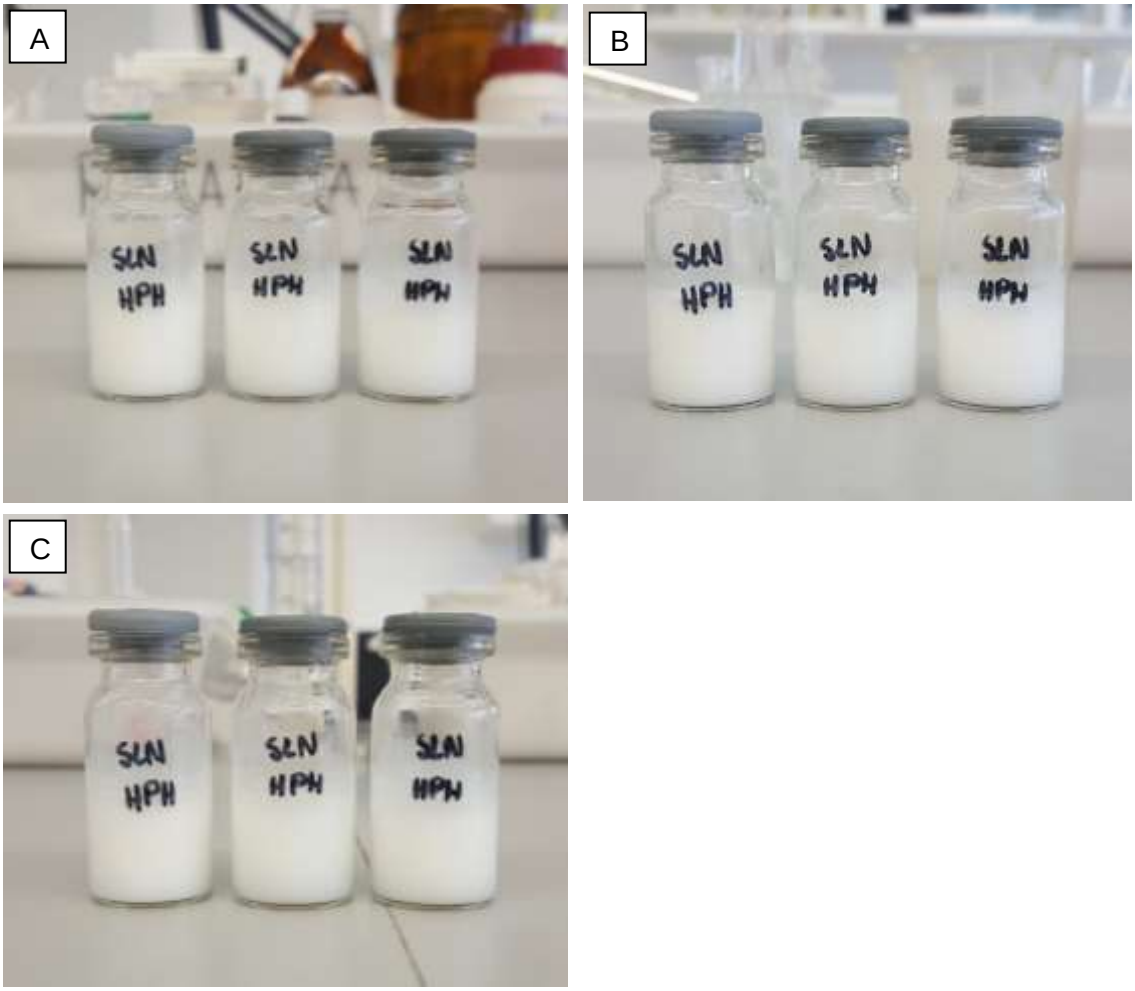

Figure 60 – Aspect of unloaded SLN dispersions prepared by hot HPH (A) after their preparation and after (B) 30 and (C) 60 days of storage at 4 ºC.

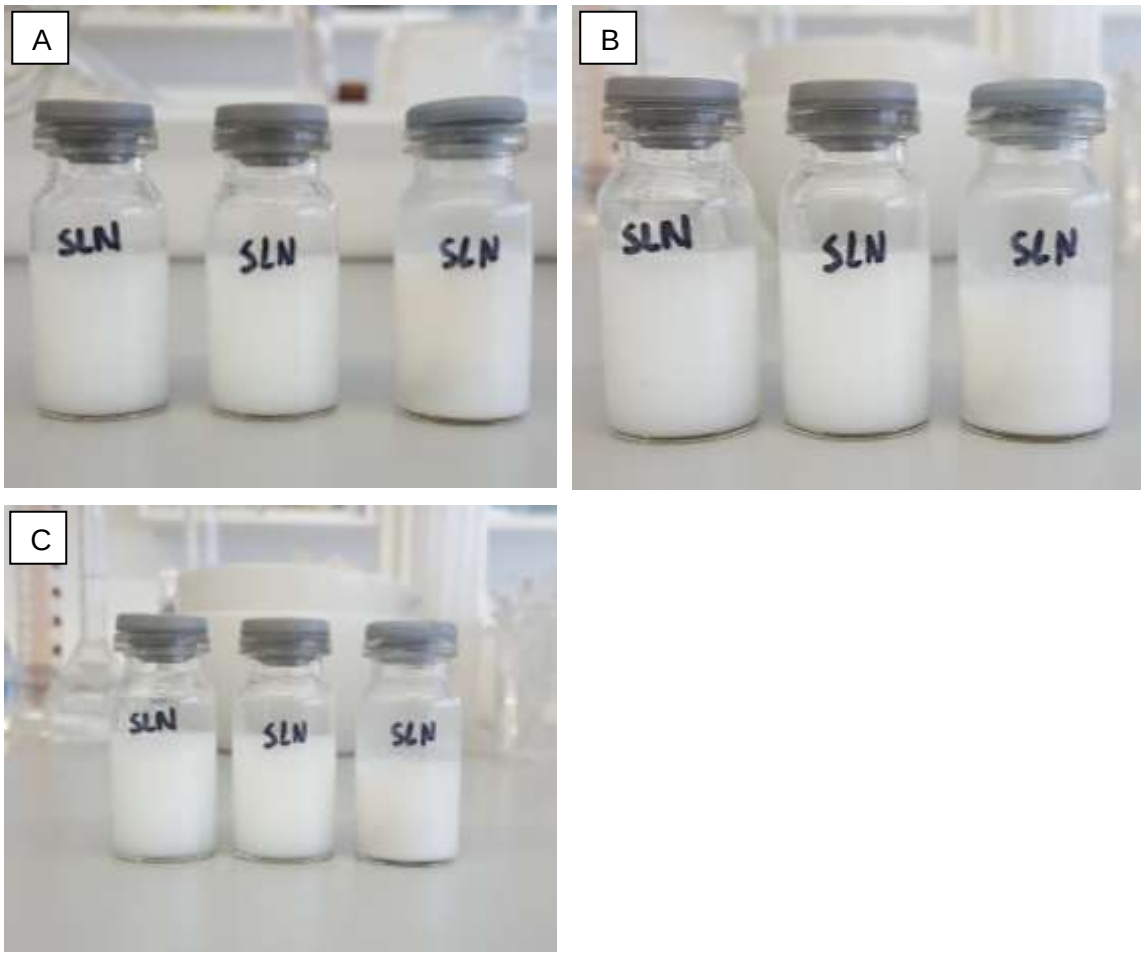

Figure 61 – Aspect of unloaded SLN dispersions prepared by ultrasonication (A) after their preparation and after (B) 30 and (C) 60 days of storage at 4 ºC.

References

1. Gordon R. Skin Cancer: An Overview of Epidemiology and Risk Factors. Semin Oncol Nurs [Internet]. 2013 Aug;29(3):160–9. Available from: https://linkinghub.elsevier.com/retrieve/pii/S0749208113000326
2. Apalla Z, Lallas A, Sotiriou E, Lazaridou E, Ioannides D. Epidemiological trends in skin cancer. Dermatol Pract Concept. 2017;
3. Goyal N, Thatai P, Sapra B. Skin cancer: Symptoms, mechanistic pathways and treatment rationale for therapeutic delivery. Therapeutic Delivery. 2017.
4. Mueller CSL, Reichrath J. Histology of melanoma and nonmelanoma skin cancer. Advances in Experimental Medicine and Biology. 2008.
5. Böni R, Schuster C, Nehrhoff B, Burg G. Epidemiology of skin cancer. Neuroendocrinol Lett. 2002;
6. Gupta V, Trivedi P. In vitro and in vivo characterization of pharmaceutical topical nanocarriers containing anticancer drugs for skin cancer treatment. In: Lipid Nanocarriers for Drug Targeting. 2018.
7. Chang AE, Karnell LH, Menck HR. The national cancer data base report on cutaneous and noncutaneous melanoma: A summary of 84,836 cases from the past decade. Cancer. 1998;
8. Mattia G, Puglisi R, Ascione B, Malorni W, Carè A, Matarrese P. Cell death-based treatments of melanoma:conventional treatments and new therapeutic strategies. Cell Death Dis [Internet]. 2018 Feb 25;9(2):112. Available from: http://www.nature.com/articles/s41419-017-0059-7
9. Geller AC, Clapp RW, Sober AJ, Gonsalves L, Mueller L, Christiansen CL, et al. Melanoma epidemic: An analysis of six decades of data from the connecticut tumor registry. J Clin Oncol. 2013;
10. World Cancer Research Fund - Skin Cancer Statistics [Internet]. 2018 [cited 2019 Jun 17]. Available from: https://www.wcrf.org/dietandcancer/cancer-trends/skin-cancer-statistics
11. Bray F, Ferlay J, Soerjomataram I, Siegel RL, Torre LA, Jemal A. Global cancer statistics 2018: GLOBOCAN estimates of incidence and mortality worldwide for 36 cancers in 185 countries. CA Cancer J Clin. 2018;
12. Bandarchi B, Ma L, Navab R, Seth A, Rasty G. From Melanocyte to Metastatic Malignant Melanoma. Dermatol Res Pract. 2010;
13. Tsao H, Olazagasti JM, Cordoro KM, Brewer JD, Taylor SC, Bordeaux JS, et al. Early detection of melanoma: Reviewing the ABCDEs. J Am Acad Dermatol [Internet]. 2015 Apr;72(4):717–23. Available from: https://linkinghub.elsevier.com/retrieve/pii/S0190962215000900
14. Helsing P, Loeb M. Small diameter melanoma: A follow-up of the Norwegian Melanoma Project. Br J Dermatol. 2004;
15. Cummins DL, Cummins JM, Pantle H, Silverman MA, Leonard AL, Chanmugam A. Cutaneous malignant melanoma. Mayo Clinic Proceedings. 2006.
16. Bataille V, De Vries E. Melanoma - Part 1: Epidemiology, risk factors, and prevention. BMJ. 2008.
17. Gallagher RP, Lee TK. Adverse effects of ultraviolet radiation: A brief review. Prog Biophys Mol Biol [Internet]. 2006 Sep;92(1):119–31. Available from: https://linkinghub.elsevier.com/retrieve/pii/S0079610706000137
18. Fahradyan A, Howell A, Wolfswinkel E, Tsuha M, Sheth P, Wong A. Updates on the Management of Non-Melanoma Skin Cancer (NMSC). Healthcare. 2017;
19. Eide MJ, Krajenta R, Johnson D, Long JJ, Jacobsen G, Asgari MM, et al. Identification of patients with nonmelanoma skin cancer using health maintenance organization claims data. Am J Epidemiol. 2010;
20. Samarasinghe V, Madan V, Lear JT. Focus on Basal Cell Carcinoma. J Skin Cancer [Internet]. 2011;2011:1–5. Available from: http://www.hindawi.com/journals/jsc/2011/328615/
21. Ting PT, Kasper R, Arlette JP. Metastatic basal cell carcinoma: Report of two cases and literature review. Journal of Cutaneous Medicine and Surgery. 2005.
22. McCormack CJ, Kelly JW, Dorevitch AP. Differences in age and body site distribution of the histological subtypes of basal cell carcinoma. A possible indicator of differing causes. Arch Dermatol. 1997;
23. Nakayama M, Tabuchi K, Nakamura Y, Hara A. Basal cell carcinoma of the head and neck. Eisele DW, editor. Head Neck [Internet]. 2012 Sep;34(9):1346–54. Available from: http://doi.wiley.com/10.1002/hed.21787
24. Didona D, Paolino G, Bottoni U, Cantisani C. Non Melanoma Skin Cancer Pathogenesis Overview. Biomedicines. 2018;
25. Stulberg DL, Crandell B, Fawcett RS. Diagnosis and treatment of basal cell and squamous cell carcinomas. American Family Physician. 2004.
26. Graham GF, Tuchayi SM. Squamous Cell Carcinoma. In: Dermatological Cryosurgery and Cryotherapy [Internet]. London: Springer London; 2016. p. 667–74. Available from: http://link.springer.com/10.1007/978-1-4471-6765-5_131
27. H. Muller R, Shegokar R, M. Keck C. 20 Years of Lipid Nanoparticles (SLN & NLC): Present State of Development & Industrial Applications. Curr Drug Discov Technol. 2011;

28. Beloqui A, Solinís MÁ, Rodríguez-Gascón A, Almeida AJ, Préat V. Nanostructured lipid carriers: Promising drug delivery systems for future clinics. Nanomedicine: Nanotechnology, Biology, and Medicine. 2016.
29. Pardeike J, Hommoss A, Müller RH. Lipid nanoparticles (SLN, NLC) in cosmetic and pharmaceutical dermal products. International Journal of Pharmaceutics. 2009.
30. Ghasemiyeh P, Mohammadi-Samani S. Solid lipid nanoparticles and nanostructured lipid carriers as novel drug delivery systems: Applications, advantages and disadvantages. Research in Pharmaceutical Sciences. 2018.
31. Saez V, Souza IDL, Mansur CRE. Lipid nanoparticles (SLN & NLC) for delivery of vitamin E: a comprehensive review. Int J Cosmet Sci [Internet]. 2018 Apr;40(2):103–16. Available from: http://doi.wiley.com/10.1111/ics.12452
32. Yoon G, Park JW, Yoon I-S. Solid lipid nanoparticles (SLNs) and nanostructured lipid carriers (NLCs): recent advances in drug delivery. J Pharm Investig [Internet]. 2013 Oct 11;43(5):353–62. Available from: http://link.springer.com/10.1007/s40005-013-0087-y
33. Müller RH, Petersen RD, Hommoss A, Pardeike J. Nanostructured lipid carriers (NLC) in cosmetic dermal products. Advanced Drug Delivery Reviews. 2007.
34. Severino P, Andreani T, Macedo AS, Fangueiro JF, Santana MHA, Silva AM, et al. Current State-of-Art and New Trends on Lipid Nanoparticles (SLN and NLC) for Oral Drug Delivery. J Drug Deliv. 2012;
35. Müller RH, Radtke M, Wissing SA. Solid lipid nanoparticles (SLN) and nanostructured lipid carriers (NLC) in cosmetic and dermatological preparations. In: Advanced Drug Delivery Reviews. 2002.
36. Mehnert W, Mäder K. Solid lipid nanoparticles: Production, characterization and applications. Advanced Drug Delivery Reviews. 2012.
37. Doktorovova S, Shegokar R, Souto EB. Role of Excipients in formulation development and biocompatibility of lipid nanoparticles (SLNs/NLCs). In: Nanostructures for Novel Therapy: Synthesis, Characterization and Applications. 2017.
38. Pardeike J, Weber S, Haber T, Wagner J, Zarfl HP, Plank H, et al. Development of an Itraconazole-loaded nanostructured lipid carrier (NLC) formulation for pulmonary application. Int J Pharm. 2011;
39. Chinsriwongkul A, Chareanputtakhun P, Ngawhirunpat T, Rojanarata T, Sila-on W, Ruktanonchai U, et al. Nanostructured Lipid Carriers (NLC) for Parenteral Delivery of an Anticancer Drug. AAPS PharmSciTech. 2012;
40. Andalib S, Varshosaz J, Hassanzadeh F, Sadeghi H. Optimization of LDL targeted nanostructured lipid carriers of 5-FU by a full factorial design. Adv Biomed Res. 2012;
41. Gönüllü Ü, Üner M, Yener G, Karaman EF, Aydoğmuş Z. Formulation and characterization of solid lipid nanoparticles, nanostructured lipid carriers and nanoemulsion of lornoxicam for transdermal delivery. Acta Pharm [Internet]. 2015 Mar 1;65(1):1–13. Available from: http://content.sciendo.com/view/journals/acph/65/1/article-p1.xml
42. Kelidari HR, Saeedi M, Akbari J, Morteza-semnani K, Valizadeh H, Maniruzzaman M, et al. Development and Optimisation of Spironolactone Nanoparticles for Enhanced Dissolution Rates and Stability. AAPS PharmSciTech. 2017;
43. Charoenputtakhun P, Opanasopit P, Rojanarata T, Ngawhirunpat T. All-trans retinoic acid-loaded lipid nanoparticles as a transdermal drug delivery carrier. Pharm Dev Technol [Internet]. 2014 Mar 28;19(2):164–72. Available from: http://www.tandfonline.com/doi/full/10.3109/10837450.2013.763261
44. Morales JO, Valdés K, Morales J, Oyarzun-Ampuero F. Lipid nanoparticles for the topical delivery of retinoids and derivatives. Nanomedicine. 2015.
45. Štecová J, Mehnert W, Blaschke T, Kleuser B, Sivaramakrishnan R, Zouboulis CC, et al. Cyproterone Acetate Loading to Lipid Nanoparticles for Topical Acne Treatment: Particle Characterisation and Skin Uptake. Pharm Res [Internet]. 2007 Apr 12;24(5):991–1000. Available from: http://link.springer.com/10.1007/s11095-006-9225-9
46. Tan SW, Billa N, Roberts CR, Burley JC. Surfactant effects on the physical characteristics of Amphotericin B-containing nanostructured lipid carriers. Colloids Surfaces A Physicochem Eng Asp. 2010;
47. Kuo YC, Chung JF. Physicochemical properties of nevirapine-loaded solid lipid nanoparticles and nanostructured lipid carriers. Colloids Surfaces B Biointerfaces. 2011;
48. Hu F-Q, Jiang S-P, Du Y-Z, Yuan H, Ye Y-Q, Zeng S. Preparation and characterization of stearic acid nanostructured lipid carriers by solvent diffusion method in an aqueous system. Colloids Surfaces B Biointerfaces [Internet]. 2005 Nov;45(3–4):167–73. Available from: https://linkinghub.elsevier.com/retrieve/pii/S092777650500247X
49. Xie S, Zhu L, Dong Z, Wang X, Wang Y, Li X, et al. Preparation, characterization and pharmacokinetics of enrofloxacin-loaded solid lipid nanoparticles: Influences of fatty acids. Colloids Surfaces B Biointerfaces [Internet]. 2011 Apr;83(2):382–7. Available from: https://linkinghub.elsevier.com/retrieve/pii/S0927776510006995
50. Khare A, Singh I, Pawar P, Grover K. Design and Evaluation of Voriconazole Loaded Solid Lipid Nanoparticles for Ophthalmic Application. J Drug Deliv. 2016;
51. Zara GP, Bargoni A, Cavalli R, Fundarò A, Vighetto D, Gasco MR. Pharmacokinetics and tissue

distribution of idarubicin-loaded solid lipid nanoparticles after duodenal administration to rats. J Pharm Sci. 2002;
52. Leiva MC, Ortiz R, Contreras-Cáceres R, Perazzoli G, Mayevych I, López-Romero JM, et al. Tripalmitin nanoparticle formulations significantly enhance paclitaxel antitumor activity against breast and lung cancer cells in vitro. Sci Rep. 2017;
53. Naguib YW, Rodriguez BL, Li X, Hursting SD, Williams RO, Cui Z. Solid lipid nanoparticle formulations of docetaxel prepared with high melting point triglycerides: In vitro and in vivo evaluation. Mol Pharm. 2014;
54. Gupta S, Kesarla R, Chotai N, Misra A, Omri A. Systematic Approach for the Formulation and Optimization of Solid Lipid Nanoparticles of Efavirenz by High Pressure Homogenization Using Design of Experiments for Brain Targeting and Enhanced Bioavailability. Biomed Res Int. 2017;
55. Raj R, Raj PM, Ram A. Preparation and characterization of solid lipid nanoparticles loaded with cytarabine: Via a micellar composition for leukemia. RSC Adv. 2016;
56. Oliveira DRB, Furtado G de F, Cunha RL. Solid lipid nanoparticles stabilized by sodium caseinate and lactoferrin. Food Hydrocoll. 2019;
57. Salvia-Trujillo L, Verkempinck S, Rijal SK, Van Loey A, Grauwet T, Hendrickx M. Lipid nanoparticles with fats or oils containing β-carotene: Storage stability and in vitro digestibility kinetics. Food Chem. 2019;
58. Nguyen HM, Hwang IC, Park JW, Park HJ. Enhanced payload and photo-protection for pesticides using nanostructured lipid carriers with corn oil as liquid lipid. J Microencapsul. 2012;
59. Zhang T, Chen J, Zhang Y, Shen Q, Pan W. Characterization and evaluation of nanostructured lipid carrier as a vehicle for oral delivery of etoposide. Eur J Pharm Sci. 2011;
60. Pathak P, Nagarsenker M. Formulation and Evaluation of Lidocaine Lipid Nanosystems for Dermal Delivery. AAPS PharmSciTech. 2009;
61. Gide PS, Gidwani SK, Kothule KU. Enhancement of transdermal penetration and bioavailability of poorly soluble acyclovir using solid lipid nanoparticles incorporated in gel cream. Indian J Pharm Sci [Internet]. 2013 Mar;75(2):138–42. Available from: http://www.ncbi.nlm.nih.gov/pubmed/24019560
62. Üner M, Karaman E, Aydoğmuş Z. Solid Lipid Nanoparticles and Nanostructured Lipid Carriers of Loratadine for Topical Application: Physicochemical Stability and Drug Penetration through Rat Skin. Trop J Pharm Res [Internet]. 2014 Sep 9;13(5):653. Available from: http://www.ajol.info/index.php/tjpr/article/view/107471
63. Lúcio M, Carvalho A, Lopes I, Gonçalves O, Bárbara E, Oliveira M. Polymeric Versus Lipid Nanoparticles: Comparative Study of Nanoparticulate Systems as Indomethacin Carriers. J Appl Solut Chem Model. 2015;
64. Boreham A, Volz P, Peters D, Keck CM, Alexiev U. Determination of nanostructures and drug distribution in lipid nanoparticles by single molecule microscopy. Eur J Pharm Biopharm. 2017;
65. El-Housiny S, Eldeen MAS, El-Attar YA, Salem HA, Attia D, Bendas ER, et al. Fluconazole-loaded solid lipid nanoparticles topical gel for treatment of pityriasis versicolor: Formulation and clinical study. Drug Deliv. 2018;
66. El-Say KM, Hosny KM. Optimization of carvedilol solid lipid nanoparticles: An approach to control the release and enhance the oral bioavailability on rabbits. Ahmad A, editor. PLoS One [Internet]. 2018 Aug 30;13(8):e0203405. Available from: http://dx.plos.org/10.1371/journal.pone.0203405
67. Huang ZR, Hua SC, Yang YL, Fang JY. Development and evaluation of lipid nanoparticles for camptothecin delivery: A comparison of solid lipid nanoparticles, nanostructured lipid carriers, and lipid emulsion. Acta Pharmacol Sin. 2008;
68. Chen C-C, Tsai T-H, Huang Z-R, Fang J-Y. Effects of lipophilic emulsifiers on the oral administration of lovastatin from nanostructured lipid carriers: Physicochemical characterization and pharmacokinetics. Eur J Pharm Biopharm [Internet]. 2010 Mar;74(3):474–82. Available from: https://linkinghub.elsevier.com/retrieve/pii/S0939641110000020
69. Araújo J, Nikolic S, Egea MA, Souto EB, Garcia ML. Nanostructured lipid carriers for triamcinolone acetonide delivery to the posterior segment of the eye. Colloids Surfaces B Biointerfaces [Internet]. 2011 Nov;88(1):150–7. Available from: https://linkinghub.elsevier.com/retrieve/pii/S0927776511003742
70. Madan J, Dua K, Khude P. Development and evaluation of solid lipid nanoparticles of mometasone furoate for topical delivery. Int J Pharm Investig. 2014;
71. Tatke A, Dudhipala N, Janga K, Balguri S, Avula B, Jablonski M, et al. In Situ Gel of Triamcinolone Acetonide-Loaded Solid Lipid Nanoparticles for Improved Topical Ocular Delivery: Tear Kinetics and Ocular Disposition Studies. Nanomaterials. 2018;
72. Zhao Y, Chang YX, Hu X, Liu CY, Quan LH, Liao YH. Solid lipid nanoparticles for sustained pulmonary delivery of Yuxingcao essential oil: Preparation, characterization and in vivo evaluation. Int J Pharm. 2017;
73. Montenegro L, Panico A, Santagati L, Siciliano E, Intagliata S, Modica M. Solid Lipid Nanoparticles Loading Idebenone Ester with Pyroglutamic Acid: In Vitro Antioxidant Activity and In Vivo Topical Efficacy. Nanomaterials. 2018;
74. Neves AR, Queiroz JF, Weksler B, Romero IA, Couraud PO, Reis S. Solid lipid nanoparticles as a vehicle for brain-targeted drug delivery: Two new strategies of functionalization with apolipoprotein e.

Nanotechnology. 2015;
75. Ali H, El-Sayed K, Sylvester PW, Nazzal S. Molecular interaction and localization of tocotrienol-rich fraction (TRF) within the matrices of lipid nanoparticles: Evidence studies by Differential Scanning Calorimetry (DSC) and Proton Nuclear Magnetic Resonance spectroscopy (1H NMR). Colloids Surfaces B Biointerfaces. 2010;
76. Madureira AR, Nunes S, Campos DA, Fernandes JC, Marques C, Zuzarte M, et al. Safety profile of solid lipid nanoparticles loaded with rosmarinic acid for oral use: In vitro and animal approaches. Int J Nanomedicine. 2016;
77. Mitri K, Shegokar R, Gohla S, Anselmi C, Müller RH. Lipid nanocarriers for dermal delivery of lutein: Preparation, characterization, stability and performance. Int J Pharm. 2011;
78. Xia Q, Saupe A, Müller RH, Souto EB. Nanostructured lipid carriers as novel carrier for sunscreen formulations. Int J Cosmet Sci. 2007;
79. Haque S, Whittaker M, McIntosh MP, Pouton CW, Phipps S, Kaminskas LM. A comparison of the lung clearance kinetics of solid lipid nanoparticles and liposomes by following the 3H-labelled structural lipids after pulmonary delivery in rats. Eur J Pharm Biopharm. 2018;
80. Suresh G, Manjunath K, Venkateswarlu V, Satyanarayana V. Preparation, characterization, and in vitro and in vivo evaluation of lovastatin solid lipid nanoparticles. AAPS PharmSciTech [Internet]. 2007 Mar;8(1):E162–70. Available from: http://link.springer.com/10.1208/pt0801024
81. Tsai MJ, Wu PC, Huang Y Bin, Chang JS, Lin CL, Tsai YH, et al. Baicalein loaded in tocol nanostructured lipid carriers (tocol NLCs) for enhanced stability and brain targeting. Int J Pharm. 2012;
82. Souto EB, Müller RH. SLN and NLC for topical delivery of ketoconazole. J Microencapsul. 2005;
83. HANAFY A, SPAHNLANGGUTH H, VERGNAULT G, GRENIER P, TUBICGROZDANIS M, LENHARDT T, et al. Pharmacokinetic evaluation of oral fenofibrate nanosuspensions and SLN in comparison to conventional suspensions of micronized drug☆. Adv Drug Deliv Rev [Internet]. 2007 Jul 10;59(6):419–26. Available from: https://linkinghub.elsevier.com/retrieve/pii/S0169409X07000397
84. Hippalgaonkar K, Adelli GR, Hippalgaonkar K, Repka MA, Majumdar S. Indomethacin-Loaded Solid Lipid Nanoparticles for Ocular Delivery: Development, Characterization, and In Vitro Evaluation . J Ocul Pharmacol Ther. 2013;
85. Bhalekar M, Upadhaya P, Madgulkar A. Formulation and characterization of solid lipid nanoparticles for an anti-retroviral drug darunavir. Appl Nanosci. 2017;
86. Choubey A, Gilhotra R, Singh S, Garg G. Formulation and characterization of nanomedicine (solid lipid nanoparticle) associate with the extract of Pterospermum acerifolium for the screening of neurochemicals and neuroendocrine effects. Asian J Neurosurg. 2017;
87. Fouad EA, Yassin AEB, Alajami HN. Characterization of celecoxib-loaded solid lipid nanoparticles formulated with tristearin and softisan 100. Trop J Pharm Res. 2015;
88. Li S, Ji Z, Zou M, Nie X, Shi Y, Cheng G. Preparation, Characterization, Pharmacokinetics and Tissue Distribution of Solid Lipid Nanoparticles Loaded with Tetrandrine. AAPS PharmSciTech. 2011;
89. Shazly GA. Corrigendum to “Ciprofloxacin Controlled-Solid Lipid Nanoparticles: Characterization, In Vitro Release, and Antibacterial Activity Assessment.” BioMed research international. 2017.
90. Liu CH, Wu CT, Fang JY. Characterization and formulation optimization of solid lipid nanoparticles in vitamin K1 delivery. Drug Dev Ind Pharm. 2010;
91. Liu CH, Wu CT. Optimization of nanostructured lipid carriers for lutein delivery. Colloids Surfaces A Physicochem Eng Asp. 2010;
92. Fang JY, Fang CL, Liu CH, Su YH. Lipid nanoparticles as vehicles for topical psoralen delivery: Solid lipid nanoparticles (SLN) versus nanostructured lipid carriers (NLC). Eur J Pharm Biopharm. 2008;
93. Ekambaram P, Abdul Hasan Sathali A. Formulation and Evaluation of Solid Lipid Nanoparticles of Ramipril. J Young Pharm [Internet]. 2011 Jul;3(3):216–20. Available from: http://www.jyoungpharm.org/article/545
94. Karami MA, Sharif Makhmal Zadeh B, Koochak M, Moghimipur E. Superoxide Dismutase-Loaded Solid Lipid Nanoparticles Prepared by Cold Homogenization Method: Characterization and Permeation Study Through Burned Rat Skin. Jundishapur J Nat Pharm Prod [Internet]. 2016 Oct 8;11(4). Available from: http://jjnpp.neoscriber.org/en/articles/13726.html
95. Jain SK, Chourasia MK, Masuriha R, Soni V, Jain A, Jain NK, et al. Solid lipid nanoparticles bearing flurbiprofen for transdermal delivery. Drug Deliv J Deliv Target Ther Agents. 2005;
96. Han F, Li S, Yin R, Liu H, Xu L. Effect of surfactants on the formation and characterization of a new type of colloidal drug delivery system: Nanostructured lipid carriers. Colloids Surfaces A Physicochem Eng Asp. 2008;
97. Zhuang CY, Li N, Wang M, Zhang XN, Pan WS, Peng JJ, et al. Preparation and characterization of vinpocetine loaded nanostructured lipid carriers (NLC) for improved oral bioavailability. Int J Pharm. 2010;
98. Amasya G, Aksu B, Badilli U, Onay-Besikci A, Tarimci N. QbD guided early pharmaceutical development study: Production of lipid nanoparticles by high pressure homogenization for skin cancer treatment. Int J Pharm. 2019;

99. Müller RH, Mäder K, Gohla S. Solid lipid nanoparticles (SLN) for controlled drug delivery - A review of the state of the art. European Journal of Pharmaceutics and Biopharmaceutics. 2000.
100. Hamishehkar H, Same S, Adibkia K, Zarza K, Shokri J, Taghaee M, et al. A comparative histological study on the skin occlusion performance of a cream made of solid lipid nanoparticles and Vaseline. Res Pharm Sci. 2015;
101. Jain S, Patel N, Shah MK, Khatri P, Vora N. Recent Advances in Lipid-Based Vesicles and Particulate Carriers for Topical and Transdermal Application. Journal of Pharmaceutical Sciences. 2017.
102. Kim H, Kim JT, Barua S, Yoo SY, Hong SC, Lee K Bin, et al. Seeking better topical delivery technologies of moisturizing agents for enhanced skin moisturization. Expert Opinion on Drug Delivery. 2018.
103. Dianzani C, Zara GP, Maina G, Pettazzoni P, Pizzimenti S, Rossi F, et al. Drug Delivery Nanoparticles in Skin Cancers. Biomed Res Int. 2014;
104. Naves LB, Dhand C, Venugopal JR, Rajamani L, Ramakrishna S, Almeida L. Nanotechnology for the treatment of melanoma skin cancer. Prog Biomater. 2017;
105. Orthaber K, Pristovnik M, Skok K, Perić B, Maver U. Skin Cancer and Its Treatment: Novel Treatment Approaches with Emphasis on Nanotechnology. J Nanomater. 2017;
106. Garcês A, Amaral MH, Sousa Lobo JM, Silva AC. Formulations based on solid lipid nanoparticles (SLN) and nanostructured lipid carriers (NLC) for cutaneous use: A review. European Journal of Pharmaceutical Sciences. 2018.
107. Venâncio JH, Andrade LM, Esteves NLS, Brito LB, Valadares MC, Oliveira GAR, et al. Topotecan-loaded lipid nanoparticles as a viable tool for the topical treatment of skin cancers. J Pharm Pharmacol. 2017;
108. Tupal A, Sabzichi M, Ramezani F, Kouhsoltani M, Hamishehkar H. Dermal delivery of doxorubicin-loaded solid lipid nanoparticles for the treatment of skin cancer. J Microencapsul. 2016;
109. Clemente N, Ferrara B, Gigliotti CL, Boggio E, Capucchio MT, Biasibetti E, et al. Solid lipid nanoparticles carrying temozolomide for melanoma treatment. Preliminary in vitro and in vivo studies. Int J Mol Sci. 2018;
110. Bharadwaj R, Das PJ, Pal P, Mazumder B. Topical delivery of paclitaxel for treatment of skin cancer. Drug Dev Ind Pharm. 2016;
111. Prado Almeida ED, Vieira Dipieri L, Rosseti FC, Maldonado Marchetti J, Lopes Badra Bentley MV, de Souza Nunes R, et al. Skin permeation, biocompatibility and antitumor effect of chloroaluminum phthalocyanine associated to oleic acid in lipid nanoparticles. Photodiagnosis Photodyn Ther. 2018;
112. Pietsch EC, Sykes SM, McMahon SB, Murphy ME. The p53 family and programmed cell death. Oncogene. 2008.
113. Bargonetti J, Manfredi JJ. Multiple roles of the tumor suppressor p53. Curr Opin Oncol [Internet]. 2002 Jan;14(1):86–91. Available from: https://insights.ovid.com/crossref?an=00001622-200201000-00015
114. Vousden KH, Lu X. Live or let die: The cell's response to p53. Nature Reviews Cancer. 2002.
115. Hao Q, Cho WC. Battle against cancer: An everlasting saga of p53. International Journal of Molecular Sciences. 2014.
116. Pflaum J, Schlosser S, MÃ¼ller M. p53 Family and Cellular Stress Responses in Cancer. Front Oncol. 2014;
117. Napoli M, Flores ER. The p53 family orchestrates the regulation of metabolism: Physiological regulation and implications for cancer therapy. British Journal of Cancer. 2017.
118. Collavin L, Lunardi A, Del Sal G. p53-family proteins and their regulators: hubs and spokes in tumor suppression. Cell Death Differ. 2010;
119. Melino G. Functional regulation of p73 and p63: development and cancer. Trends Biochem Sci [Internet]. 2003 Dec;28(12):663–70. Available from: https://linkinghub.elsevier.com/retrieve/pii/S0968000403002706
120. Müller M, Schleithoff ES, Stremmel W, Melino G, Krammer PH, Schilling T. One, two, three-p53, p63, p73 and chemosensitivity. Drug Resist Updat. 2006;
121. Ferraiuolo M, Di Agostino S, Blandino G, Strano S. Oncogenic Intra-p53 Family Member Interactions in Human Cancers. Front Oncol. 2016;
122. Bourdon JC. p53 and its isoforms in cancer. British Journal of Cancer. 2007.
123. Haupt Y, Blandino G. Editorial: Human Tumor-Derived p53 Mutants: A Growing Family of Oncoproteins. Front Oncol. 2016;
124. Murray-Zmijewski F, Lane DP, Bourdon JC. p53/p63/p73 isoforms: An orchestra of isoforms to harmonise cell differentiation and response to stress. Cell Death and Differentiation. 2006.
125. Li L, Li L, Li W, Chen T, Bin Zou, Zhao L, et al. TAp73-induced phosphofructokinase-1 transcription promotes the Warburg effect and enhances cell proliferation. Nat Commun. 2018;
126. Sznarkowska A, Kostecka A, Kawiak A, Acedo P, Lion M, Inga A, et al. Reactivation of TAp73 tumor suppressor by protoporphyrin IX, a metabolite of aminolevulinic acid, induces apoptosis in TP53-deficient cancer cells. Cell Div. 2018;
127. Coates PJ. Regulating p73 isoforms in human tumours. J Pathol. 2006;
128. Melino G, De Laurenzi V, Vousden KH. p73: Friend or foe in tumorigenesis. Nat Rev Cancer. 2002;2(8):605–15.

129. Stiewe T, Pützer BM. Role of p73 in malignancy: Tumor suppressor or oncogene? Cell Death and Differentiation. 2002.
130. Tomasini R, Tsuchihara K, Wilhelm M, Fujitani M, Rufini A, Cheung CC, et al. TAp73 knockout shows genomic instability with infertility and tumor suppressor functions. Genes Dev. 2008;
131. Tuve S, Wagner SN, Schitrek B, Pützer BM. Alterations of ΔTA-p73 splice transcripts during melanoma development and progression. Int J Cancer. 2004;
132. DeYoung MP, Ellisen LW. p63 and p73 in human cancer: Defining the network. Oncogene. 2007.
133. Box NF, Vukmer TO, Terzian T. Targeting p53 in melanoma. Pigment Cell Melanoma Res. 2014;
134. Inoue K, Fry EA. Alterations of p63 and p73 in human cancers. Subcell Biochem. 2014;
135. Rufini A, Agostini M, Grespi F, Tomasini R, Sayan BS, Niklison-Chirou MV, et al. p73 in Cancer. Genes Cancer [Internet]. 2011 Apr 1;2(4):491–502. Available from: http://gan.sagepub.com/lookup/doi/10.1177/1947601911408890
136. Gomes S, Raimundo L, Soares J, Loureiro JB, Leão M, Ramos H, et al. New inhibitor of the TAp73 interaction with MDM2 and mutant p53 with promising antitumor activity against neuroblastoma. Cancer Lett [Internet]. 2019 Apr;446:90–102. Available from: https://linkinghub.elsevier.com/retrieve/pii/S0304383519300266
137. Wu H, Leng RP. MDM2 mediates p73 ubiquitination: a new molecular mechanism for suppression of p73 function. Oncotarget. 2015;
138. Vassilev LT, Vu BT, Graves B, Carvajal D, Podlaski F, Filipovic Z, et al. In Vivo Activation of the p53 Pathway by Small-Molecule Antagonists of MDM2. Science (80-). 2004;
139. Di Agostino S, Cortese G, Monti O, Dell'Orso S, Sacchi A, Eisenstein M, et al. The disruption of the protein complex mutantp53/p73 increases selectively the response of tumor cells to anticancer drugs. Cell Cycle. 2008;
140. Kravchenko JE, Ilyinskaya G V., Komarov PG, Agapova LS, Kochetkov D V., Strom E, et al. Small-molecule RETRA suppresses mutant p53-bearing cancer cells through a p73-dependent salvage pathway. Proc Natl Acad Sci. 2008;
141. Lau LMS, Nugent JK, Zhao X, Irwin MS. HDM2 antagonist Nutlin-3 disrupts p73-HDM2 binding and enhances p73 function. Oncogene. 2008;
142. Hong B, Prabhu V V., Zhang S, Van Den Heuvel APJ, Dicker DT, Kopelovich L, et al. Prodigiosin rescues deficient p53 signaling and antitumor effects via upregulating p73 and disrupting its interaction with mutant p53. Cancer Res. 2014;
143. Xie B, Nagalingam A, Kuppusamy P, Muniraj N, Langford P, Gyorffy B, et al. Benzyl Isothiocyanate potentiates p53 signaling and antitumor effects against breast cancer through activation of p53-LKB1 and p73-LKB1 axes. Sci Rep. 2017;
144. Gelperina S, Kisich K, Iseman MD, Heifets L. The potential advantages of nanoparticle drug delivery systems in chemotherapy of tuberculosis. American Journal of Respiratory and Critical Care Medicine. 2005.
145. Mudshinge SR, Deore AB, Patil S, Bhalgat CM. Nanoparticles: Emerging carriers for drug delivery. Saudi Pharmaceutical Journal. 2011.
146. Silva AC, Amaral MH, Sousa Lobo JM, Tichota D. Design, characterization, and clinical evaluation of argan oil nanostructured lipid carriers to improve skin hydration. Int J Nanomedicine [Internet]. 2014 Aug;3855. Available from: http://www.dovepress.com/design-characterization-and-clinical-evaluation-of-argan-oil-nanostruc-peer-reviewed-article-IJN
147. Eiras F. Desenvolvimento, caracterização e avaliação da biocompatibilidade e do potencial irritativo de formulações cosméticas à base de nanopartículas lipídicas. Faculdade de Farmacia da Universidade do Porto; 2016.
148. Tamjidi F, Shahedi M, Varshosaz J, Nasirpour A. Nanostructured lipid carriers (NLC): A potential delivery system for bioactive food molecules. Innovative Food Science and Emerging Technologies. 2013.
149. Souto EB, Almeida AJ, Müller RH. Lipid nanoparticles (SLN®, NLC®) for cutaneous drug delivery: Structure, protection and skin effects. Journal of Biomedical Nanotechnology. 2007.
150. Chaturvedi SP, Kumar V. Production techniques of lipid nanoparticles: A review. Research Journal of Pharmaceutical, Biological and Chemical Sciences. 2012.
151. Ganesan P, Narayanasamy D. Lipid nanoparticles: Different preparation techniques, characterization, hurdles, and strategies for the production of solid lipid nanoparticles and nanostructured lipid carriers for oral drug delivery. Sustainable Chemistry and Pharmacy. 2017.
152. Mehnert W, Mader K. NLS Production, characterization and applications. 2001;47:165–96.
153. Tzachev CT, Svilenov HL. Lipid nanoparticles at the current stage and prospects - A review article. International Journal of Pharmaceutical Sciences Review and Research. 2013.
154. Garud A, Singh D, Garud N. Solid Lipid Nanoparticles (SLN): Method, Characterization and Applications. Int Curr Pharm J [Internet]. 2012 Oct 3;1(11):384–93. Available from: https://www.banglajol.info/index.php/ICPJ/article/view/12065
155. Attama. A, Momoh. M, Builders. P. Lipid Nanoparticulate Drug Delivery Systems: A Revolution in Dosage

Form Design and Development. In: Recent Advances in Novel Drug Carrier Systems [Internet]. InTech; 2012. Available from: http://www.intechopen.com/books/recent-advances-in-novel-drug-carrier-systems/lipid-nanoparticulate-drug-delivery-systems-a-revolution-in-dosage-form-design-and-development
156. Malvern Instruments Limited. A basic guide to particle characterization. Whitepaper. 2015.
157. Gumustas M, Sengel-Turk CT, Gumustas A, Ozkan SA, Uslu B. Effect of Polymer-Based Nanoparticles on the Assay of Antimicrobial Drug Delivery Systems. In: Multifunctional Systems for Combined Delivery, Biosensing and Diagnostics. 2017.
158. Stetefeld J, McKenna SA, Patel TR. Dynamic light scattering: a practical guide and applications in biomedical sciences. Biophysical Reviews. 2016.
159. Lim J, Yeap SP, Che HX, Low SC. Characterization of magnetic nanoparticle by dynamic light scattering. Nanoscale Res Lett. 2013;
160. Danaei M, Dehghankhold M, Ataei S, Hasanzadeh Davarani F, Javanmard R, Dokhani A, et al. Impact of particle size and polydispersity index on the clinical applications of lipidic nanocarrier systems. Pharmaceutics. 2018.
161. Badran M. Formulation and in vitro evaluation of flufenamic acid loaded deformable liposomes for improved skin delivery. Dig J Nanomater Biostructures. 2014;
162. Putri DCA, Dwiastuti R, Marchaban M, Nugroho AK. OPTIMIZATION OF MIXING TEMPERATURE AND SONICATION DURATION IN LIPOSOME PREPARATION. J Pharm Sci Community [Internet]. 2017 Nov 30;14(2):79–85. Available from: http://e-journal.usd.ac.id/index.php/JFSK/article/view/728
163. Yingchoncharoen P, Kalinowski DS, Richardson DR. Lipid-Based Drug Delivery Systems in Cancer Therapy: What Is Available and What Is Yet to Come. Pharmacol Rev. 2016;
164. Park S-J, Seo M-K. Intermolecular Force. In: Interface Science and Technology [Internet]. 2011. p. 1–57. Available from: https://linkinghub.elsevier.com/retrieve/pii/B9780123750495000013
165. Clogston JD, Patri AK. Zeta Potential Measurement. Methods Mol Biol. 2011;
166. Smith MC, Crist RM, Clogston JD, McNeil SE. Zeta potential: a case study of cationic, anionic, and neutral liposomes. Anal Bioanal Chem. 2017;
167. Bagul US, Pisal V V, Solanki N V, Karnavat A. Current status of solid lipid nanoparticles: a review. Mod Appl Bioequivalence Bioavailab. 2018;3(MS. ID. 555617):1–9.
168. Agrawal Y, Patel V. Nanosuspension: An approach to enhance solubility of drugs. J Adv Pharm Technol Res [Internet]. 2011;2(2):81. Available from: http://www.japtr.org/text.asp?2011/2/2/81/82950
169. Bhattacharjee S. DLS and zeta potential – What they are and what they are not? J Control Release [Internet]. 2016 Aug;235:337–51. Available from: https://linkinghub.elsevier.com/retrieve/pii/S0168365916303832
170. Lu GW, Gao P. Emulsions and Microemulsions for Topical and Transdermal Drug Delivery. In: Handbook of Non-Invasive Drug Delivery Systems [Internet]. Elsevier; 2010. p. 59–94. Available from: https://linkinghub.elsevier.com/retrieve/pii/B9780815520252100034
171. Vincent P. NanoFASE - ELS [Internet]. [cited 2019 Jun 22]. Available from: http://nanofase.eu/show/ELS_1278
172. Dahimiwal SM, Thorat DB, Jain NP, Jadhav VB, Patil PB. A review on high performance liquid chromatography. Int J Pharm Res. 2013;5(3):1–6.
173. Malviya R, Bansal V, Pal OP, Sharma PK. High performance liquid chromatography: A short review. Journal of Global Pharma Technology. 2010.
174. Petrova O, Sauer K. High-Performance Liquid Chromatography (HPLC)-Based Detection and Quantitation of Cellular c-di-GMP. In: c-di-GMP Signaling [Internet]. Weinheim, Germany: Wiley-VCH Verlag GmbH & Co. KGaA; 2017. p. 33–43. Available from: http://doi.wiley.com/10.1002/9783527629237.ch21
175. Czaplicki S. Chromatography in Bioactivity Analysis of Compounds. In: Column Chromatography [Internet]. InTech; 2013. p. 99–122. Available from: http://www.intechopen.com/books/column-chromatography/chromatography-in-bioactivity-analysis-of-compounds
176. Fornstedt T, Forssén P, Westerlund D. Basic HPLC Theory and Definitions: Retention, Thermodynamics, Selectivity, Zone Spreading, Kinetics, and Resolution. In: Analytical Separation Science. 2015.
177. Wang IH, Moorman R, Burleson J. Isocratic reversed-phase liquid chromatographic method for the simultaneous determination of (S)-methoprene, MGK264, piperonyl butoxide, sumithrin and permethrin in pesticide formulation. J Chromatogr A. 2003;
178. Moreira ARS. Development of proliposomes as a vehicle to deliver new molecules with antitumor activity [Internet]. Faculdade de Farmácia, Universidade do Porto; 2015. Available from: https://repositorio-aberto.up.pt/bitstream/10216/85998/2/36423.pdf
179. Schellinger AP, Carr PW. Isocratic and gradient elution chromatography: A comparison in terms of speed, retention reproducibility and quantitation. J Chromatogr A [Internet]. 2006 Mar;1109(2):253–66. Available from: https://linkinghub.elsevier.com/retrieve/pii/S002196730600166X
180. Shabir GA. A Practical Approach to Validation of HPLC Methods Under Current Good Manufacturing Practices. J Valid Technol. 2004;10:210–8.
181. Shabir GA. Validation of high-performance liquid chromatography methods for pharmaceutical analysis:

Understanding the differences and similarities between validation requirements of the US Food and Drug Administration, the US Pharmacopeia and the International Conf. In: Journal of Chromatography A. 2003.
182. International Conference on Harmonization of Technical Requirements for Registration on Pharmaceuticals for Human Use [ICH]. ICH Q2 (R1) Validation of Analytical Procedures : Text and Methodology. International Conference on Harmonization. 2005.
183. Bhagyasree T, Neelam I, Ajitha A, Rao UM. International Journal of Pharmaceutical Research & Analysis. Int J pharmacutical recearch Anal. 2014;4(8):444–8.
184. Kumar V, Bharadwaj R, Gupta G, Kumar S. An Overview on HPLC Method Development, Optimization and Validation process for drug analysis. Pharm Chem J. 2015;2(2):30–40.
185. FDA Guidance for Industry. Validation of Chromatographic Methods. Reviewer Guidance. Cent Drug Evalutaion Res. 1994;
186. Das S, Ng WK, Tan RBH. Sucrose ester stabilized solid lipid nanoparticles and nanostructured lipid carriers: I. Effect of formulation variables on the physicochemical properties, drug release and stability of clotrimazole-loaded nanoparticles. Nanotechnology [Internet]. 2014 Mar 14;25(10):105101. Available from: http://stacks.iop.org/0957-4484/25/i=10/a=105101?key=crossref.6dfeeb1de934d08e7d7ef1cd0659aeeb
187. FUJIFILM Irvine Scientific. Protocol for Mesenchymal Stem Cell Expansion | FUJIFILM Irvine Scientific [Internet]. [cited 2019 Jun 25]. Available from: http://www.irvinesci.com/protocol-for-mesenchymal-stem-cell-expansion
188. Soares J, Pereira NAL, Monteiro Â, Leão M, Bessa C, Dos Santos DJVA, et al. Oxazoloisoindolinones with in vitro antitumor activity selectively activate a p53-pathway through potential inhibition of the p53-MDM2 interaction. Eur J Pharm Sci. 2015;
189. Mahmood T, Yang P-C. Cell lysis to extract protein Western Blot: technique, theory, and trouble shooting. Am J Med Sci. 2012;
190. Vallejo-Illarramendi A, Marciano DK, Reichardt LF. A novel method that improves sensitivity of protein detection in PAGE and Western blot. Electrophoresis. 2013;
191. Mishra M, Tiwari S, Gomes A V. Protein purification and analysis: Next generation western blotting techniques. Expert Review of Proteomics. 2017.
192. Bass JJ, Wilkinson DJ, Rankin D, Phillips BE, Szewczyk NJ, Smith K, et al. An overview of technical considerations for Western blotting applications to physiological research. Scandinavian Journal of Medicine and Science in Sports. 2017.
193. Murphy RM, Lamb GD. Important considerations for protein analyses using antibody based techniques: Down-sizing Western blotting up-sizes outcomes. Journal of Physiology. 2013.
194. Gherasim O, Popescu RC, Gherasim TG, Grumezescu V, Andronescu E. Pharmacotherapy and nanotechnology. In: Nanoparticles in Pharmacotherapy [Internet]. Elsevier; 2019. p. 275–82. Available from: https://linkinghub.elsevier.com/retrieve/pii/B9780128165041000028
195. Ruland A, Kreuter J. Influence of various penetration enhancers on the in vitro permeation of amino acids across hairless mouse skin. Int J Pharm [Internet]. 1992 Sep;85(1–3):7–17. Available from: https://linkinghub.elsevier.com/retrieve/pii/037851739290128O
196. Loftsson T. Effect of Oleic Acid on Diffusion of Drugs Through Hairless Mouse Skin. Acta Pharm Nord. 1989;1:17–22.
197. Mathur V, Satrawala Y, Rajput M. Physical and chemical penetration enhancers in transdermal drug delivery system. Asian J Pharm [Internet]. 2010;4(3):173. Available from: http://www.asiapharmaceutics.info/text.asp?2010/4/3/173/72115
198. Verma D. Particle size of liposomes influences dermal delivery of substances into skin. Int J Pharm [Internet]. 2003 Jun 4;258(1–2):141–51. Available from: https://linkinghub.elsevier.com/retrieve/pii/S0378517303001832
199. Verma DD, Verma S, Blume G, Fahr A. Liposomes increase skin penetration of entrapped and non-entrapped hydrophilic substances into human skin: A skin penetration and confocal laser scanning microscopy study. Eur J Pharm Biopharm. 2003;
200. Hua S. Lipid-based nano-delivery systems for skin delivery of drugs and bioactives. Front Pharmacol [Internet]. 2015 Sep 30;6. Available from: http://journal.frontiersin.org/Article/10.3389/fphar.2015.00219/abstract
201. Chen M, Liu X, Fahr A. Skin penetration and deposition of carboxyfluorescein and temoporfin from different lipid vesicular systems: In vitro study with finite and infinite dosage application. Int J Pharm. 2011;
202. CHROMacademy. The Theory of HPLC: Chromatographic Parameters. Crawford Scientific. 2014.
203. Taylor R. Interpretation of the Correlation Coefficient: A Basic Review. J Diagnostic Med Sonogr [Internet]. 1990 Jan;6(1):35–9. Available from: http://journals.sagepub.com/doi/10.1177/875647939000600106
204. Debbasch C, Brignole F, Pisella PJ, Warnet JM, Rat P, Baudouin C. Quaternary ammoniums and other preservatives' contribution in oxidative stress and apoptosis on Chang conjunctival cells. Investig Ophthalmol Vis Sci. 2001;42(3):652–652.
205. National Center for Biotechnology Information. Cetrimide | C17H38BrN - PubChem [Internet]. [cited 2019 Sep 9]. Available from: https://pubchem.ncbi.nlm.nih.gov/compound/Cetrimide

206. Lachenmeier DW. Antiseptic Drugs and Disinfectants. In: Ray S, editor. Side Effects of Drugs Annual [Internet]. Elsevier B.V.; 2016. p. 211–6. Available from: http://dx.doi.org/10.1016/bs.seda.2016.07.006
207. Debbasch C, De Saint Jean M, Pisella P-J, Rat P, Warnet J-M, Baudouin C. Quaternary ammonium cytotoxicity in a human conjunctival cell line. J Fr Ophtalmol. 1999;22(9):950–8.
208. Yasun E, Li C, Barut I, Janvier D, Qiu L, Cui C, et al. BSA modification to reduce CTAB induced nonspecificity and cytotoxicity of aptamer-conjugated gold nanorods. Nanoscale. 2015;
209. Alkilany AM, Nagaria PK, Hexel CR, Shaw TJ, Murphy CJ, Wyatt MD. Cellular Uptake and Cytotoxicity of Gold Nanorods: Molecular Origin of Cytotoxicity and Surface Effects. Small [Internet]. 2009 Mar 20;5(6):701–8. Available from: http://doi.wiley.com/10.1002/smll.200801546
210. Debbasch C, Rat P, Warnet J-M, De Saint Jean M, Baudouin C, Pierre-Jean P. Evaluation of toxicity of benzalkonium chloride to the ocular surface. J Toxicol - Cutan Ocul Toxicol. 2008;19(2):105–15.
211. Shamas-Din A, Kale J, Leber B, Andrews DW. Mechanisms of Action of Bcl-2 Family Proteins. Cold Spring Harb Perspect Biol [Internet]. 2013 Apr 1;5(4):a008714–a008714. Available from: http://cshperspectives.cshlp.org/lookup/doi/10.1101/cshperspect.a008714